[illegible] A

[illegible]

[illegible] Unlimited

19951220 032

[illegible]

[illegible] SUBMITTED TO [illegible]

[illegible] (ALPHA): APPROVED FOR PUBLIC RELEASE; DISTRIBUTION

UNLIMITED [redacted]

[redacted]

[illegible]

DEPARTMENT OF DEFENSE
PLASTICS TECHNICAL EVALUATION CENTER
ARRADCOM, DOVER, N. J. 07806

DTIC QUALITY INSPECTED 3

This is an authorized facsimile
printed by microfilm/xerography on acid-free paper
in 1982 by
UNIVERSITY MICROFILMS INTERNATIONAL
Ann Arbor, Michigan, U.S.A.
London, England

DTIC
S ELECTE D
DEC 27 1995
B

DISTRIBUTION STATEMENT A
Approved for public release
Distribution Unlimited

INFORMATION TO USERS

This was produced from a copy of a document sent to us for microfilming. While the most advanced technological means to photograph and reproduce this document have been used, the quality is heavily dependent upon the quality of the material submitted.

The following explanation of techniques is provided to help you understand markings or notations which may appear on this reproduction.

1. The sign or "target" for pages apparently lacking from the document photographed is "Missing Page(s)". If it was possible to obtain the missing page(s) or section, they are spliced into the film along with adjacent pages. This may have necessitated cutting through an image and duplicating adjacent pages to assure you of complete continuity.

2. When an image on the film is obliterated with a round black mark it is an indication that the film inspector noticed either blurred copy because of movement during exposure, or duplicate copy. Unless we meant to delete copyrighted materials that should not have been filmed, you will find a good image of the page in the adjacent frame. If copyrighted materials were deleted you will find a target note listing the pages in the adjacent frame.

3. When a map, drawing or chart, etc., is part of the material being photographed the photographer has followed a definite method in "sectioning" the material. It is customary to begin filming at the upper left hand corner of a large sheet and to continue from left to right in equal sections with small overlaps. If necessary, sectioning is continued again—beginning below the first row and continuing on until complete.

4. For any illustrations that cannot be reproduced satisfactorily by xerography, photographic prints can be purchased at additional cost and tipped into your xerographic copy. Requests can be made to our Dissertations Customer Services Department.

5. Some pages in any document may have indistinct print. In all cases we have filmed the best available copy.

University
Microfilms
International

300 N. ZEEB RD., ANN ARBOR, MI 48106

8118883

LO, JIELIN

FLAMMABILITY AND PHOTO-STABILITY OF SELECTED POLYMER SYSTEMS

Polytechnic Institute of New York Ph.D. 1981

University
Microfilms
International 300 N. Zeeb Road, Ann Arbor, MI 48106

Accession For
NTIS GRA&I ☑
DTIC TAB ☐
Unannounced ☐
Justification [illegible]
By
Distribution/
Availability Codes

Dist	Avail and/or Special
A-1	

© 1981

JEELIN LO

All Rights Reserved

FLAMMABILITY AND PHOTO-STABILITY OF SELECTED POLYMER SYSTEMS

DISSERTATION

Submitted in Partial Fulfillment
of the Requirements for the
Degree of

DOCTOR OF PHILOSOPHY (Chemistry)

At the

POLYTECHNIC INSTITUTE OF NEW YORK

by

Jeelin Lo

June 1981

Approved:

Eli Pearce

Department Head

May 1, 198

Approved by the Guidance Committee

__Major__. Polymer Chemistry

Eli M. Pearce, (Chairman)
Professor and Head
Department of Chemistry

Yoshiyuki Okamoto
Professor
Department of Chemistry

__Minor__: Polymer Science and
Engineering

Jovan Mijovic
Assistant Professor
Department of Chemical
Engineering

__Additional Member__:

Bernard J. Bulkin
Professor and
Dean of Arts and Sciences

Microfilm or other copies of this dissertation are obtainable from

University Microfilms
300 N. Zeeb Road
Ann Arbor, Michigan
48106

VITA

Jeelin Lo was born on [redacted] [redacted] in [redacted] [redacted] [redacted] [redacted] He moved to the Province of Taiwan during the civil war in China in late 1949, and completed his primary, high school, and college education. He received his B.Sc. at Fu-Jen Catholic University in Taipei, Taiwan in 1971. After two years military service in China he joined the Polytechnic Institute of New York in September, 1974 and continued his education in Chemistry.

During his tenure as a graduate student he was awarded a Teaching Assistantship and a Research Fellowship until June, 1981, at which time he completed the requirements for the Degree of Doctor of Philosophy.

The author is currently a member of the Society of Plastics Engineers as well as the American Chemical Society.

DEDICATION

To My Parents

ACKNOWLEDGEMENT

The author wishes to express his sincere gratitude to Professor Eli M. Pearce for his guidance and encouragement during the course of this research. The author is deeply grateful to Dean Bernard J. Bulkin for his helpful discussions and guidance in the FT-IR studies.

The financial assistance from AMP Incorporated, the Army Research Office and the National Aeronautics and Space Administration is gratefully acknowledged.

AN ABSTRACT

FLAMMABILITY AND PHOTO-STABILITY
OF SELECTED POLYMER SYSTEMS

BY

Jeelin Lo

Adviser: Eli M. Pearce

Submitted in Partial Fulfillment of the Requirement
for the Degree of
Doctor of Philosophy (Chemistry)
June 1981

A systematic approach to the improvement of the flammability of epoxy resins, bisphenol-A polycarbonate , poly(butylene terephthalate), and Nylon 6.6 by introducing halogens and loop functionality into the flame retardants is described. The phthalides (the loop functionality containing molecules) include 3,3-bis(4-bromophenyl)-phthalide, 3,3-bis(4-chlorophenyl)phthalide, and phenolphthalein. The phthalide containing epoxy resins are synthesized and characterized in comparison with the bisphenol-A epoxy resins in terms of flammability in the copolymer systems. The resins include diglycidyl ethers of phenolphthalein, bisphenol-A, tetrabromobisphenol-A, and tetrabromophenolphthalein. The vaporization of the phthalide additive in the polymers is observed in Thermal Gravimetric Analysis. The flame retardancy is primarily due to the presence of halogens. In the poly(butylene terephthalate) system, the cleavage of the $C_{aromatic}$-Br bond

of the flame retardant additive enhances the crosslinking reactions between the aromatic rings resulting in an increase of char formation. In the epoxy resin systems, loop functionality contributes to char formation to a larger extent. The interaction between the epoxy resin and poly(butylene terephthalate) follows the mechanism of insertion of the oxirane ring into the ester bond. This mechanism is studied by FT-IR.

The investigation of the thermal properties of the char-forming phenol-formaldehyde resins is conducted to provide information for the systematic design of high temperature flame-resistant phenolics. NMR and FT-IR are used to characterize the oligomeric resins and the cured resins. The curing agents used in the study include formaldehyde, s-trioxane and terephthaloyl chloride. The brominated phenolic resins are found to have higher oxygen indices with lower char yields. The nonhalogen-containing phenolic resins give a linear relationship between char yield and oxygen index according to the following equation:

$$\%OI = 2.4 + 0.57\ (\%\text{ char yield at } 800^{\circ}\text{C } N_2).$$

The differences in structure of the cured resins are observed from the FT-IR spectra. The s-trioxane cured resins contain long chain ethers and cyclic acetals along with the methylene linkages. The terephthaloyl chloride cured resins are crosslinked through the hydroxyls and contain the inter- and intra-molecular ester linkages.

In the study of the photo-Fries rearrangement the fluorene-based polyarylates prepared include 9,9'-bis(4-hydroxyphenyl)fluorene isophthalate (BPF-I), 9,9'-biscresol fluorene isophthalate (BCF-I), and 9,9'-bis(3,5-dimethyl-4-hydroxyphenyl)fluorene isophthalate (BDMPF-I). The formatio of the o-hydroxybenzophenone moiety upon UV irradiation of BPF-I and BCF-I can be observed in the UV and IR spectra. The degradation of the polymer structure of BDMPF-I is due to its inability to rearrange into the o-hydroxybenzophenone structure which can function as an internal UV-stabilizer. A mechanism for this degradation is postulated based on the evidence from the IR spectra.

TABLE OF CONTENTS

Page

Abstract

1. Introduction 1

1.1 Elements in Flame Retardation 2

1.2 Structure-Flammability Relationship 4

1.3 Flame Retardant Additives 7

1.4 Modified and Flame Resistant Phenolic Resins 9

1.5 Photo-Stability of Fluorene-Based Polyarylates 13

1.5.1 Basic Approaches 13

1.5.2 Polymer Photo-Rearrangement 17

2. Experimental 19

2.1 Standard Procedure for the Preparation of Phthalides 19

2.2 Phthalides Used as Additive in Polymers 20

2.3 Standard Procedure for the Preparation of Epoxy Resins 21

2.3.1 Preparation of 4,5,6,7-Tetrabromophenolphthalein 22

2.3.2 Epoxy Resin Preparation 23

2.4 Characterization of Epoxy Resins 24

2.5 Brominated Epoxy Resins Used as Commoners in the DGEBA System 26

2.6 Epoxy Resins/Poly(butylene terephthalate) System 30

2.7 Standard Procedure for the Preparation of the Oligomeric Phenol-Formaldehyde Resins 30

2.8 Characterization of the Oligomeric Phenol-Formaldehyde Resins 30

2.9 Standard Procedure for the Crosslinking of Phenol-Formaldehyde Resins 32

2.9.1 Crosslinking Through Ester Linkages with Terephthaloyl Chloride 32

2.9.2 Crosslinking Through Methylene Linkages 32

2.9.2.1 Crosslinking with s-Trioxane 32

TABLE OF CONTENTS (Continued)

Page

2.9.2.2. Crosslinking with Formaldehyde 33

2.10 Characterization of Cured Phenol-Formaldehyde Resins 33

2.11 Preparation of Fluorene-Based Polyarylates 33

2.11.1 Preparation of Bisphenols 33

2.11.2 Preparation of Polymers 35

2.12 Studies of Photo-Fries Rearrangement 37

2.12.1 Irradiation Chamber 37

2.12.2 UV Spectroscopic Studies 37

2.12.3 FT-IR Spectroscopic Studies 37

3. Results and Discussion 38

3.1 Flame Retardants Containing Loop Functionality 38

3.1.1 Effects of Phthalides on Thermal Properties of Polymers 38

3.1.1.1 Bisphenol-A Polycarbonate System 38

3.1.1.2 Poly(butylene Terephthalate) and Nylon 6.6 Systems 48

3.1.2 Effects of Phthalide Containing Epoxy Resins on the Thermal Properties of Polymers 52

3.1.2.1 Epoxy Copolymer Resins 52

3.1.2.2 FT-IR Studies on Curing Reactions of the Epoxy Resins 55

3.1.2.3 Epoxy Resin/Poly(butylene terephthalate) System 62

3.1.2.4 FT-IR Studies of DGEHEFP/Poly-(butylene terephthalate) System 62

3.1.3 Conclusion 69

3.2 Phenol-Formaldehyde Resins 70

3.2.1 Structural Studies of the Oligomeric Resins 70

3.2.2 Number Average Molecular Weight Determination 93

TABLE OF CONTENTS (Concluded)

Page

3.2.3 Thermal Properties of Cured Phenolic Resins 94

3.2.4 Conclusion 104

3.3 Photo-Fries Rearrangement of Fluorene-Based Polyarylates 105

3.3.1 UV Spectroscopic Studies 105

3.3.2 FT-IR Spectroscopic Studies 110

3.3.3 Conclusion 118

Bibliography 119

LIST OF TABLES

Table No.		Page
1	Thermal Analytical Data of Polymers Containing Phthalide Additives	49
2	Thermal Analytical Data of Epoxy Resins	53
3	Thermal Analytical Data of Poly(butylene terephthalate) Containing Different Epoxy-Resin Additives	65
4	Number Average Molecular Weights, $\bar{M}n$, of Oligomeric Phenolic Resins	95
5	Thermal Analytical Data of Phenolic Resins Crosslinked via Methylene Linkages	96
6	Thermal Analytical Data of Phenolic Resins Crosslinked via Ester Linkages	97
7	Char Yields as a Function of Degree of Crosslinking of Phenol-formaldehyde Polymer	101

LIST OF FIGURES

Figure No.		Page
1	Effect of Aromatic Structure on Char Yield	5
2	Correlation Between OI and Cr	6
3	DSC Thermogramsof DGEPP	27
4	DSC Thermogramsof DGETBPP	28
5	DSC Thermograms of DGETBBA AND DGEBA	29
6	Schematic Diagram of Reflectance Attachment	31
7	Effect of 3,3-bis(4-Bromophenyl)phthalide Additive upon Char Yield of Bisphenol-A Polycarbonate as Measured by TGA at 10°C/min under N_2	39
8	Effect of 3,3-bis(4-Chlorophenyl)phthalide Additive upon Char Yield of Bisphenol-A Polycarbonate as Measured by TGA at 10°C/min under N_2	40
9	Effect of Phenolphthalein Additive Upon Char Yield of Bisphenol-A Polycarbonate as Measured by TGA at 10°C/min under N_2	41
10	Relationship of Oxygen Index with Additive Content in Bisphenol-A Polycarbonate	42
11	Infrared Spectra of HCl (A) and the Gases Evolved Between 300°-400°C in a TGA Measurement of Bisphenol-A Polycarbonate Containing 30%, 3,3-bis(4-Chlorophenyl)-phthalide (B). IR Gas Cell; 25°C.	46
12	Effect of Phenolphthalein Upon the Thermal Stability of Bisphenol-A Polycarbonate as Measured by DSC	47
13	Effect of 30% of 3,3-bis(4-Bromophenyl)-phthalide on Char Yield of Nylon 6,6 as Measured by TGA at 10°C/min under N_2	50
14	Effect of 30% of 3,3-bis(4-Bromophenyl)-phthalide on Char Yield of Poly(butylene terephthalate) as Measured by TGA at 10°C /min under N_2	51

LIST OF FIGURES (Continued)

Figure No. Page

15 TGA Thermograms of Epoxy Resin Copolymers Cured with Phthalic Anhydride
(A) DGEBA/DGETBPP (50/50).
(B) DGEBA/DGETBBA (50/50); N_2. 10°C/min. 54

16 Infrared Spectra of DGEBA/DGETBPP Cured with Phthalic Anhydride
(A) Initial Mixture.
(B) after Curing at 100°C for 30 min..
(C) after Curing at 100°C for 2 Hr..
(D) after Additional Heating at 180°C for 1 hr. KBr Pellet; 25°C. 56

17 Difference Spectra Obtained from Figure 16 by Subtracting the 1510 cm^{-1} Band to the Base Line 57

18 Infrared Spectrum of DGEBA 58

19 Infrared Spectrum of DGETBPP 59

20 Infrared Spectrum of DGETBBA 60

21 Infrared Spectrum of Phthalic Anhydride 61

22 Infrared Spectra of DGEBA/DGETBBA Cured with Phthalic Anhydride.
(A) after Curing at 120°C for 1 hr..
(B) after Additional Heating at 170°C for 25 min.,
(C) Cured Resin. KBr Pellet; 25°C. 63

23 Difference Spectra Obtained from Figure 22 by Subtracting the 1510 cm^{-1} Band to the Base Line 64

24 Infrared Spectra of Poly(Butylene terephthalate)/DGETBPP (A) Melt Mixture
(B) Sum Spectrum Constructed by a 0.5:1 Addition of the Individual Spectra of DGETBPP and Poly(Butylene terephthalate) 66

25 Difference Spectrum Obtained from Figure 24 by Subtracting the 1770 cm^{-1} Band to the Base Line 68

LIST OF FIGURES (Continued)

Figure No.		Page
26	NMR Chemical Shift Region for Different Functional Groups of Phenol-Formaldehyde Resins in Dilute Solutions in Acetone	72
27	NMR Spectra of Phenol-Formaldehyde Dimers	74
28	NMR Spectrum of Phenol-Formaldehyde Resin in d-Acetone	75
29	NMR Spectrum of p-Bromophenol-Formaldehyde Resin in d-Acetone	76
30	NMR Spectrum of m-Bromophenol-Formaldehyde Resin in d-Acetone.	77
31	NMR Spectrum of p-Chlorophenol-Formaldehyde Resin in d-Acetone	78
32	NMR Spectrum of m-Chlorophenol-Formaldehyde Resin in d-Acetone	79
33	NMR Spectrum of p-Cresol-Formaldehyde Resin in d-Acetone	80
34	NMR Spectrum of m-Cresol-Formaldehyde Resin in d-Acetone	81
35	NMR Spectra of an o-Chlorophenol-Formaldehyde Polymer (A) and the Corresponding Dehalogenated Polymer (B)	83
36	IR Spectra of (A) PF, and (B) X(C)pCPF	85
37	IR Spectra of (A) pCF, and (B) mCF	86
38	IR Spectra of (A) pBPF, and (B) mBPF	87
39	IR Spectra of (A) pCPF, and (B) mCPF	88
40	IR Spectra of (A) PF, (B) PF Cured with Formaldehyde, and (C) PF Cured with Terephthaloyl Chloride	90
41	Correlation of Oxygen Index and Char Yield of Phenolic Resins	98

LIST OF FIGURES (Concluded)

Figure No.		Page
42	IR Spectra of (A) X(T)mCPF, (B) X(F)mCPF, and (C) X(F)PF	102
43	UV Spectra of BPF-I in Methylene Chloride Solution before and after Irradiation for Different Periods of Time.	106
44	UV Spectra of BCF-I in Methylene Chloride Solution before and after Irradiation for Different Periods of Time.	107
45	UV Spectra of BDMPF-I in Methylene Chloride Solution before and after Irradiation for Different Periods of Time	108
46	Changes in Absorbance at 350 nm with Irradiation time : (A) BPF-I, (B) BCF-I, and (C) BDMPF-I	109
47	Infrared Spectra of (A) BPF-I, (B) BPF-I after 60 min. Irradiation and (C) Difference Spectrum B-A	111
48	Infrared Spectra of (A) BCF-I, (B) BCF-I after 60 min. Irradiation and (C) Difference Spectrum B-A	112
49	Infrared Spectra of (A) BDMPF-I, (B) BDMPF-I after 60 min. Irradiation and (C) Difference Spectrum B-A	113

ABBREVIATIONS

In addition to the common symbols and abbreviations, the following are designated for the various monomers and polymers.

DGEBA	Diglycidyl Ether of Bisphenol-A
DGETBBA	Diglycidyl Ether of Tetrabromobisphenol-A
DGEPP	Diglycidyl Ether of Phenolphthalein
DGETBPP	Diglycidyl Ether of Tetrabromophenolphthalein
PF	Oligomeric Phenol-Formaldehyde Resin
mCPF	Oligomeric meta-Chlorophenol-Formaldehyde Resin
mBPF	Oligomeric meta-Bromophenol-Formaldehyde Resin
mCF	Oligomeric meta-Cresol-Formaldehyde Resin
pCPF	Oligomeric para-Chlorophenol-Formaldehyde Resin
pBPF	Oligomeric para-Bromophenol-Formaldehyde Resin
pCF	Oligomeric para-Cresol-Formaldehyde Resin
X(F)-	Crosslinked with Formaldehyde
X(T)-	Crosslinked with s-Trioxane
X(C)-	Crosslinked with Terephthaloyl Chloride
BPF	9,9'-Bis(4-hydroxyphenyl)-fluorene
BPF-I	Polyisophthalate of BPF
BCF	9,9'-Biscresol-fluorene
BCF-I	Polyisophthalate of BCF
BDMPF	9,9'-Bis(3,5-dimethyl-4-hydroxyphenyl)fluoren
BDMPF-I	Polyisophthalate of BDMPF

1. INTRODUCTION

The growing use of polymers in a variety of applications has created a great deal of concern over their performance in many aspects including flammability and photostability.

The initial goals of the research in flammability are mainly focused on the flame retardation of polymers and not their flame proofing due to the balance of properties required in these systems. As a result, many flame retardants and flame retardant polymers have been and still are being developed.

Recent advances in space and other technologies have continued the development of high temperature resistant polymers. Theories and approaches in synthesizing these polymers are mainly based on structure-flammability relationships.

One objective of this work is to utilize the structural features of some high temperature polymers in designing new and better flame retardants. An attempt has also been made to introduce halogen systematically into the structure of high temperature phenol-formaldehyde resins and to study their flame retardation.

Developments in the area of organic photochemistry have given assistance to the interpretation of photodegradation processes and to the search for novel methods of stabilization. Consequently, many "tailor-made" stabilizers are being developed for specific polymers. However, the use of monomeric stabilizers has some critical limitations: (1) incompatibility with the polymers, (2) potential migration of the additives, (3) impairing the mechanical properties of the polymers, (4) extractability and "blooming".

Taking this into account, the sytheses of photo-resistant polymers have considerable interests. Stabilizing groups can be introduced into the polymer during the synthesis and function as internal stabilizers. In this study the nature of this type of stabilizing process in fluorene-based polyarylates has been investigated. The interpretations are based on the spectroscopic observations.

1.1 Elements in Flame Retardation

Upon examining the different means of achieving flame retardation, a number of guidelines have been established. The ideal flame-retardant polymer system should have (1) a high resistance to ignition and flame propagation, (2) reduced smoke generation and low toxicity of the combustion gases, (3) durability, (4) acceptibility in appearance and properties for specific end-uses, and (5) little or no economic penalty(1).

A brief anatomy of a combustion process can be shown by the following scheme:

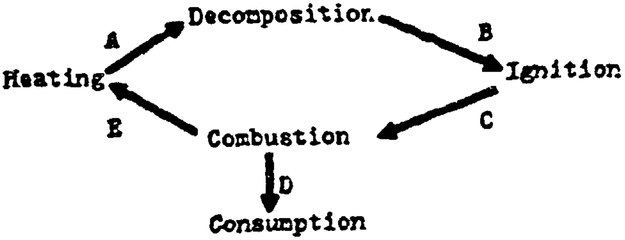

The burning of a polymer requires a heat source which causes degradation and decomposition of the polymer. Decomposition leads to the formation of various fragments which are susceptible to ignition and combustion. Heat generated from the combustion process supports further decomposition of the material. Flame retardation can be achieved by interrupting the burning process at one of the arrows shown in the scheme. At stage A decomposition of a polymer is usually initiated by oxidation resulting in the formation of active free radicals. This process can be interrupted by chain transfer agents, such as amines, phenols and halogen compounds. Materials used in stages B and C to prevent ignition and combustion usually are the chemicals which can develop noncombustible gases, such as H_2O, hydrogen halides, CO_2 and NH_3 when decomposed. These noncombustible gases may act as gas-phase diluents for the combustible decomposition products obtained from the polymer. In addition to being a gas-phase diluent, the water released from materials, such as $Al_2O_3 \cdot 3H_2O$ can also dissipate the heat generated at stage E and thus inhibit the burning process. There are materials which are active in the condensed phase to prevent ignition and combustion. Such materials can form nonvolatile char or glassy coatings which minimize the oxygen diffusion to the polymers and also reduce the heat transferred from the flame to the polymer(2).

There are many ways to measure the flammability of a material. A test that has been widely used on a laboratory scale in recent years since its initial development in 1966 is the Oxygen Index (OI) test(3). In the OI test, the material in the form of either a rod or a sheet is clamped vertically and ignited at the top, so that it burns in a candle-like manner in an upward-flowing mixture of oxygen and nitrogen. The oxygen concentration of the gas is then adjusted until the minimum level for sustained burning is reached. The OI is then defined as:

$$OI = (100 X [O_2])/([N_2] + [O_2])$$

where $[O_2]$ and $[N_2]$ are the volume concentrations of oxygen and nitrogen, respectively.

1.2 Structure-Flammability Relationship

A number of studies have been concerned with developing correlations between the structure of the polymers and their char formation. Char yield thus becomes an important measurement in flammability studies. It is defined as the char residue in weight % at 800°C in a Thermal Gravimetric Analysis under nitrogen atmosphere. Parker, *et al.*(4) have correlated char yield with the number of moles of multiple bonded aromatic rings per gram of polymers (Figure 1). Van Krevelen(5) has developed a linear relationship between char yields and oxygen indices of polymers (Figure 2) and a prediction of the amount of char yield from the number of aromatic units in the polymer. Besides aromatic structures, char formation can also be increased by introducing cyclic functional side groups (cardo groups) in the polymers. Such polymers are termed

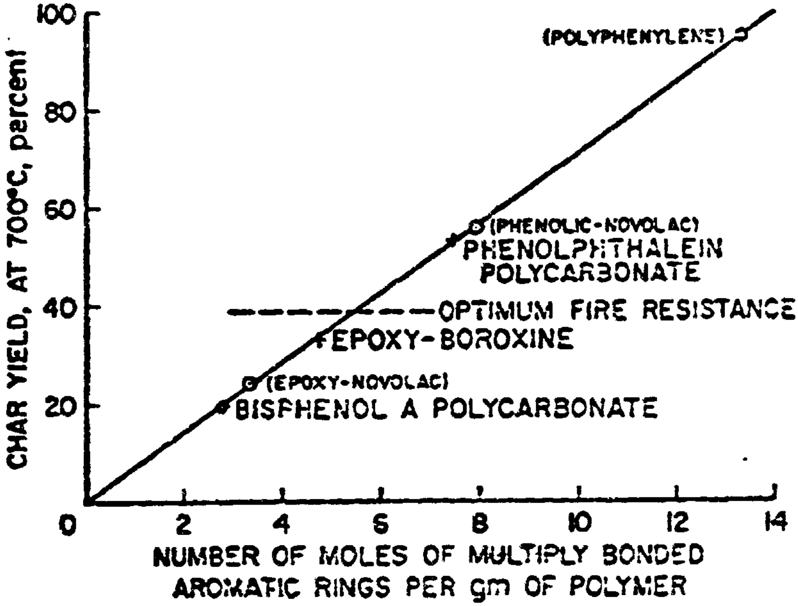

Figure 1: Effect of Aromatic Structure on Char Yield.

J. A. Parker, G. M. Fohlen, and P. M. Sawko, Paper Presented at Conference on Transparent Aircraft Enclosures, Las Vegas, Nevada, Feb. 5-8, 1973.

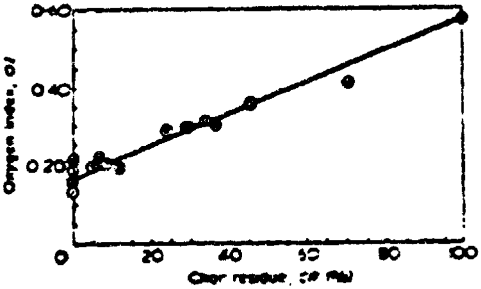

Figure 2 Correlation between *OI* and *CR* 1, Polyformaldehyde; 2, polyethylene, polypropylene; 3, polystyrene, polyisoprene; 4, nylon; 5, cellulose; 6, poly(vinyl alcohol); 7, PETP; 8, polyacrylonitrile; 9, PPO®; 10, polycarbonate; 11, Nomex®; 12, polysulphone; 13, Kynol®; 14, polyimide; 15, carbon

D. W. Van Krevelan, Polymer, 16, 615(1975).

"cardo polymers". These polymers have been the subject of an excellent review(6). Systematic studies on cardo polymers have begun with the syntheses of high molecular weight polyarylates from phenolphthalein and various dicarboxylic acids in 1961(7). So far numerous cardo polymers with various cardo groups (see below) have been synthesized.

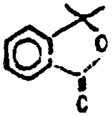

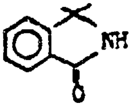

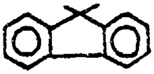

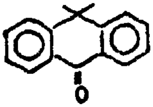

It has been found that the presence of cardo groups in different hetero- and cardo-chain polymers endows them with not only enhanced thermal stability but also excellent solubility, which is of particular importance in aromatic polymers with rigid chains.

1.3 Flame Retardant Additives

For the evaluation of specific contribution of cardo-group containing additives to the thermal behavior of polymers, a series of compounds based on the phthalide group have been synthesized. The effects of varying amounts of the phthalide additives on the flammability of bisphenol-A polycarbonate, poly(butylene terephthalate), and nylon 6,6 have been studied by thermal analytical techniques and Fourier Transform Infrared Spectroscopy (FT-IR).

Flame-retardant resins can also be used as the additives incorporated into nonhalogenated resins in order to impart some useful degree of flame retardancy to the material. One example is the use of tetrabromophthalic anhydride polyester resins in nonhalogenated polyester resins(8). Using a polymer resin as a flame-retardant additive has the advantage that the additive would not subsequently leach out of the system once the resin system is crosslinked. In addition it can be easily mixed with a polymer resin at a variety of levels depending on the degree of flame retardancy desired for a particular application.

The syntheses of flame retardant epoxy resins of tetrabromo- and tetrachloro-bisphenol-A have been reported in detail(9,10). The use of tetrabromobisphenol-A epoxy resin as an additive in the acrylonitrile-butadiene-styrene copolymer system(11) and polycarbonate system(12) has been reported in the literature. These halogenated resins, however, are too viscous for many applications(13). Cardo group containing epoxy resins, on the other hand, are mostly solid resins due to the fact that the cyclic side groups increase the glass transition temperature (T_g) of the polymer(14). The solid resins provide no unusual problems in sample handling and formulation.

The diglycidyl ether of 4,5,6,7-tetrabromophenolphthalein (DGETBPP) has been synthesized and copolymerized with the diglycidyl ether of bisphenol-A (DGEBA) and evaluated as an additive in poly(butylene terephthalate). The DGETBPP/DGEBA system actually forms a copolymer once the resin is cured by phthalic anhydride. The evaluation of the cured DGETBPP/DGEBA copolymer in terms of thermal properties is based on a comparison with the system using the diglycidyl ether of tetrabromobisphenol-A (DGETBBA).

The degree of curing has always been an important factor in determining the properties of the final products. It is also important to monitor the curing reaction in order to adjust the curing conditions. For this purpose FT-IR has been used to follow the curing reactions. In addition, the spectral subtraction routine is applied to the determination of the changes in chemical structures.

In the poly(butylene terephthalate) system the curing is caused by the interaction of the oxirane ring with the ester groups and proceeds by the mechanism of "insertion" of the fragment of the oxirane ring into the ester bond without scission of the molecular chain of the polyester(15). The effects of various amounts of DGETBBA and DGETBPP on char yield and oxygen index of poly(butylene terephthalate) are compared.

It is also interesting to know how much contribution to the flame retardancy is due to the presence of bromine in the resin. The diglycidyl ether of phenolphthalein has been synthesized and formulated in the same fashion as that of the brominated resins. The analysis of the results gives an evaluation of the effectiveness of bromine and cardo groups for flame retardation.

1.4 Modified and Flame Resistant Phenolic Resins

That phenols and formaldehyde react has been known as far back as 1872 by Bayer(16) and others. The substances obtained by these investigations were merely of theoretical interest and no attempt was made to utilize them commercially. With the advent of cheap commercial formaldehyde, Kleeberg(17) continued the investigation and obtained a cross-linked, insoluble resin by the reaction of an excess of formaldehyde in the presence of hydrochloric acid. Luft(18) was the first one to develop technical applications for curable phenolic resins. The process involved an acid catalyst, i.e., sulfuric acid, and a suitable solvent system, such as a mixture of formalin and glycerin. The resin was able to be molded or drawn into threads. In 1907 Baekeland applied for his "heat and pressure" patent(19) for the processing of phenol-formaldehyde resins. This technique made possible the worldwide application of phenolic resins.

The conditions, mainly pH and temperature, under which reactions of phenols with formaldehyde are carried out, have a profound influence on the character of the products obtained. Resol resins are the products of the reaction between phenol and an excess of formaldehyde (1:1.5-2) in the alkaline pH-range(20). Initially, phenoxide ions are formed from phenol under alkaline conditions. Delocalization of the electron pair on the oxygen ion results in increased electron densities at the o- and p-positions. This effect leads to substitution of phenol by electrophiles at the o- and p-positions. The first-step product, o- and p-methylolphenols (see below), are more reactive towards

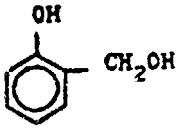

o-Hydroxymethylphenol

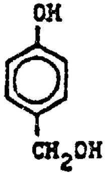

p-Hydroxymethylphenol

formaldehyde than the original phenol and rapidly undergo further substitution with the formation of di- and trimethylol derivatives (see below)(21).

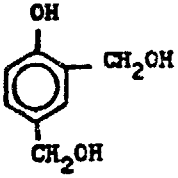

o,p-Dihydroxymethylphenol

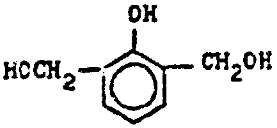

o,o'-Dihydroxymethylphenol

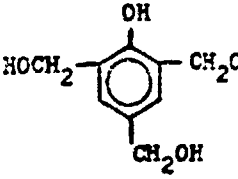

Trihydroxymethylphenol

The methylolphenols then undergo self-condensation to form dinuclear and polynuclear phenols in which the phenolic nuclei are linked by methylene groups. The crosslinked polymers are obtained simply by heating(22).

Novolak resins are normally prepared by the interaction of a molar excess of phenol with formaldehyde (1.25:1) under acidic conditions(23). In the first step, the formation of a hydroxymethylene carbonium ion from methylene glycol occurs:

$$\mathrm{HO{-}CH_2{-}OH} \xrightarrow{H^+} {}^+\mathrm{CH_2{-}OH} + \mathrm{H_2O}$$

The second step is the addition of the hydroxymethylene carbonium ion to phenol:

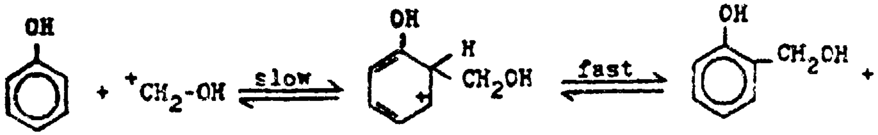

In the presence of acid the initial products, o- and p-methylolphenols, are present only transiently in very small concentrations. They are converted to benzylic carbonium ions which rapidly react with free phenol to form dihydroxydiphenylmethanes(24-26):

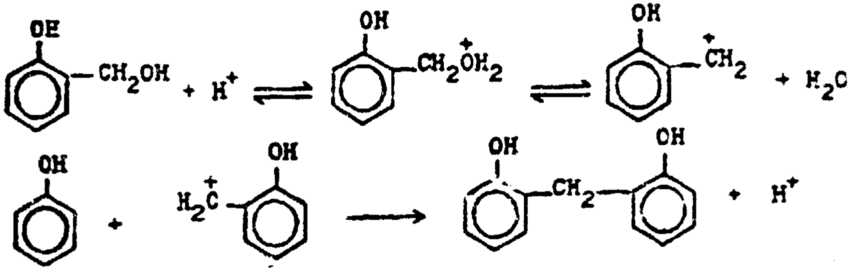

Polynuclear phenols are produced by further methylolation and methylene link formation. The final resin can be cured by the addition of a crosslinking agent.

Cured phenolic resins have good heat stability, resistance to most chemical reagents, and good mechanical properties. The principle uses include thermosetting molding powders, laminates, adhesives, binders and surface coatings. The highly crosslinked fiber named Kynol(27) has been developed from phenolic resins and is largely used in flame-proof apparel.

The thermo-oxidative resistance of phenolic resins can be further improved by chemical modifications. The following methods have been used(28),

1. Etherification or esterification of the phenolic hydroxyl groups,
2. Complex formation with polyvalent elements (Ca, Mg, Zn, Cd,···),
3. Replacement of the methylene linking groups by heteroatoms (O, S, N, Si,···).

The present study is initiated with a view to making modifications of the flammability behaviors of phenolic resin by using substituted phenols. Also, esterification of phenolic hydroxyl groups has been applied to the system by using terephthaloyl chloride as the curing agent. This makes possible the crosslinking of p-substituted phenolic resins. Modification by esterification has also been reported by Lei(29) in the synthesis of p-chlorophenolic fiber. The crosslinking of the fiber involves reactions between the hydroxyls and the diacid chloride.

1.5 Photo-Stability of Fluorene-Based Polyarylates

1.5.1 Basic Approaches

Polymers containing certain chromophores can absorb light followed by photochemical reactions which function as one mode for the dissipation of the absorbed energy. Such photochemical reactions have included the formation of free radicals, photoionizations, cyclizations, intramolecular rearrangements, and fragmentations.

Many polymers have been protected against photodegradation by the addition of stabilizers. These additives have been of two general types: light screens and ultraviolet (UV) absorbers. Light screens function either by absorbing damaging radiation before it reaches the polymer surface or by limiting its penetration into the polymer bulk. Coatings and pigments are classified as light screens. Carbon black is by far the most effective pigment. Its effectiveness can be attributed to a combination of being light screen and an absorber through energy dissipating mechanisms in its polynuclear aromatic structures(30). The UV absorbers functions by absorbing and dissipating UV irradiation through photo-physical processes. Most important is the internal conversion process which changes electronic energy into vibrational energy by a radiationless route without a change in spin multiplicity ($S_1 \longrightarrow S_0$, $S_2 \longrightarrow S_1$). It has been a major proposed mechanism for photostabilization by additives such as o-hydroxybenzophenones (I), o-hydroxyphenylbenzotriazoles (II), and salicylates (III)(31),

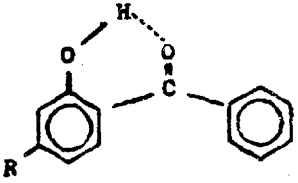

(I)

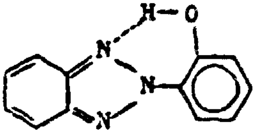

(II)

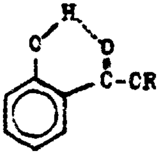

(III)

These compounds have a common structural feature, the intramolecular hydrogen bond. The photo-stabilization mechanism is considered to be the result of a rapid charge-transfer transition,

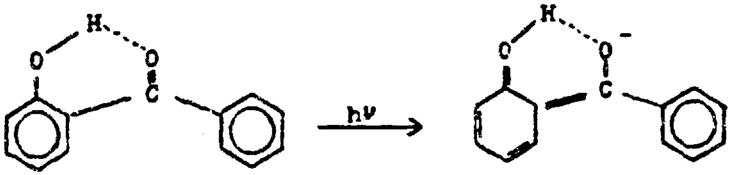

which may be facilitated by the strong intramolecular hydrogen bond(32,33).

The protective action has also been found in the case of resorcinol monobenzoate which is almost as effective as 2,4-dihydroxybenzophenone. The comparable effectiveness is due to the fact that resorcinol monobenzoate is converted by sunlight into 2,4-dihydroxybenzophenone by a photo-Fries rearrangement(34).

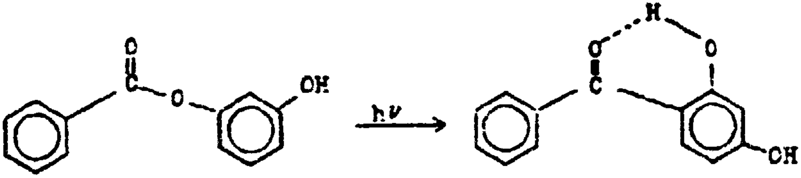

The photo-Fries rearrangement has been first reported by Anderson and Reese(35) in 1960. A simple example is the rearrangement of phenylacetate in ethanol to give o- and p-hydroxyacetophenones and phenol:

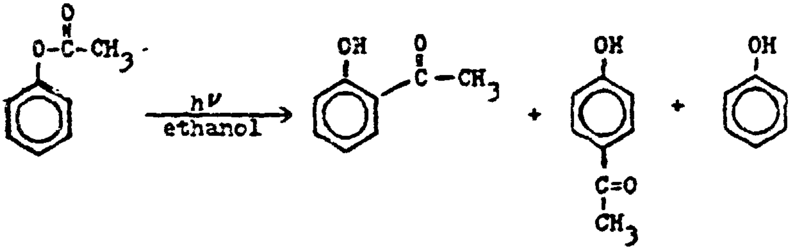

The rearrangement has been found to occur for many derivatives of phenol:phenyl esters(35-37), arylalkylcarbonates(38,39), phenoxyacetic acids(40), and hydroxyphenyl cinnamates(41). A recent review of the photo-Fries rearrangement has been published by Bellus(42).

Two mechanisms have been proposed for the photo-Fries rearrangement. Anderson and Reese(43) have suggested a "molecular" pathway, involving a bridged intermediate of type (I)

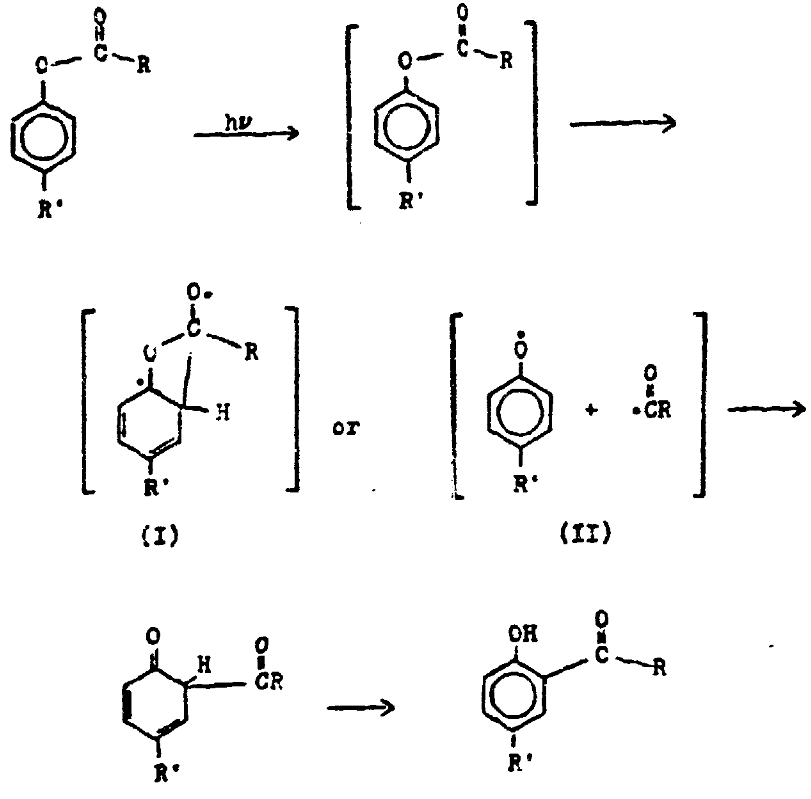

A similar intermediate is considered for the *para*-rearrangement. Kobsa(36) and Finnegan and Mattice(37) have proposed a "cage radical pair" intermediate (II), in which C-O homolysis is followed by the attack of the resulting acyl radical on the *ortho* or *para* position of the phenoxy radical with subsequent enolization.

1.5.2 Polymer Photo-Rearrangement

It has been demonstrated that many photochemical reactions shown by small organic molecules can be induced in polymers when the same chronophores are bonded to a polymer backbone(44). The rearrangement of poly(4,4'-diphenylol-propane isophthalate) to *o*-hydroxybenzophenone moieties can be taken as a typical representation of the photo-Fries rearrangement in a polymeric system(45).

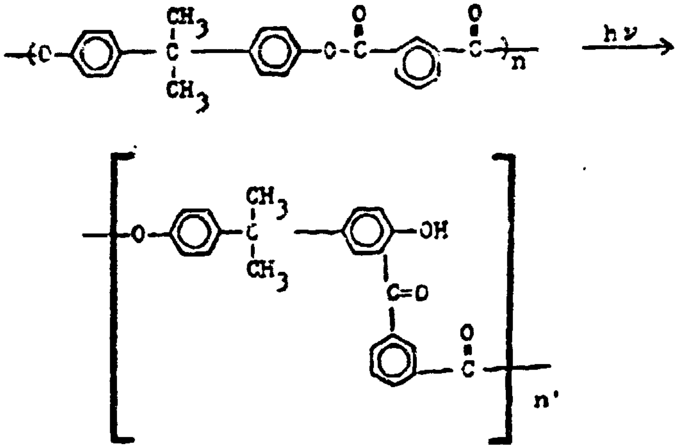

In the work of Cohen, Young and Markhart(46), the photo-Fries rearrangement products in poly(aryl esters) and Poly(aryl carbonates) are considered to be the internal UV stabilizer of the hydroxybenzophenone type. Korshak et al.(47) have also reported the synthesis of polymers capable of self-stabilization.

It is suggested that the rearranged polymer functions as a coating to prevent further deterioration of the polymer bulk.

In the present work we have investigated the chemical changes which occur during the UV irradiation of fluorene-based polyarylates. The derivatives of fluorene-based polyarylate substituted in the phenol ring ortho-positions by methyl groups have also been synthesized and studied. The results have provided an insight into the structural requirement for producing photo-Fries rearrangements in polymers.

2. EXPERIMENTAL

2.1 Standard Procedure for the Preparation of Phthalides

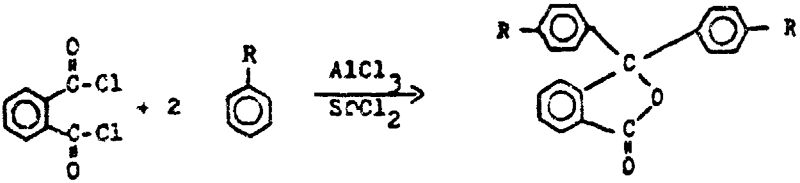

(R = Br, Cl, OH)

Phthalides prepared for the study include 3,3-bis(4-bromophenyl)phthalide, 3,3-bis(4-chlorophenyl)-phthalide, and phenolphthalein.

To a mixture of (0.25 mole) of phthaloyl chloride (Aldrich) and 78.5 g (1.50 mole) of bromobenzene (Aldrich), 16.7 g (0.125 mole) of anhydrous aluminum chloride (Fisher) is added in small portions. A few drops of thionyl chloride (Aldrich) are added as co-catalyst. The mixture is charged into a 500 ml round bottom flask connected with a reflux condenser and heated in an oil bath with stirring at 110°C for 24 hours. The reaction mixture is then steam distilled to remove the unreacted bromobenzene. The residue left in the flask is extracted with hot dilute hydrochloric acid to remove aluminum salts. The residue is then filtered and washed with dilute sodium chloride solution. The product is dissolved in hot acetone and decolorized over decolorizing carbon. One crystallization from acetone gives 96.5 g (87%) of fine light yellow crystals. Further purification gives white crystals, m.p. 184.5-185°C. IR: 1860 cm^{-1} (γ-lactone), 1080 cm^{-1} (BrC_6H_4-). TLC: one component.

Anal. *Calcd*. for $C_{20}H_{22}O_2Br_2$: C, 54.10; H, 2.71; Br, 36.02.
Found: C 54.25; H, 2.68; Br, 36.15.

3,3-Bis(4-chlorophenyl)phthalide

Yield : 90%
m.p. : 154.5-155°C. (Baeyer(96) reported 155-156°C)
IR : 1760 cm^{-1} (γ-lactone), 1096 cm^{-1} (ClC_4H_4-).
TLC : one component.

Anal. *Calcd*. for $C_{20}H_{22}O_2Cl_2$: C, 67.68; H, 3.38; Cl, 19.97.
Found: C, 67.33; H, 3.44; Cl, 19.74.

The same product was obtained in 84% yield by Blicke *et al*.(97) Bradlow *et al*.(98) reported the preparation of 3,3-bis(4-fluorophenyl)phthalide in 92% yield by the similar method. The *para*-isomers are considered to be the main products.(99)

2.2 Phthalides Used as Additive in Polymers

Bisphenol-A polycarbonate (Polysciences), Nylon 6,6 (Monsanto), and poly(butylene terephthalate) (AMP) are selecte for the study. Polymer films containing phthalides are cast from trifluoroacetic acid and dried at 25°C under vacuum.

Thermal Gravimetric Analysis (TGA) measurements of the resulting films are made under nitrogen using a Du Pont 99 Thermal Gravimetric Analyzer and 950 Thermal Analyzer. Oxygen indices are taken by using GeneralElectric CR 280 FM 11B Oxygen Index Flammability Gauge. Infrared spectrum of the gaseous products is taken on a Digilab FTS-20B Fourier Transform Spectrometer.

2.3 Standard Procedure for the Preparation of Epoxy Resins

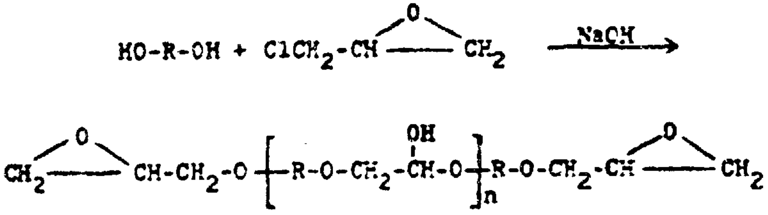

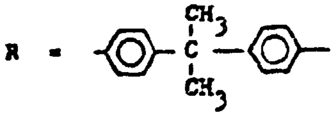

DGEBA

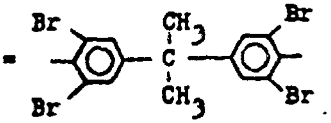

DGETBBA

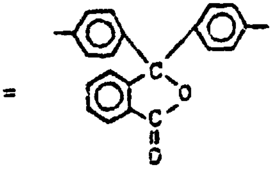

DGEPP

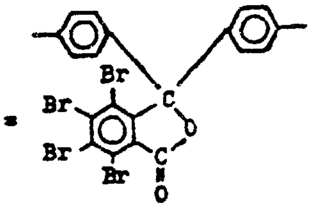

DGETBPP

2.3.1 Preparation of 4,5,6,7-Tetrabromophenolphthalei

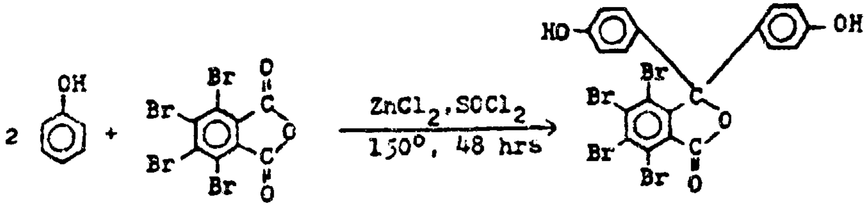

Approximately 29.5 g (6.35x10^{-2}mole) of tetrabromophthalic anhydride (Aldrich) is added to 46.6 g (0.5 mole) of purified phenol (Aldrich) in a 500 ml round bottom flask connected with a reflux condenser. To the mixture 10 g (0.07 mole) of zinc chloride and 1 ml of thionyl chloride are added. The flask containing the reaction mixture is then immersed in an oil-bath and heated to 150°C with stirring. Hydrogen chloride gas is evolved during the first few hours of reaction. After 48 hours the reaction mixture turns dark and viscous. The resulting mass is then steam distilled to remove excess phenol. The solid residue is collected and dissolved in a large amount of 2N sodium hydroxide solution. The solution is filtered through Celite and precipitated into a large amount of dilute hydrochloric acid solution. The precipitate is collected and washed with distilled water. The crude material is dissolved in acetone and decolorized over charcoal followed by reprecipitation in distilled water. Repeated recrystallizations from hot 95% alcohol are performed by careful saturation of the clear solution with distilled water. Colorless powders, m.p. 314°C (DSC) is obtained. The yield is over 90%.

Anal. Calcd. for $C_{20}H_{10}Br_4O_4$: C, 37.90; H, 1.59; Br, 50.42. Found: C, 37.78; H, 1.71; Br, 50.00.

The NMR spectrum shows a symmetrical AA'XX' pattern for the aromatic protons (see below), indicating that phenols are para-substituted.(100)

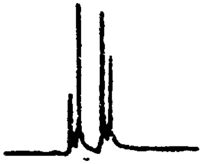

2.3.2 Epoxy Resin Preparation

To a 50 ml four-necked flask equipped with a stirrer, a thermometer, a dropping funnel, and a reflux condenser is added 28 g (4.4×10^{-2} mole) of 4,5,6,7-tetrabromophenolphthalein and 81.7 g (8.8×10^{-2} mole) of distilled epichlorohydr (Aldrich). The reaction mixture is heated with stirring to 80-90°C. The 40% NaOH solution (8.8×10^{-2} mole) is then added dropwise over a period of 30 minutes. The reaction mixture turns from deep purple to orange color in 2 hours. After another one hour the reaction mixture is cooled and filtered. The clear aqueous upper layer is siphoned off and the resin is slurried with 200 ml of distilled water. The mixture is heated at 60-80°C. After settling, the aqueous layer is again siphoned off. This washing procedure is repeated sever times until 100 ml of the wash water consumes less than 0.15 ml of 0.1 N HCl upon titration (indicator: Methyl Red). The resin is vacuum distilled at 120°C. The resin soldifies upon cooling. The solid resin is then dried at 100°C at reduced pressure overnight.

2.4 Characterization of Epoxy Resins

Diglycidyl Ester of Bisphenol-A (DGEBA)

This resin is characterized by using ASTM D-1652-73 method(48). The solid resin is heated to melt and filtered through glass wool. To a solution of 10 ml of 50 volume percent of chlorobenzene in chloroform, 0.5 g of the resin is added. The solution is stirred with a magnetic stirrer. Four drops of 0.1 percent of crystal violet (4,4',4"-methylidyne tris-(N,N-dimethyl-aniline)) solution in glacial acetic acid is used as the indicator. The solution is titrated with 0.1 N of hydrogen bromide in acetic acid (standardized by 0.4 g of potassium hydrogen phthalate). The solution turns from light green to red indicating the end-point.

$$\text{Weight per epoxide equivalent} = \frac{(W)(1000)}{(S-B)\ (N)}$$

W = Weight of sample
S = Milliliters of HBr used in titrating sample
B = Milliliters of HBr used in titrating blank
N = Normality of HBr.

The weight per epoxide equivalent of DGEBA is found to be 192 g.

Diglycidyl Ether of Phenolphthalein (DGEPP)

Weight per epoxide equivalent: 247.

Diglycidyl Ether of Tetrabromobisphenol-A (DGETBBA)

Weight per epoxide equivalent: 800.

Diglycidyl Ether of Tetrabromophenolphthalein (DGETBPP)

Determination of epoxy content of DGETBPP by ASTM method has failed to provide a reliable result due to the ambiguous end-point upon titration. Another procedure for determination of epoxide equivalent by the pyridinium chloride method(49) is used.

Exactly 0.317 g of epoxy resin is dissolved in 25 ml of 0.2 N pyridinium chloride-pyridine solution (16 ml conc. HCl per liter of pyridine) in a round bottom flask connected with a reflux condenser. The solution is heated to reflux with stirring for 25 minutes. After refluxing, the solution is cooled with the condenser in place. Fifty ml of methanol is added through the reflux condenser and let drain. The solution is then titrated with 0.5 N standardized methanolic NaOH to a pink end point of 15 drops of phenolphthalein.

$$\text{Weight per epoxide equivalent} = \frac{(16)(\text{sample weight, g})}{(\text{g of oxirane oxygen in sample})}$$

Grams of oxirane oxygen in sample = (A-B)(N)(0.016)

A = Milliliters of NaOH for blank
B = Milliliters of NaOH for sample
N = Normality of NaOH
0.016 = Milliequivalent weight of oxygen in grams.

The weight of resin per epoxide equivalent is found to be 537 g.

Anal. *Calcd.* for $C_{26}H_{18}O_6Br_4$: C, 41.86; H, 2.43; Br, 42.84; Molecular weight, 746. Found: C, 41.63;

H, 2.54; Br, 39.84; Average molecular weight, 805.

NMR (δ): 6.85-7.22 ppm (aromatic protons)
2.73-2.91 ppm ($-\overset{|}{C}H_2$)
3.23-3.35 ppm ($-CH-$)
3.64-4.28 ppm ($-OCH_2-$).

The DSC traces of the uncured resins (Figures 3-5) are taken on a DuPont 910 Differential Scanning Calorimeter and 1090 Thermal Analyzer. The absence of T_m in DGEPP and DGETBPP suggests that both resins are highly amorphous. The appearance of an endothermic glass transition in DGETBPP is due to the "hysteresis effects" caused by slow cooling (after vacuum-oven dried at 70°C) and subsequent fast heating (10°C/min temperature run).(101) The glass transition temperatures (T_g) of DGEBA and DGETBBA are resolved by quenching the samples at the molten state (T_m) followed by 10°C/min temperature runs. Crystallization of the samples does not occur fast enough at this heating rate to give endothermic melting curves. The melting peak of DGETBBA reappears after annealing the sample at 115°C for 12 hours.

2.5 Brominated Epoxy Resins Used as Commoners in the DGEBA System

Equal amounts of DGEBA and DGETBPP (or DGETBBA) are mixed at 120°C with a calculated amount of phthalic anhydride (0.6 equivalent per equivalent of epoxy group). The resin is initially maintained at 120°C for one hour and is then cured for 1-2 hours at 170°-180°C. The curing reaction is monitore by taking the sample out of the batch at the various stages o cure and examining the changes of absorbance in the IR spectr The cured resin is characterized by TGA and OI.

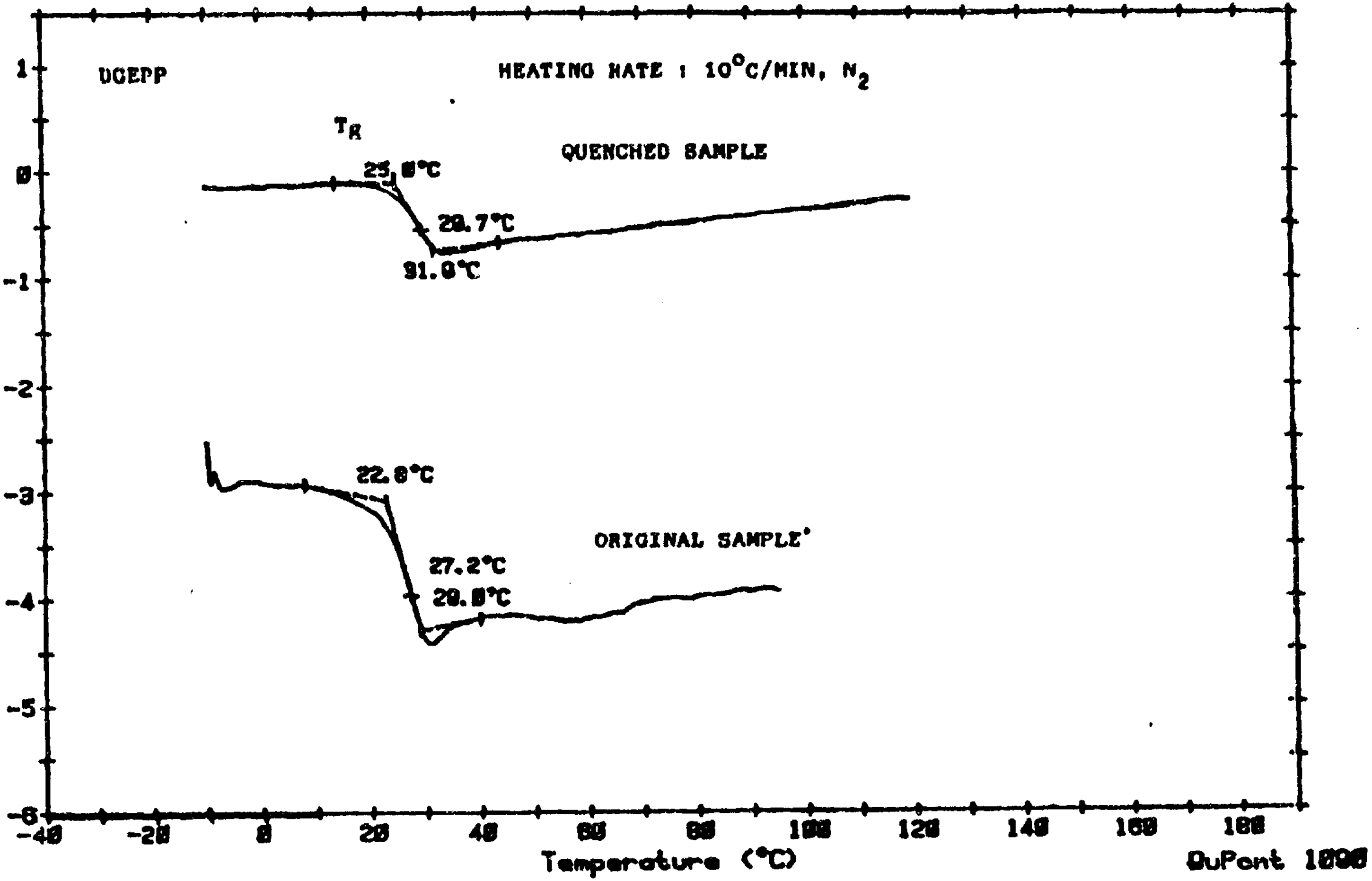

DSC Thermograms of DGEPP

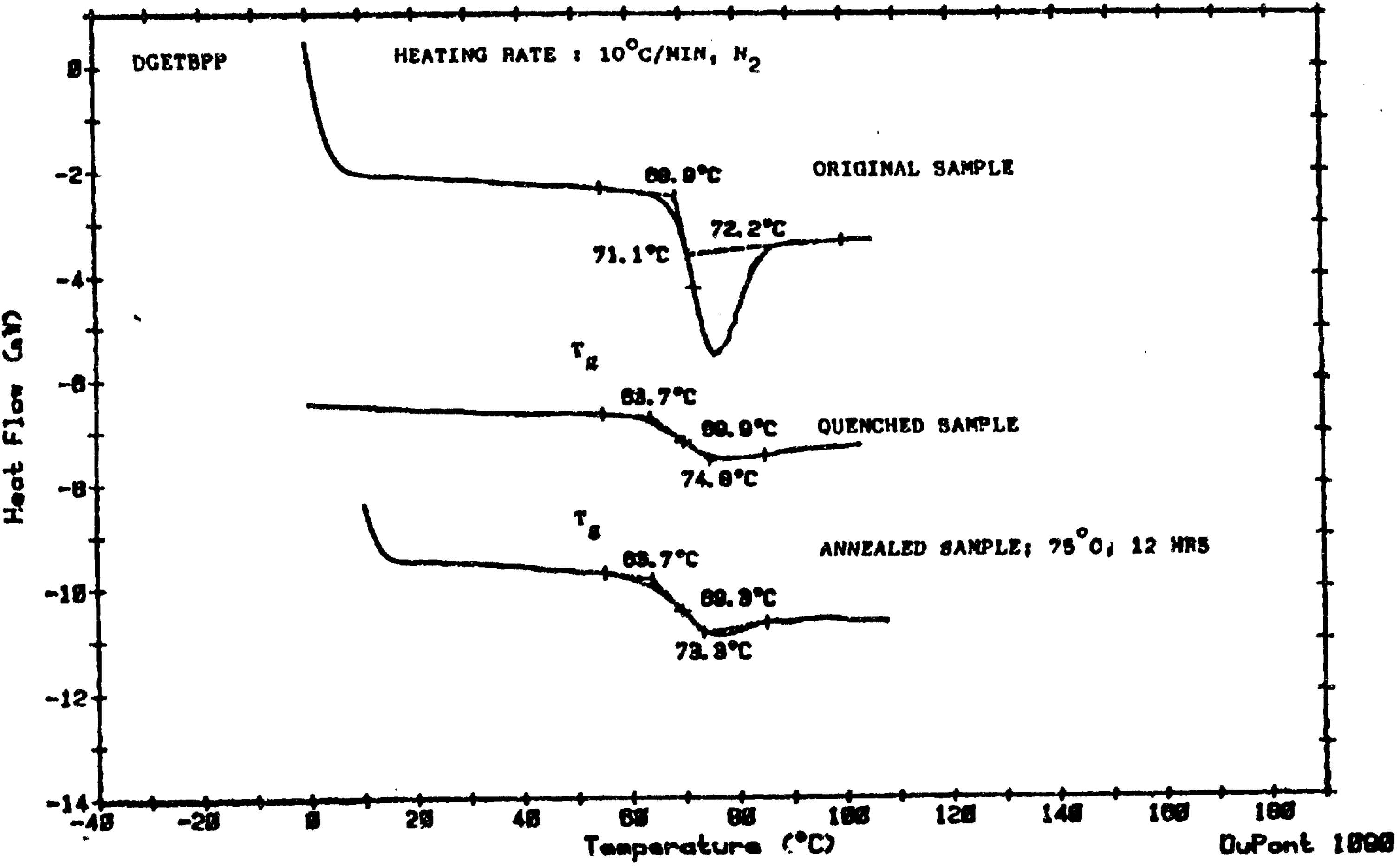

Figure 4: DSC Thermograms of DGETBPP.

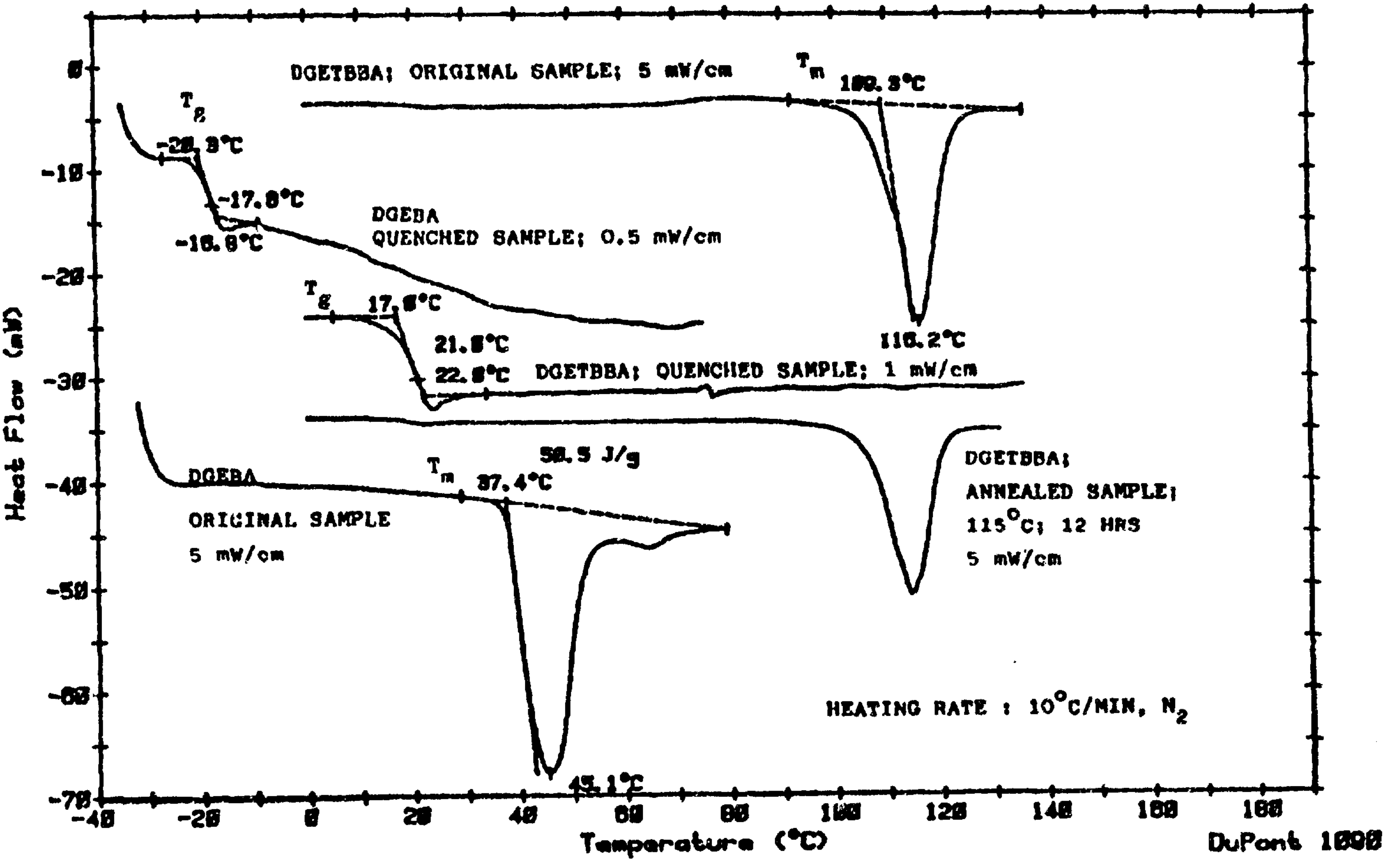

Figure 5: DSC Thermograms of DGETBBA and DGEBA.

2.6 Epoxy Resins/Poly(butylene terephthalate) System

Samples are prepared by mixing poly(butylene terephthalate) and the additive resins at the specified weight ratios and are melted with stirring in the aluminum dishes. Char yields and oxygen indices are taken. The reactions between DGETBPP and poly(butylene terephthalate) are followed by FT-IR. IR spectra are taken on the thin films of the samples coated on the aluminum plates using a Reflectance Attachment (Figure 6).

2.7 Standard Procedure for the Preparation of the Oligomeric Phenol-Formaldehyde Resins

The phenolic monomers used in the syntheses include phenol, m- and p-cresols, m- and p-chlorophenols, and m- and p-bromophenols.

One mole of phenolic monomer, 66.2 g (0.83 mole) of a 37.8% aqueous solution of formaldehyde, and 1.5 g of oxalic acid are reacted by refluxing at 95-97°C with stirring. The precipitation of the resin is observed during the reaction. Excess water and the unreacted phenolic monomer are removed by vacuum distillation. The solid resin is then dissolved in menthanol and precipitated in a large amount of acidified water (pH 3.4). Th precipitate is collected, washed with water, and dried under vacuum at room temperature. The resins are obtained in 80-95% yield.

2.8 Characterization of the Oligomeric Phenol-Formaldehyde Resins

The melting points of the resins are determined by DSC. The number-average molecular weights are determined by NMR

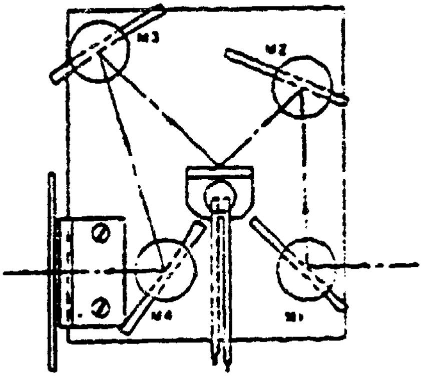

Figure 6: Schematic Diagram of Reflectance Attachment.

using a Varian HR/NTC TT-220 proton NMR spectrometer. The number of repeating units is calculated from the ratio of the total aromatic protons and the hydroxyl protons to the total number of methylene protons.

2.9 Standard Procedure for the Crosslinking of Phenol-Formaldehyde Resins

2.9.1 Crosslinking Through Ester Linkages with Terephthaloyl Chloride

To a resin kettle equipped with two dropping funnels and a mechanical stirrer is added 5.0 g of oligomeric resin (containing 2.7-4.8x10^{-2}mole of phenolic hydroxyls) in 300 ml acetone (Aldrich, distilled). Excess (9.6 g, 4.7x10^{-2} mole) of terephthaloyl chloride (Aldrich, recrystallized fro hexane) in 100 ml acetone is slowly charged into the solutio Simultaneously triethylamine (9.6 g, 9.5x10^{-2}mole) is added dropwise into the reaction mixture over a period of 15 minutes. The reaction is kept at room temperature for 12 hours. At the end of the reaction the crosslinked resin precipitates from the solution. The product is washed successively with acetone, distilled water, dilute ammonium hydroxide solution, distilled water, dilute oxalic acid solution, water, and acetone. The final resin is then dried under reduced pressure.

2.9.2 Crosslinking Through Methylene Linkages

2.9.2.1 Crosslinking with s-Trioxane

To a resin kettle is added a solution of 5.0 g of oligomeric resin, a large excess (36.0 g, 0.4 mole) of s-trioxane, and 3.0 g of p-toluenesulfonic acid in 200 ml of bis(2-ethoxyethyl) ether. The solution is heated at 95-100°C with stirring for 48 hours. The cured resin is washed with distilled water and methanol, and dried under reduced pressure.

2.9.2.2 Crosslinking with Formaldehyde

To a resin kettle is added 5.0 g oligomeric resin, 200 g of 37.8% formaldehyde, and 3.0 g of p-toluenesulfonic acid. The mixture is heated to 92-94°C and refluxed with stirring for 5 hours. The cured resin is then washed with distilled water and methanol.

2.10 Characterization of Cured Phenol-Formaldehyde Resins

Selected samples of cured resins are analyzed by FT-IR. Thermal properties are determined by TGA and OI.

2.11 Preparation of Fluorene-Based Polyarylates

2.11.1 Preparation of Bisphenols

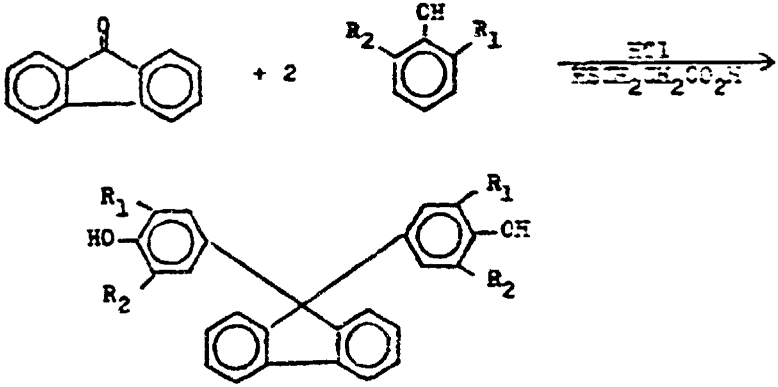

1. 9.9'-Bis(4-hydroxyphenyl)fluorene (BPF), $R_1 = R_2 = H$
2. 9.9'-Biscresol fluorene (BCF), $R_1 = CH_3$, $R_2 = H$
3. 9.9'-Bis(3,5-dimethyl-4-hydroxyphenyl)fluorene (BDMPF

$R_1 = R_2 = CH_3$

Bisphenols are prepared by following Morgan's(50) procedure. Excess phenol, cresol and 2,6-dimethylphenol are used in the condensation reaction with fluorenone. A small amount of mercaptoacetic acid is used as co-catalyst. Dry hydrogen chloride is bubbled through the reaction mixture for 20 minutes while the reaction is kept at 140°-150°C. At the end of the reaction the viscose mass is washed with hot water several times and dissolved in NaOH solution. The product is obtained by titrating with concentrate HCl. One recrystallization from toluene gives white crystals.

BPF: m.p. 224°-225°C, yield 56%.

Anal. Calcd. for $C_{25}H_{18}O_2$: C, 85.71; H, 5.1; Found: C, 85.62; H, 5.21.

NMR (δ): 6.78 ppm (phenolic protons)
7.10-7.80 ppm (fluorenyl protons)
8.10 ppm (hydroxyl protons)

BCF: m.p. 110°-111°C, yield 70%.

Anal. Calcd. for $C_{27}H_{22}O_2$: C, 85.7; H, 5.8%; Found: C, 85.2; H, 5.43.

BDMPF: m.p. 271-272°C, yield 35%

Anal. Calcd. for $C_{27}H_{26}O_2$: C, 85.71; H, 6.40; Found: C, 85.52; H, 6.26.

NMR (δ): 2.13 (methyl protons)
6.73 (phenolic protons)
7.10-7.72 (fluorenyl protons).

2.11.2 Preparation of Polymers

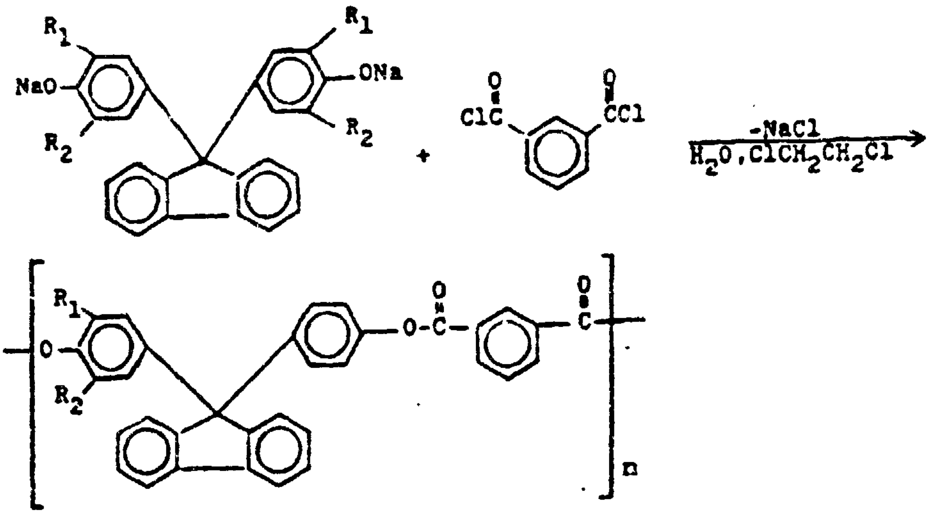

1. Polyisophthalate of 9,9'-bis(4-hydroxyphenyl)-fluorene (BPF-I); $R_1 = R_2 = H$
2. Polyisophthalate of 9,9'-biscresol fluorene (BCF-I); $R_1 = CH_3$; $R_2 = H$
3. Polyisophthalate of 9,9'-bis(3,5-dimethyl-4-hydroxyphenyl)fluorene (BDMPF-I); $R_1 = R_2 = CH_3$.

The polyarylates are synthesized by interfacial polycondensation using the procedure similar to that for the polyterephthalate of 9,9'-bis(4-hydroxyphenyl)fluorene. For a typical run, 3.5 g (0.01 mole) of BPF, 1.6 g (0.04 mole) of sodium hydroxide and 2.1 g (0.01 mole) of tetraethylammonium bromide are dispersed in 120 ml of water in a blender. To this mixture is added quickly with vigorous stirring 2.03 g (0.01 mole) of isophthaloyl chloride in 30 ml of 1,2-dichloroethane. After stirring for 3 minutes, the addition of 200 ml of n-hexane is made. The separated polymer is collected, washed with water and dried. The product is redissolved in methylene chloride and precipitated in 500 ml methanol to yield 4.0 g (95%) of polymer.

BPF-I

Anal. Calcd. for $C_{33}H_{20}C_4$: C, 82.50; H, 4.17; Found: C, 83.79; H, 4.76.

η_{inh} : 0.91 (0.45 g/dl, methyl chloride, 25°C)
T_g : 265°C
T_d : 500°C
Char yield, 800°C : 59%
OI : 37.

BCF-I

Anal. Calcd. for $C_{35}H_{24}O_4$: C, 80.6; H, 4.72; Found: C, 82.6; H, 4.76.

η_{inh} : 0.25 (0.45 g/dl, methylene chloride, 25°C)
T_g : 287°C
T_d : 520°C
Char yield, 800°C: 40%
OI : 36.

BDMPF-I

Anal. Calcd. for $C_{37}H_{28}O_4$: C, 82.84; H, 5.22; Found: C, 79.77; H, 5.36.

η_{inh} : 0.85 (0.45 g/dl, methylene chloride, 25°C)
T_g : 315°C
T_d : 510°C
Char yield, 800°C: 34%
OI : 35.

2.12 Studies of Photo-Fries Rearrangement

2.12.1 Irradiation Chamber

The equipment for photo-Fries rearrangement consists of a power source (Hanovia 27801), an ultraviolet light source (Mercury-Xenon Compact Arc Lamp, Hanovia 508B0090) with 1000 watts of power and a lamp housing system (Schoeffel Instrument Co., LH 152 N Lamp Housing).

2.12.2 UV Spectroscopic Studies

Polymer samples are dissolved in methylene chloride (Aldrich, distilled) to make 6.0×10^{-4} M solutions. After the initial UV-Visible spectra are taken the quartz curvettes containing the sample solutions are then placed in the irradiation chamber for irradiation. Spectra are taken after certain periods of irradiation time.

2.12.3 FT-IR Spectroscopic Studies

The aluminum plates coated with polymer films are subjected to UV irradiation. Infrared spectra are taken before and after irradiation, using Reflectance Attachment.

3. RESULTS AND DISCUSSION

3.1 Flame Retardants Containing Loop Functionality

3.1.1 Effects of Phthalides on Thermal Properties of Polymers

3.1.1.1 Bisphenol-A Polycarbonate System

Table 1 summarizes the valuesof char yield and oxygen index for all the polymer samples incorporated with different amounts of additives. Bisphenol-A polycarbonate containing phthalide additives show slight weight changes in TGA at 800°C as compared to the polymer without the additives. The amount of weight change actually corresponds to the amount of additives incorporated into the polymers indicating the additives are not active in the condensed phase. The TGA curves (Figures 7-9) show two areas of weight losses corresponding to the evaporation of phthalides and the decomposition of the polymers (discussed later). A plot of oxygen index as a function of the percentage of three different phthalide additives in bisphenol-A polycarbonate is illustrated in Figure 10 . The substituted bisphenyl phthalides are found to increase the oxygen index in a linear fashion with increasing weight % of the additives. In substituted phenylphthalides the relative order of effectiveness is Br > Cl > CH_3, based on the slope of the plot.

Although a large body of research into the mechanism of halogen fire retardants have been reported, considerable uncertainty remains concerning the relative importance of

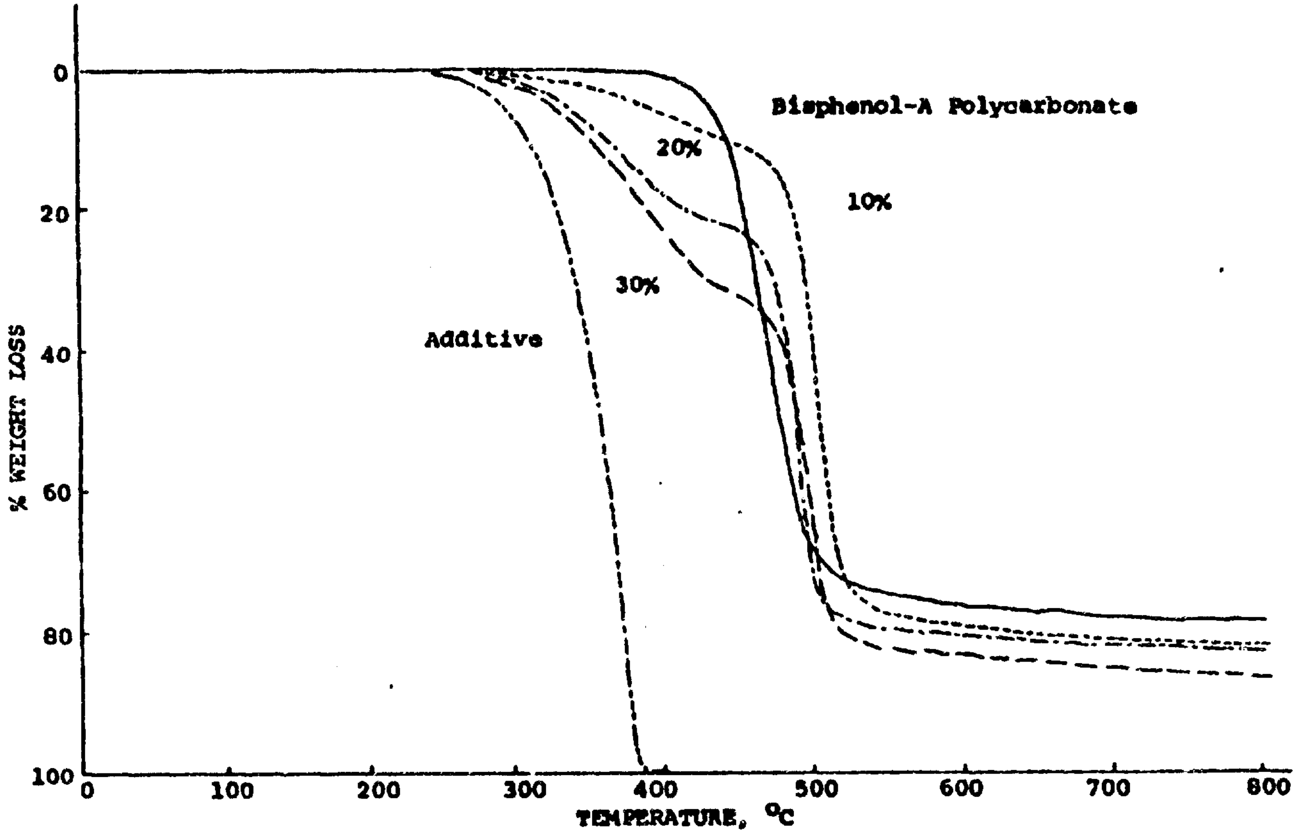

Figure 7: Effect of 3,3-bis(4-Bromophenyl)phthalide Additive upon Char Yield of Bisphenol-A Polycarbonate as Measured by TGA at 10°C/min under N_2.

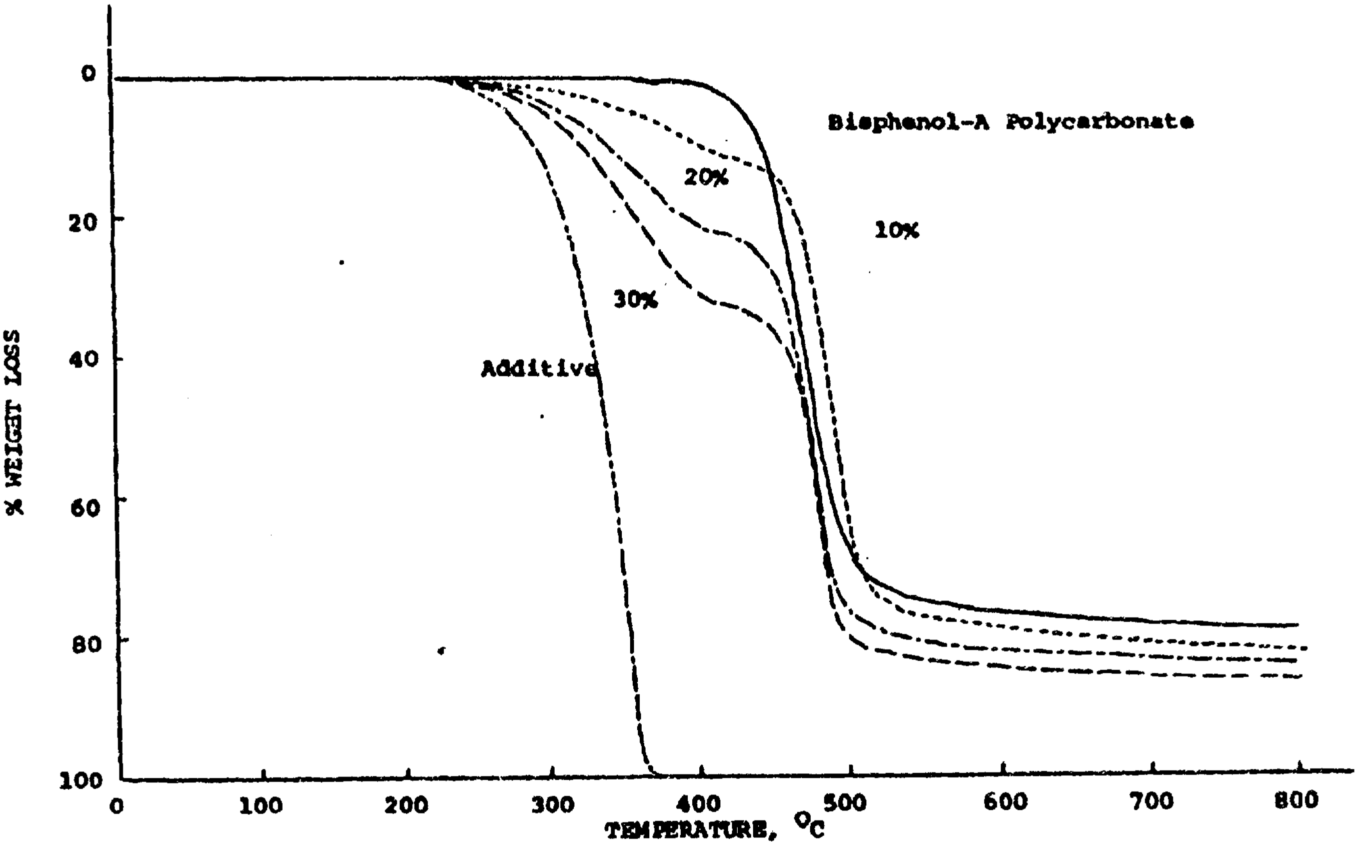

Figure 8: Effect of 3,3-bis(4-Chlorophenyl)phthalide Additive upon Char Yield of Bisphenol-A Polycarbonate as Measured by TGA at 10°C/min under N_2.

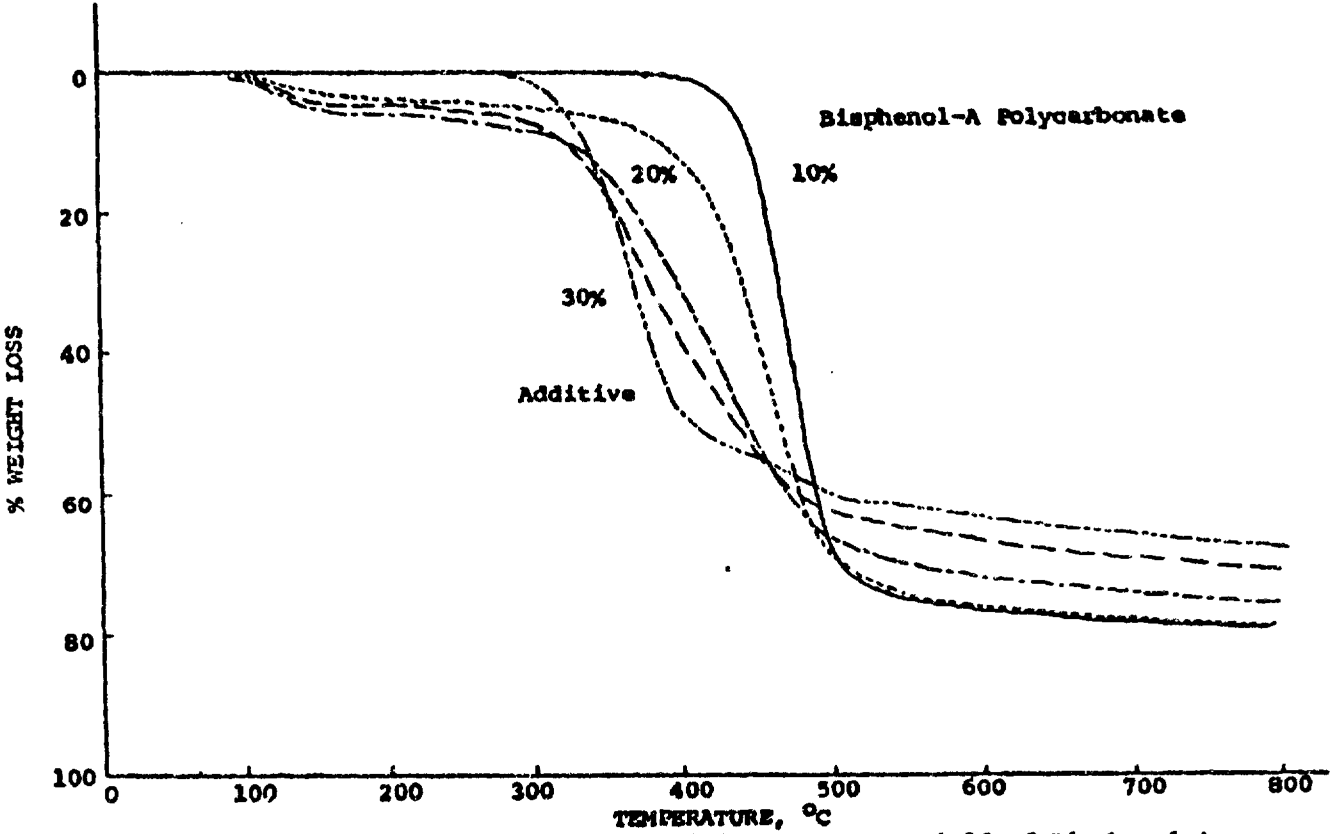

Figure 9: Effect of Phenolphthalein Additive upon Char Yield of Bisphenol-A Polycarbonate as Measured by TGA at 10°C/min under N_2.

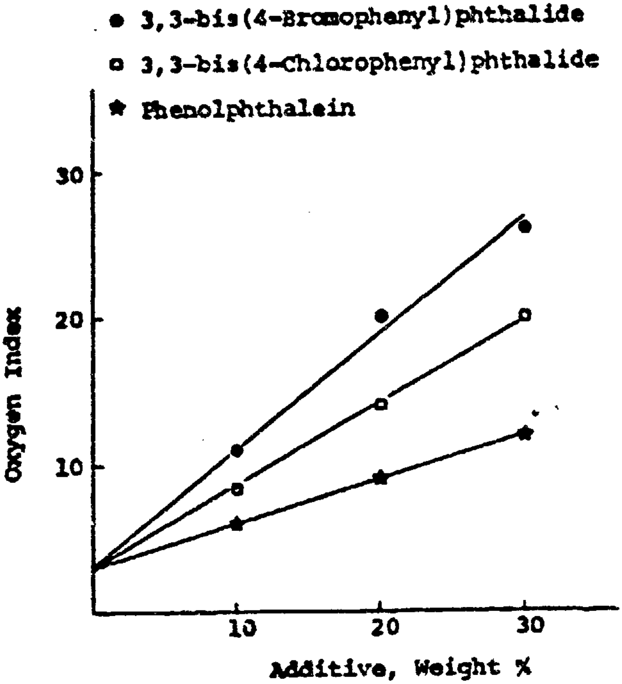

Figure 10: Relationship of Oxygen Index with Additive Content in Bisphenol-A Polycarbonate.

hydrogen halide gas versus free radical reactions. The role of hydrogen halide as the primary inhibiting species in gas-phase reactions is supported by the fact that the inhibiting effect (as measured by the flame velocity) of bromine (Br_2) and chlorine (Cl_2) in a carbon monoxide-oxygen flame can be increased by the addition of hydrogen (H_2)(51,50). The halogens are considered to be dissociated or converted to HX molecules. The diatomic halogen molecule is hence not expected to be the inhibitor, but rather the halogen atom or HX molecules(56). Nevertheless, Fenimore and Martin (53) have found that the injection of hydrogen chloride or chlorine into the oxygen-nitrogen mixture used in their oxygen index measurements has little or no effect upon oxygen index. The inhibiting effect is found only when chlorine is substituted in the polymer. The halogen flame inhibition can not be considered to be only due to the blanketing and cooling actions of the gases evolved since certain halogen containing materials are much more effective than inert gases such as carbon dioxide and nitrogen(54). Therefore, the actions of halogenated fire retardants are mainly chemical in nature. The mechanisms associated with polymer combustion and its suppression has been reviewed by Warren(55). Rosser et al.(57) have proposed a mechanism for the suppression of the gas-phase radical reactions. It consists of the replacement of the radical chain carriers by less reactive halogen atoms (X·):

$$\begin{aligned} HR + X\cdot &\longrightarrow HX + R\cdot \\ H\cdot + HX &\longrightarrow X\cdot + H_2 \\ OH\cdot + HX &\longrightarrow X\cdot + H_2O \end{aligned}$$

where HR represents the fuel or other hydrogen containing species. The substitution of X for H and OH results in a reduction of diffusion of such species and the possible exothermic propagation reaction:

$$OH\cdot + CO \longrightarrow H\cdot + CO_2$$

and chain branching reactions:

$$\begin{aligned} H\cdot + O_2 &\longrightarrow OH\cdot + O\cdot \\ H_2 + O\cdot &\longrightarrow OH\cdot + H\cdot\,. \end{aligned}$$

Creitz(58) has indicated, however, that the halogen acids might not be the primary inhibiting species based on the experimental results that the inhibitor (HX), when added to the fuel, is little more effective than the equivalent amount of nitrogen(59). It appears that the halogen acids can not survive under the oxidizing conditions in the reaction zone. It is more likely that the inhibition takes place in the oxygen-rich, recombination region which is out side of the reaction zone of a diffusion flame. Removal of the active oxygen atoms accounts for the inhibition effect according to the following mechanisms.

$$\begin{aligned} O\cdot + X\cdot + M &\longrightarrow OX + M^{*} \\ O\cdot + X_2 &\longrightarrow XO\cdot + X\cdot \\ O\cdot + OX\cdot &\longrightarrow X\cdot + O_2 \\ XO\cdot + \cdot OH &\longrightarrow HX + O_2\,. \end{aligned}$$

The relative effectiveness of the various halogens as flame inhibitors has been found to be directly proportional to their atomic weights, i.e., F:Cl:Br:I = 1.0:1.9:4.2:6.7(60). Perhaps the differences in efficiency among the halogens can be explained by the differences in bond energy(61) (C-X bond energy in Kcal/mole: C-F, 107.0; C-Cl, 66.5; C-Br, 54.0; and C-I, 56.5).

Infrared spectra (Figure 11) of the pyrolysis gases from the TGA experiment on bisphenol-A polycarbonate containing chlorophthalide show a trace of HCl formation at the early stages of heating. The weight loss in the range of 300°-400°C (Figure 8) may be due to the evaporation of the additives.

The chemistry of additive phenolphthalein in bisphenol-A polycarbonate involves reactions taking place at 160°-180°C. This is clearly shown by the Differential Scanning Calorimetry (DSC) thermogram (Figure 12) of the sample. The weight loss starting from 120°C in TGA thermogram (Figure 9) may be due to the evaporation of water which is proposed to be one of the possible products of the following reactions:

$$R_1OH \longrightarrow R_1\cdot + \cdot OH$$

$$\cdot OH + R_2H \longrightarrow H_2O + R_2\cdot$$

(R_1OH: phenolphthalein; R_2H: polymer)

Consequently phenolphthalein changes the mechanisms of pyrolytic degradation of the polymer and alters fuel production process resulting in flame retardation.

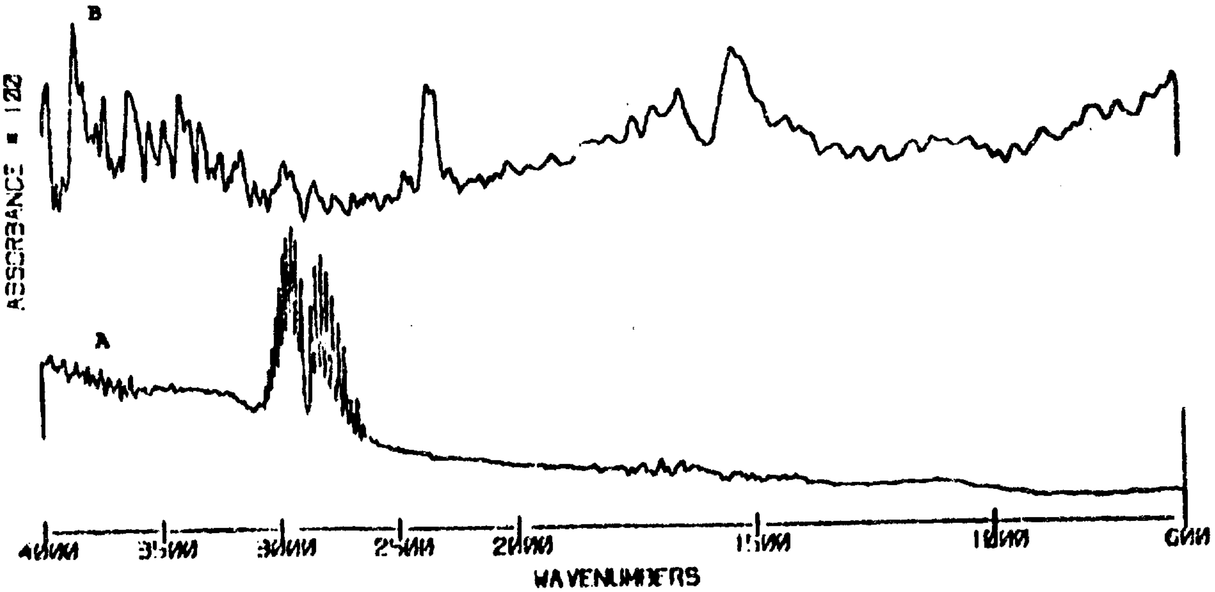

Figure 11: Infrared Spectra of HCl (A) and the Gases evolved between 300°-400°C in a TGA Measurement of Bisphenol-A Polycarbonate Containing 30% 3,3-bis (4-Chlorophenyl)phthalide (B). IR Gas Cell; 25°C.

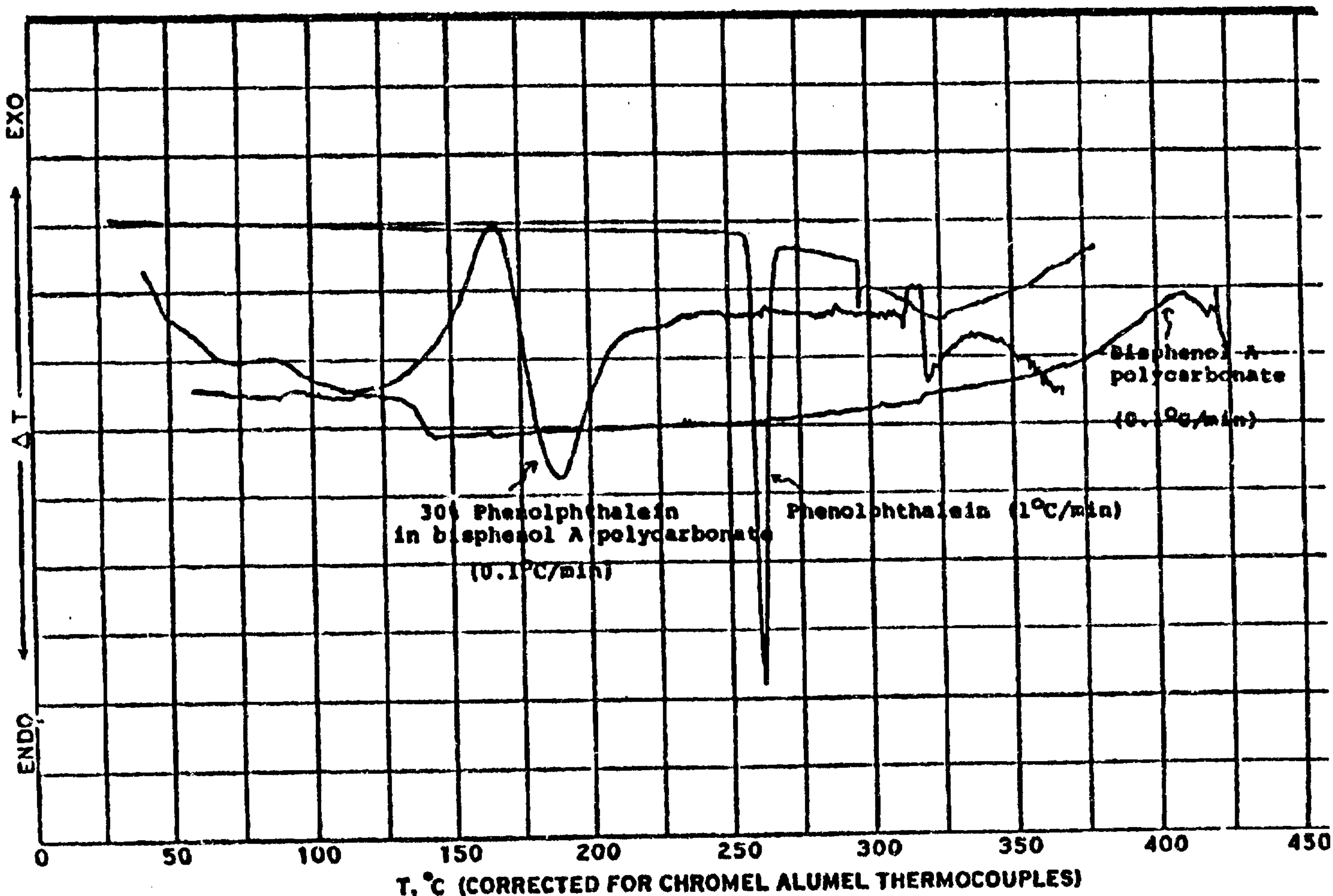
EXO
ΔT
ENDO
0
50
100
150
200
250
300
350
400
450
T, °C (CORRECTED FOR CHROMEL ALUMEL THERMOCOUPLES)
30% Phenolphthalein
in bisphenol A polycarbonate
(0.1°C/min)
Phenolphthalein (1°C/min)
Bisphenol A
polycarbonate
(0.1°C/min)

3.1.1.2 Poly(butylene terephthalate) and Nylon 6.6 Systems

The bromophthalide additive in poly(butylene terephthalate) leads to an increase in char yield and an increase in oxygen index as indicated in Table 1. The condensed phase activity can be attributed to the loss of bromine and the crosslinking of the aromatic rings of the additive and the polymer by free-radical coupling reactions:

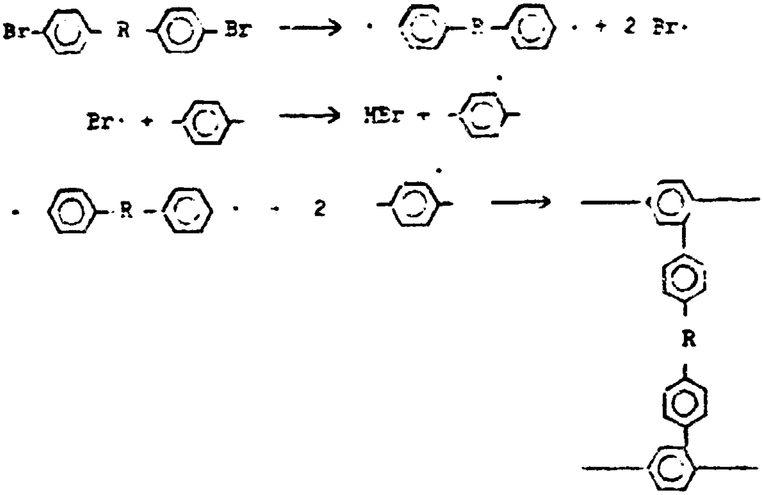

Nylon 6.6 does not provide crosslinking sites resulting in an unchanged char yield.

The char forming activity is reduced due to the evaporation of the additive in the 200°-350°C range as indicated in Figures 13 and 14. This result leads to an

Table 1.

Thermal Analytical Data of Polymers Containing Phthalide Additives

Polymer	Additive(a)	Parts by Wt. %	Char Yield % at $800^{\circ}C.N_2$	Oxygen Index,%
Bisphenol-A Poly-carbonate	None	-	20.7	21.5
	3,3-bis(4-Bromo-phenyl)-phthalide	10	17.7	25.5
		20	17.0	30.0
		30	13.3	33.0
	3,3-bis(4-Chloro-phenyl)-phthalide	10	17.3	24.3
		20	15.8	27.0
		30	13.6	30.0
	Phenol-phthalein	10	21.0	23.0
		20	24.4	24.5
		30	29.0	26.0
PBT	None		1.1	23.0
	3,3-bis(4-Bromo-phenyl)-phthalide	30	2.6	31.0
Nylon 6.6	None	-	5.9	24.0
	3,3-bis(4-Bromo-phenyl)-phthalide	30	6.1	32.0

(a) 3,3-bis(4-bromophenyl)-phthalide

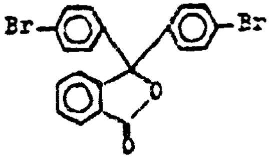

3,3-bis(4-Chlorophenyl)-phthalide

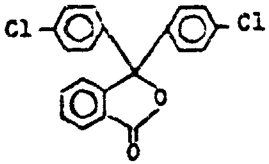

Phenolphthalein

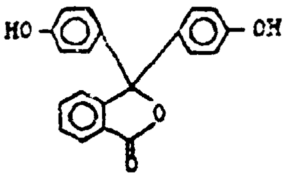

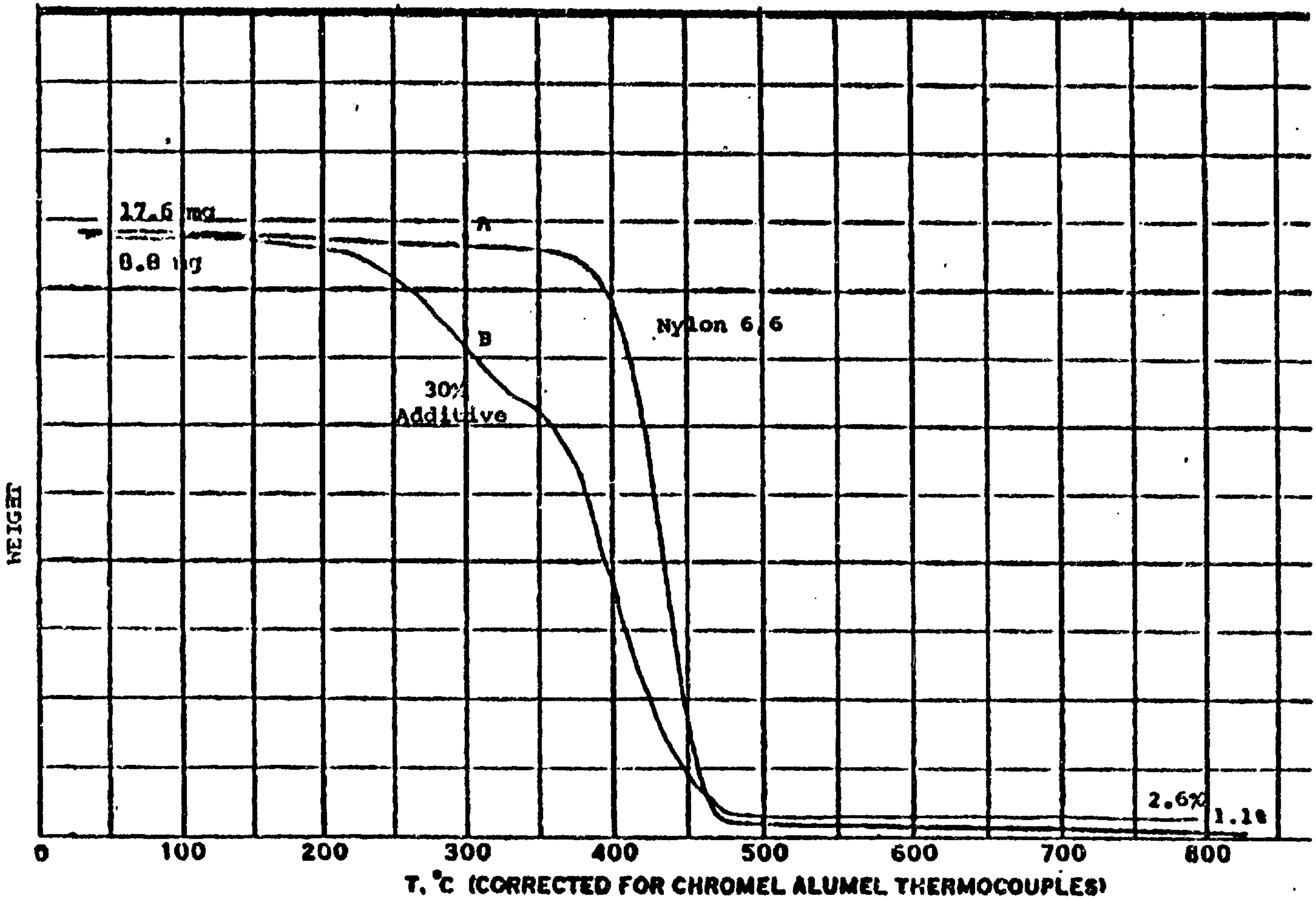

Figure 13: Effect of 30% of 3,3-bis(4-Bromophenyl)phthalide on Char Yield of

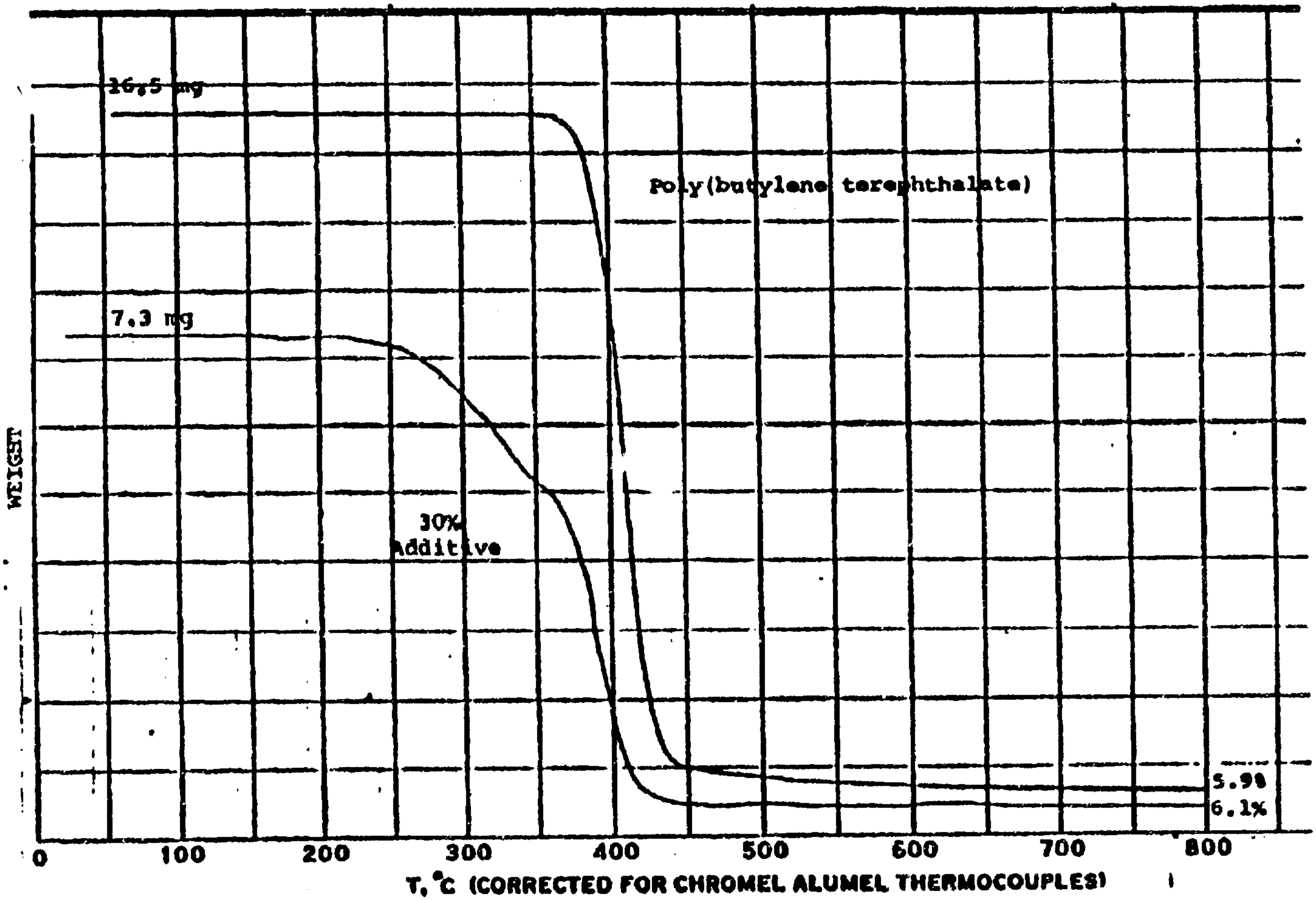

Figure 14: Effect of 30% of 3,3-bis(4-Bromophenyl)phthalide on Char Yield of

expectation that less volatile material such as an oligomeric additive should retain its effectiveness at high temperature. In the later sections it will be demonstrated that a high degree of char forming ability will result with the incorporation of an epoxy resin additive.

3.1.2 Effects of Phthalide Containing Epoxy Resins on the Thermal Properties of Polymers

3.1.2.1 Epoxy Copolymer Resins

Summaries of the thermal analytical data of the phthalic anhydride cured DGEBA, DGEBA/DGETBBA, and DGEBA/DGETBPP resins are shown in Table 2. The presence of DGETBBA in DGEBA leads to an increase of char yield from 7.3% to 13.6% and an increase of oxygen index from 21 to 31. The TGA thermograms in Figure 15 show no sign of the evaporation of the additives. The char formation mechanism is similar to the one described previously. The increase of char formation has been observed in other halogenated polymer systems such as styrene-vinyl benzyl chloride copolymers(60) and chlorine-substituted aromatic polyamides(61). In these systems the cleavage of the $C_{aromatic}$-Cl bond enchances the c linking of the aromatic rings.

The replacement of DGETBBA by DGETBPP in the copolymer resin leads to another increase in char yield from 13.6% to 22% and an increase in oxygen index from 31 to 34, suggesting that the loop functionality of DGETBPP contributes to char formation and overall flame retardancy of the resin.

Table 2.

Thermal Analytical Data of Epoxy Resins

Resin[a]	Bromine Content,%	Char Yield,% at 800°C, N_2	OI
DGEBA	0	7.3	21
DGEBA/DGETBEA	45	13.6	31
DGEBA/DGETBPP	50	22.0	34

(a) Cured with phthalic anhydride.

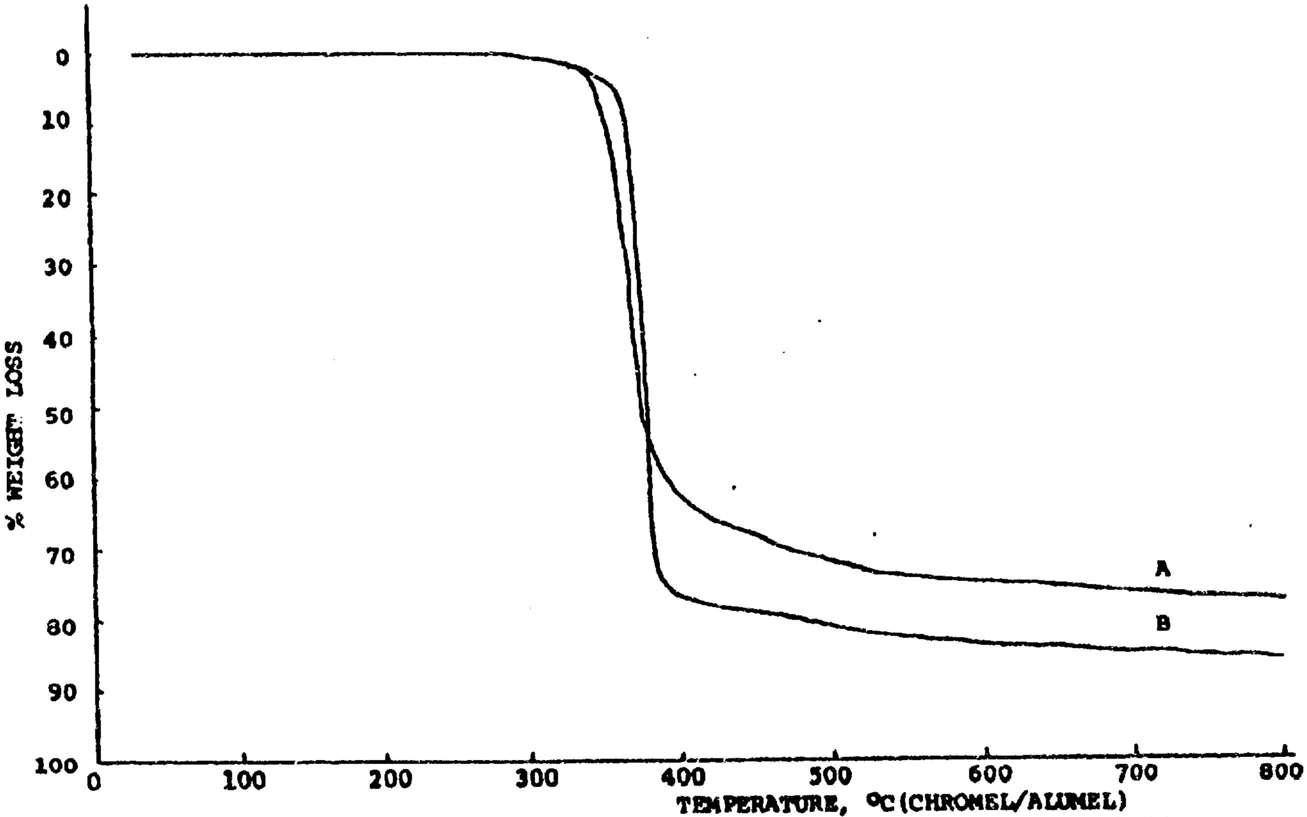

Figure 15: TGA Thermograms of Epoxy Rosin Copolymers Cured with Phthalic Anhydride (A) DGEBA/DGETBPP (50/50) (B) DGEBA/DGETBBA (50/50); N_2, 10°C/min.

3.1.2.2 FT-IR Studies on Curing Reactions of the Epoxy Resins

The curing reactions of DGEBA/DGETBPP with phthalic anhydride are studied by infrared spectroscopy (Figure 16). The curing reaction involves opening of the anhydride ring by an active hydrogen(64):

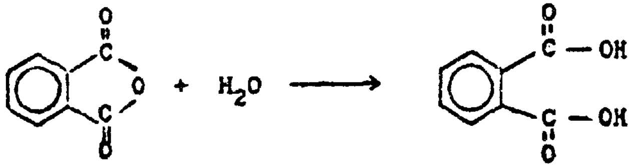

The initial reaction is addition esterification:

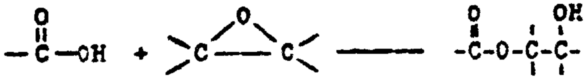

The bands near 1850, 1765, and 715 cm^{-1}, which decrease in intensity during the curing reaction, are related to the structure of phthalic anhydride. The increase in intensity of the band near 1070 cm^{-1} results from the formation of an ether linkage. The crosslinked structure is formed at the expense of oxirane rings of the epoxy resins. Accordingly, the oxirane ring breathing adsorptions at 1260 and 910 cm^{-1} decrease in intensity. The changes in intensity are clearly demonstrated in the difference spectra obtained by subtracting the 1510 cm^{-1} band (semicircle stretching of the benzene ring) to the base line (Figure 17). The spectra of the individual components are shown in Figures 18-21.

Similar changes in the infrared spectra are observed during the curing reaction of DGEBA/DGETBBA with phthalic

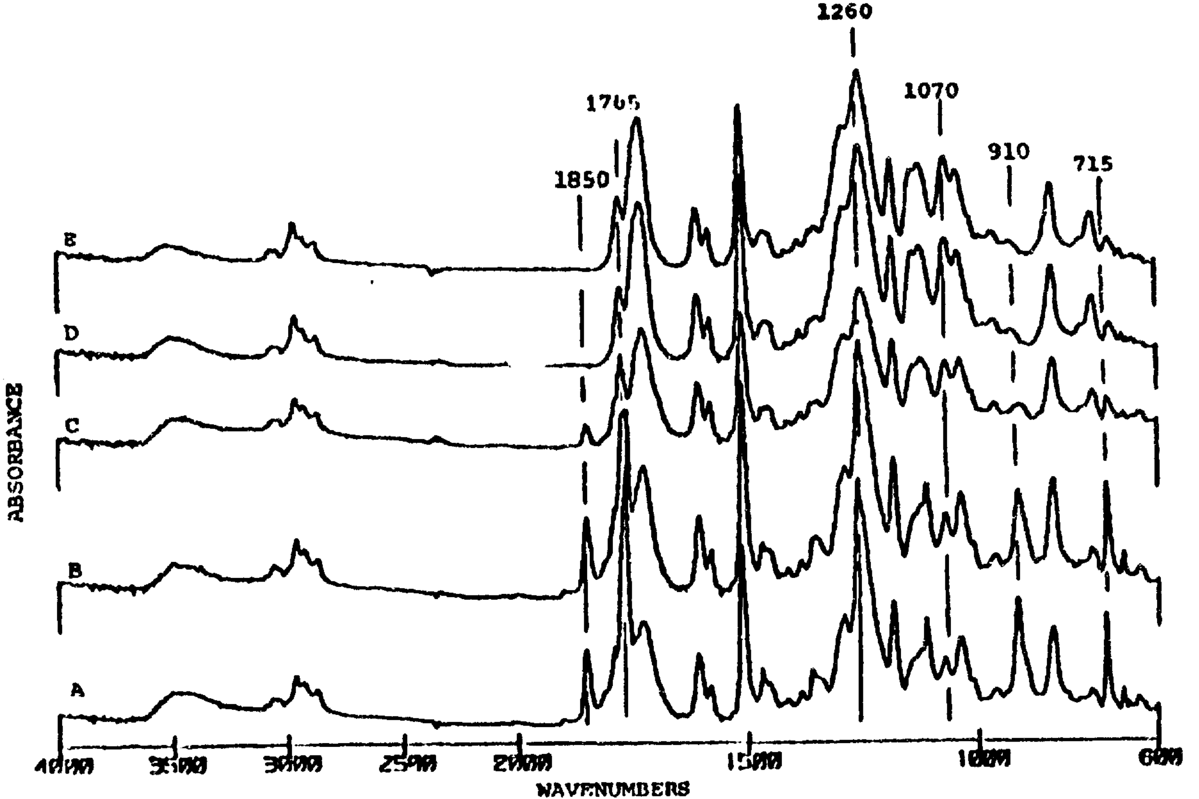

Figure 16: Infrared Spectra of DGEBA/DGETBPP Cured with Phthalic Anhydride (A) Initial Mixture (B) after Curing at 100°C for 30 Min. (C) after Curing at 100°C for 2 Hr. (D) after Additional Heating at 180°C for 1 Hr. KBr Pellet; 25°C.

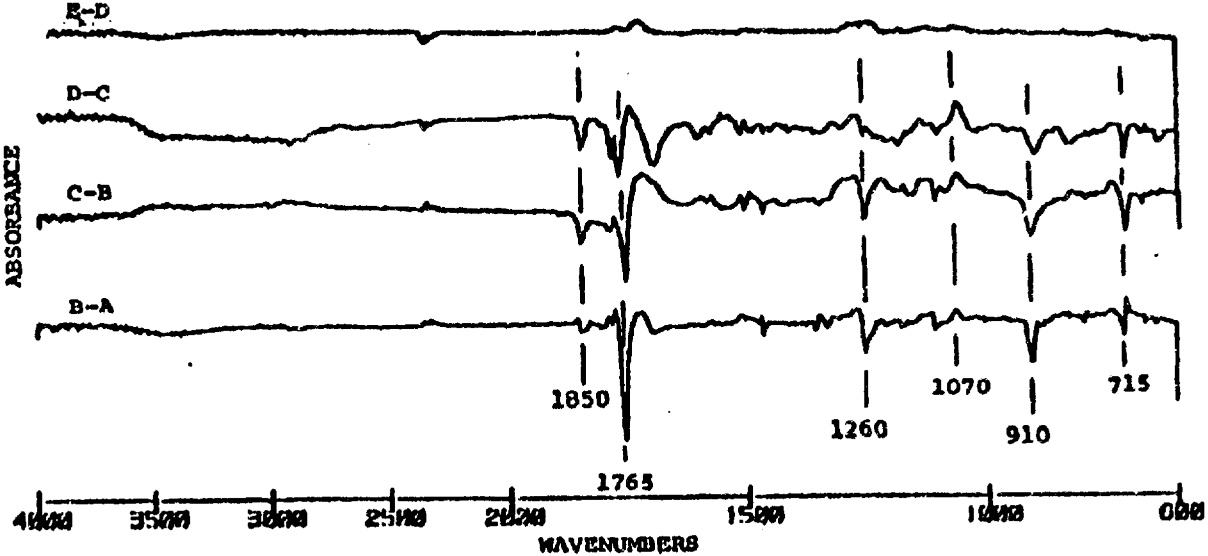

Figure 17: Difference Spectra Obtained from Figure 16 by Subtracting the 1510 cm^{-1} Band to the Base Line.

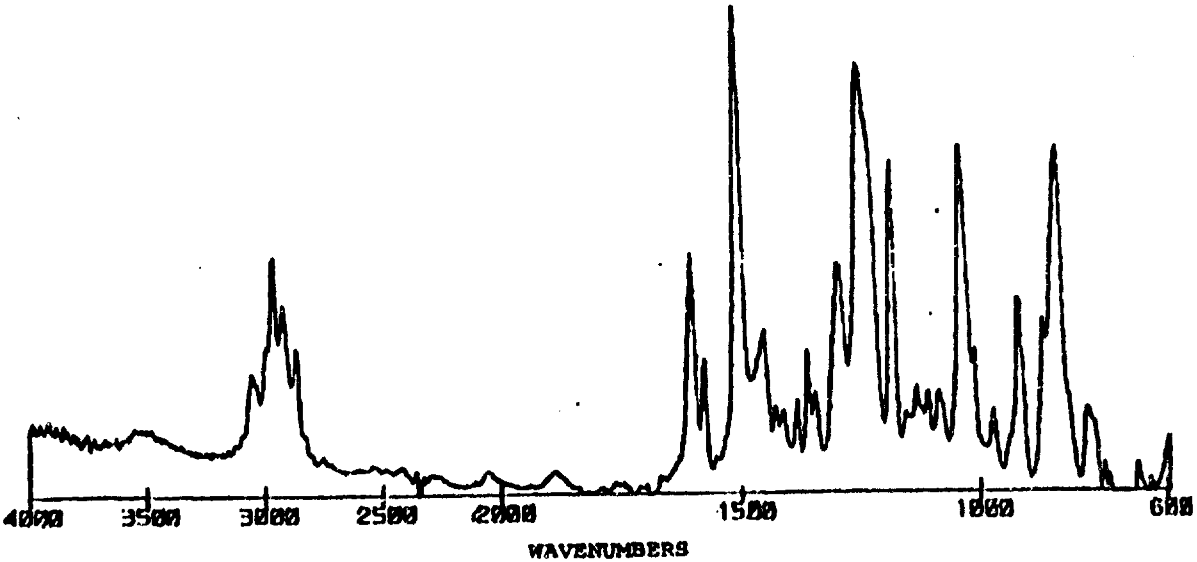

Figure 18: Infrared Spectrum of DGEBA. Reflectance Attachment.

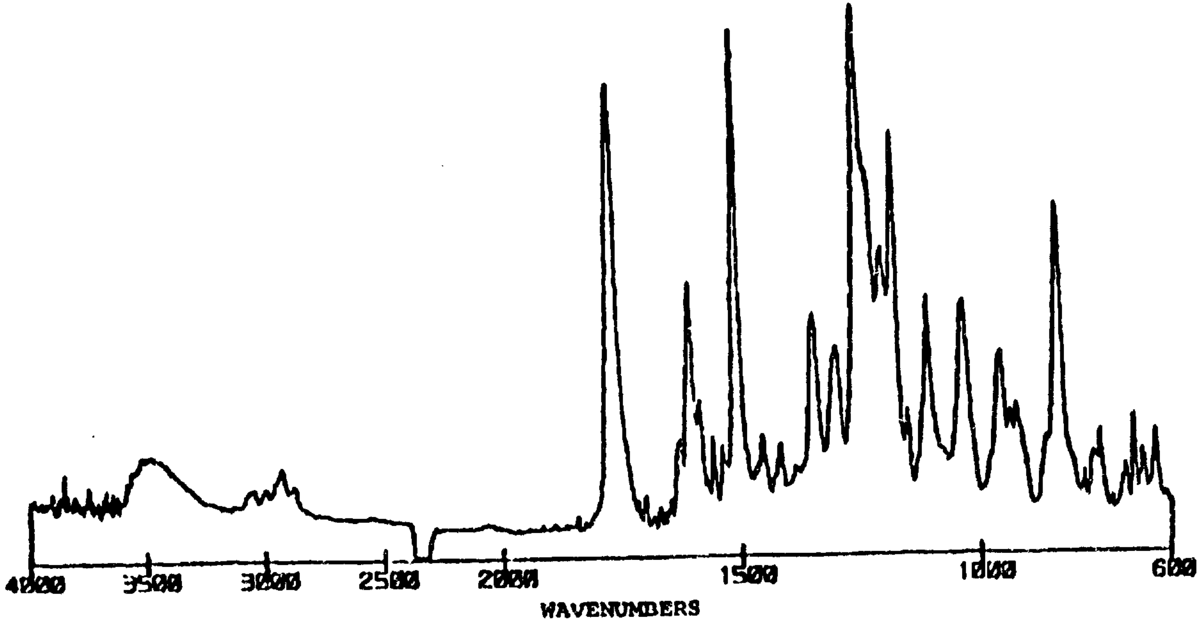

Figure 19; Infrared Spectrum of DGETBPP. Reflectance Attachment.

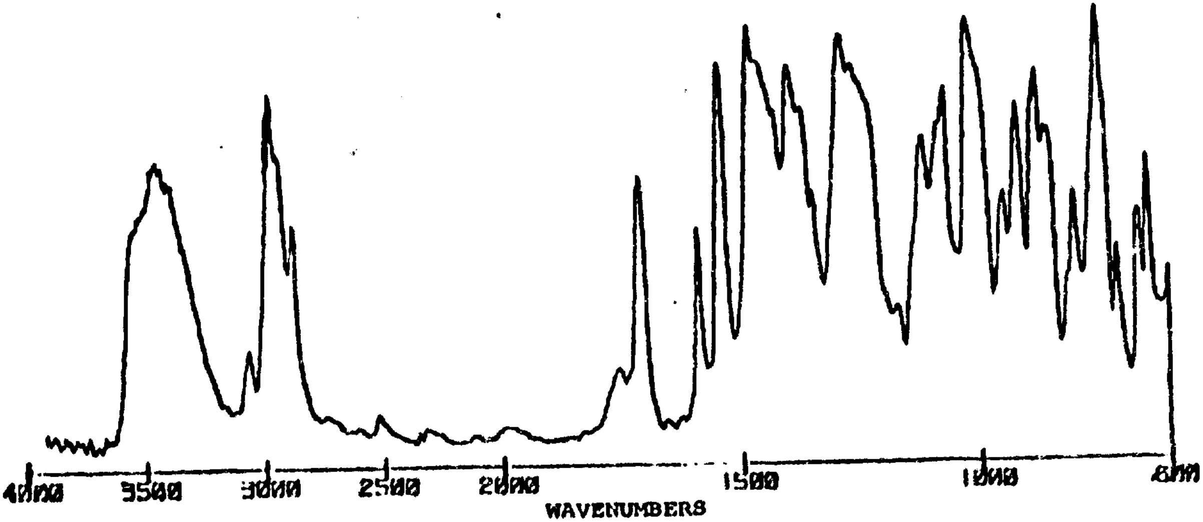

Figure 20: Infrared Spectrum of DGETBBA. Reflectance Attachment.

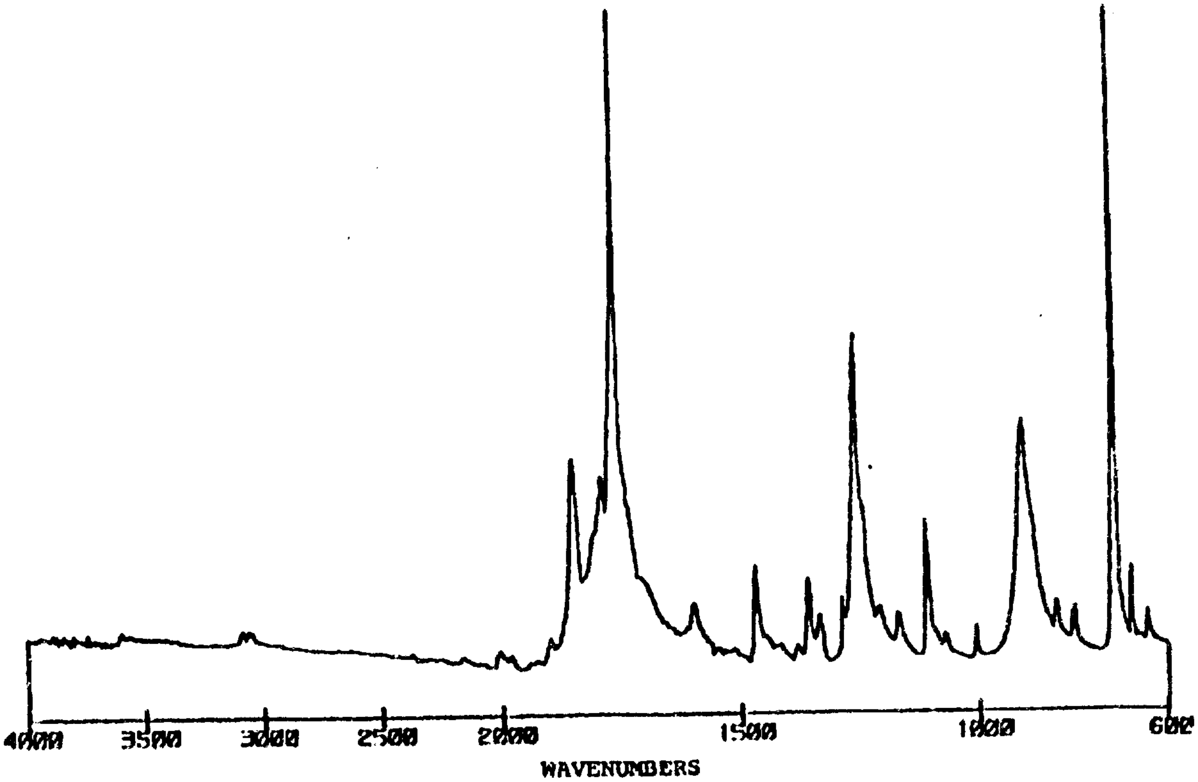

Figure 21: Infrared Spectrum of Phthalic Anhydride. KBr Pellet.

anhydride. The decreases of bands at 1850, 1765, 1260, and 715 cm^{-1} associated with phthalic anhydride are shown in Figure 22. The sample after curing at 120°C for one hour already shows the presence of an additional band at 1070 cm^{-1} (ether linkage) which does not increase much after further heating, indicating that the curing reaction is near completion. The difference spectra are shown in Figure 23.

3.1.2.3 Epoxy Resin/Poly(butylene terephthalate) System

The thermal analytical data of poly(butylene terephthalate) containing different epoxy resin additives are shown in Table 3. By comparing the data one can find that DGEPP and DGETBBA have an equivalent influence on oxygen index. However, the loop functionality of DGEPP increases the char yield. The presence of bromine in DGETBPP causes a slight decrease in char yield and an increase of oxygen index by one unit as compared to the DGEPP system.

If one takes into account the char yields of the additives, the actual increased char formation will be 11.5%, 6.9% and 9% from DGEPP, DGETBBA, and DGETBPP, respectively. The values are obtained from the differences between the experimental char yields and the calculated char yields in Table 3.

3.1.2.4 FT-IR Studies of DGETBPP/Poly(butylene terephthalate) System

The spectral changes which occur upon heating the mixture of DGETBPP and poly(butylene terephthalate) at melting are shown in Figure 24. In order to compare the spectrum of

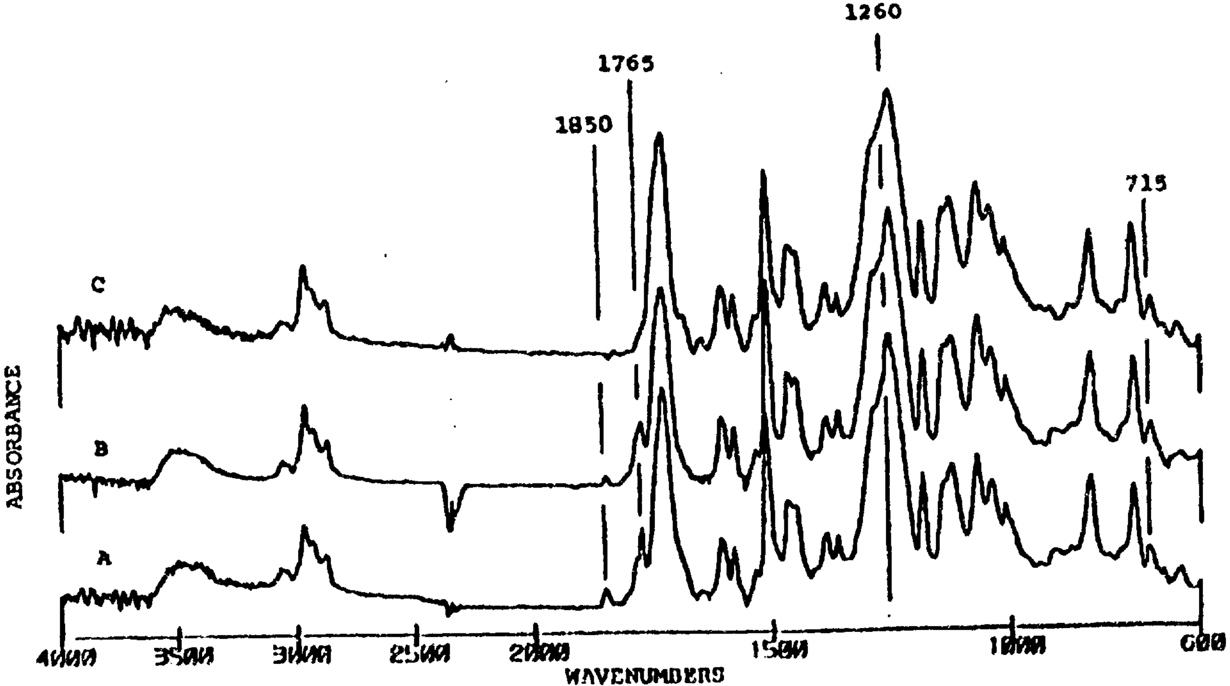

Figure 22: Infrared Spectra of DGEBA/DGETBBA Cured with Phthalic Anhydride. (A) after Curing at 120°C for 1 Hr. (B) after Additional Heating at 170°C for 25 Min. (C) Cured Resin. KBr Pellet. 25°C.

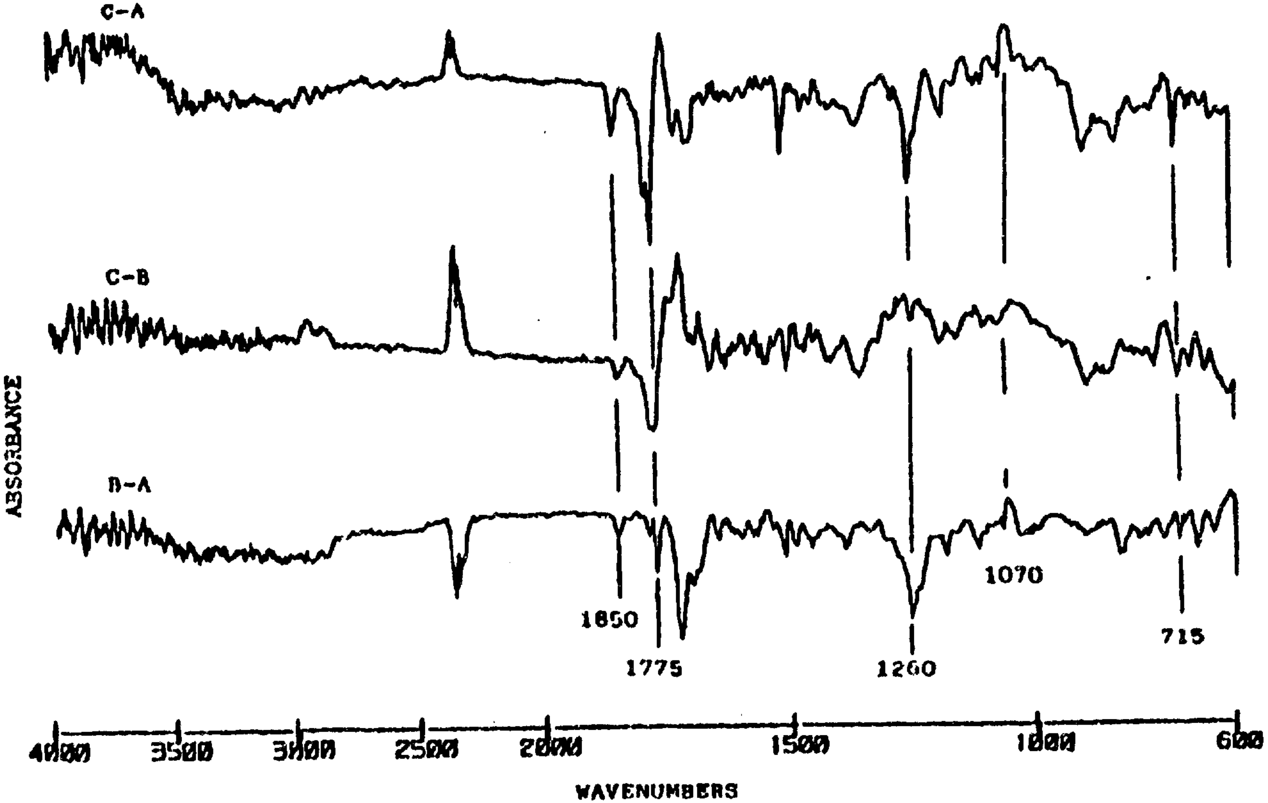

Figure 23: Difference Spectra Obtained from Figure 22 by Subtracting the $1510\ \mathrm{cm}^{-1}$ Band to the Base Line.

Table 3.

Thermal Analytical Data of Poly(butylene terephthalate) Containing Different Epoxy-Resin Additives

Additives	% Weight	Char Yield,% at 800°C, N_2	Oxygen Index,%
None	-	1	24
DGEPP	30	20, (8.5)[a]	27
DGETBBA	30	10, (3.1)[a]	27
DGETBPP	30	18, (11)[a]	28

(a) Calculated values based on 30% contribution from the char yield of the additive (DGEPP, 26%; DGETBBA, 8%; DGETBPP, 34%.

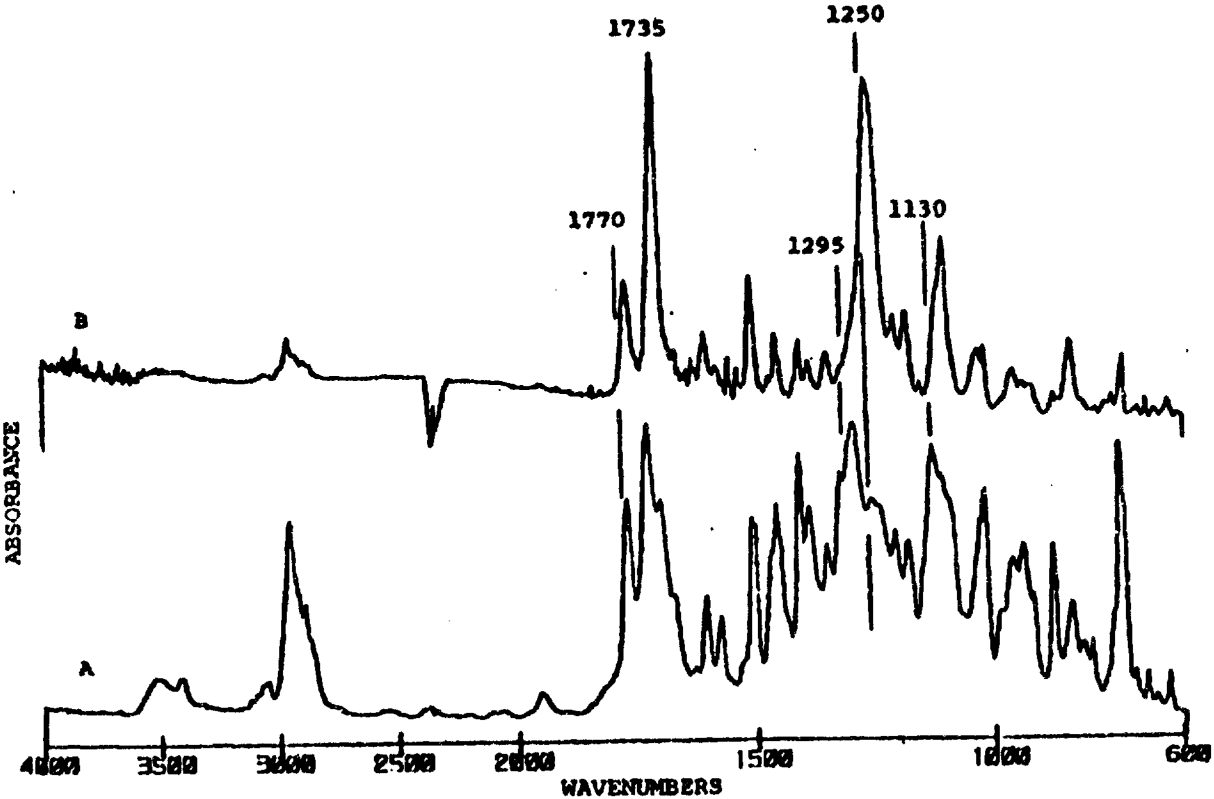

Figure 24: Infrared Spectra of Poly(Butylene terephthalate)/DGETBPP (A) Melt Mixture (B) Sum Spectrum Constructed by a 0.5:1 Addition of the Individual Spectra of DGETBPP and Poly(Butylene terephthalate).

the mixture with that of the original sample, a sum spectrum of DGETBPP and poly(butylene terephthalate) (Figure 24) is constructed by a 0.5:1 addition of the individual spectrum. A new band at 1130 cm^{-1} associated with ether linkage (C-O-C) is observed. The newly formed ester bond (O-CO) shows a band at 1295 cm^{-1}. The decrease of the band at 1250 cm^{-1} associated with oxirane ring breathing absorption is clearly observed. As a result of the stiffer structure, the carbonyl C=O shifts to 1735 cm^{-1}. Opening of the oxirane ring in DGETBPP results in the formation of -OH groups so that the increase in intensity of the bands in the region of 3400-3600 cm^{-1} is observed. These spectral changes are clearly demonstrated in the difference spectrum (Figure 25), obtained by subtracting the 1770 cm^{-1} band (lactone ring stretching vibration) to the base line. The positive difference bands at 1130 cm^{-1} and 1295 cm^{-1} are observed. The decrease in intensity of the band at 1250-1260 cm^{-1} and a shift of carbonyl absorption are also clearly resolved. The change in the degree of crystallinity of poly(butylene terephthalate) caused by the melt process is demonstrated by the appearance of a sharp positive difference band at 730 cm^{-1}(65). The subtraction criterion for the reduction of the 1770 cm^{-1} band to the base line is to eliminate one component (DGETBPP) from the mixture. The other component may leave a few difference bands in the spectrum. For this reason the difference spectrum shown in Figure 25 is contracted 5 times to avoid confusion.

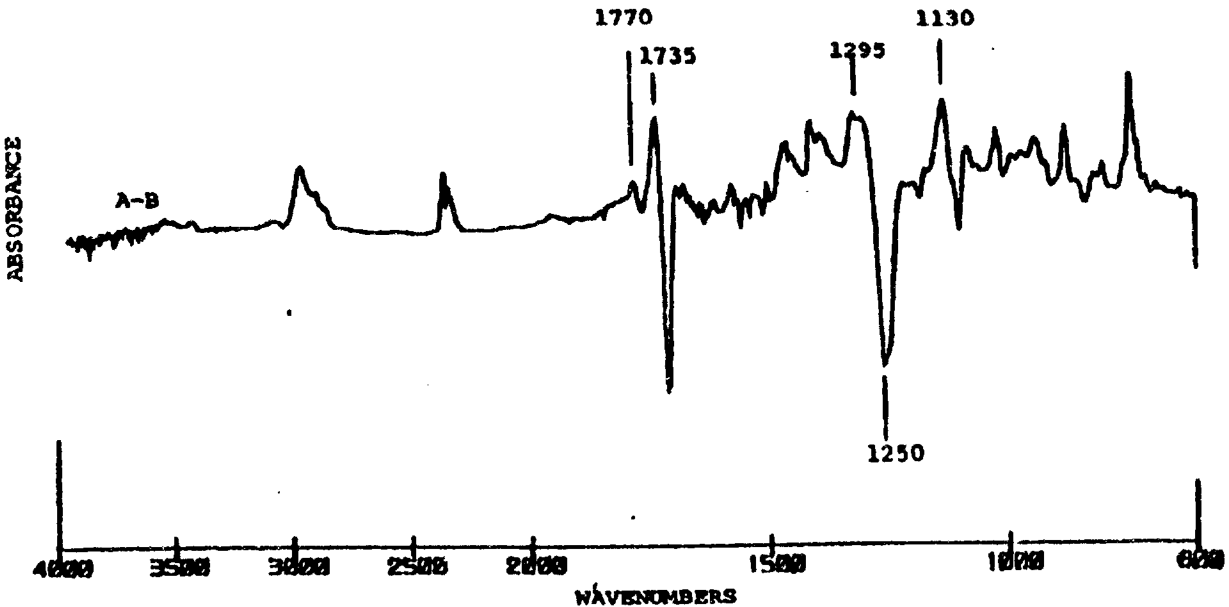

Figure 25: Difference Spectrum Obtained from Figure 24 by Subtracting the 1770 cm^{-1} Band to the Base Line.

From the above analysis, the interaction of DGETBPP with poly(butylene terephthalate) may be assumed to proceed according to the following mechanisms(15),

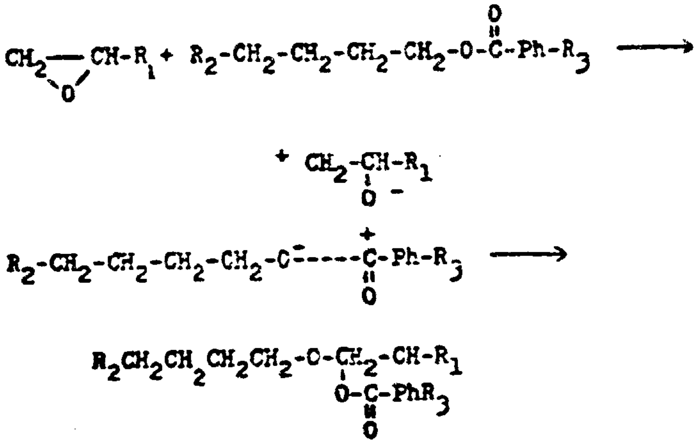

$$\underset{\diagdown O \diagup}{CH_2\text{—}CH}\text{-}R_1 + R_2\text{-}CH_2\text{-}CH_2\text{-}CH_2\text{-}CH_2\text{-}O\text{-}\overset{O}{\overset{\|}{C}}\text{-}Ph\text{-}R_3 \longrightarrow$$

$$^{+}\;CH_2\text{-}\underset{O^{-}}{\underset{|}{CH}}\text{-}R_1$$

$$R_2\text{-}CH_2\text{-}CH_2\text{-}CH_2\text{-}CH_2\text{-}O^{-}\text{-----}\underset{O}{\underset{\|}{\overset{+}{C}}}\text{-}Ph\text{-}R_3 \longrightarrow$$

$$R_2CH_2CH_2CH_2CH_2\text{-}O\text{-}\underset{O\text{-}\underset{O}{\underset{\|}{C}}\text{-}PhR_3}{\underset{|}{CH_2}}\text{-}CH\text{-}R_1$$

The final product is completely soluble in phenol at elevated temperature. Further heating of the sample at 300°C for 3 hours after mixing leads to insoluble materials attributed to a crosslinked structure. The increase in char formation is indicative of the formation of the intermediate compound during the heating process that is capable of altering the mode of decomposition of poly(butylene terephthalate).

3.1.3 Conclusion

Small molecules containing loop functionality used as additives do not affect the char formation of bisphenol-A polycarbonate. The increased flame retardancy appears to be mainly due to the presence of halogens. However, in poly(butylene terephthalate) the cleavage of the

$C_{aromatic}$-Br bond of the flame retardant additive seems to enhance the crosslinking reactions between the aromatic rings resulting in a higher char yield.

The only apparent evidence for the char-forming activity due to loop functionality is found in the epoxy-resin systems.

3.2 Phenol-Formaldehyde Resins

3.2.1 Structural Studies of the Oligomeric Resins

In the syntheses of phenol-formaldehyde resins, numerous different types of reactions may occur. Among these are hydroxymethylations of phenolic rings:

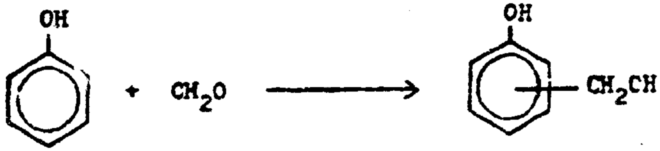

(I)

(II)

Further reactions of the hydroxymethylated phenols, II, with formaldehyde gives hemiformals and polyformals.

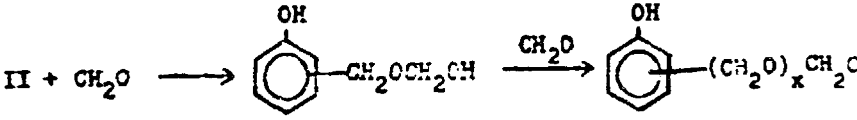

(III)

$$HO(CH_2O)_xH + CH_2O \longrightarrow HO(CH_2O)_{x+1}H$$

(IV)

Diphenylmethane-type methylene bridges (V) and dibenzyl ether-type bridges (VI) are the products of condensation type reactions:

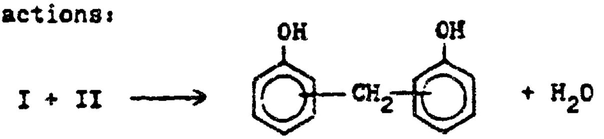

(V)

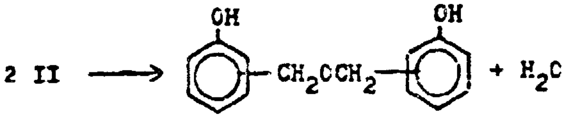

(VI)

The mechanisms and the rates of these reactions mainly depend on pH, type of catalyst, and temperature(66). As a general observation, resol resins contain appreciable methylol and ether groups, while novalak resins contain very little methylol and ether groups(67).

Model compounds have been studied by Woodbrey, *et al.*(68). The results (Figure 26) show the different chemical shifts in NMR spectra for different type of methylene bridges. The shift differences observed between methylene protons of *o*- and *p*-hydroxymethyl groups are primarily due to the strong intramolecular hydrogen bonding between *o*-hydroxymethyl and the phenolic hydroxyl groups.

The methylene bridges formed during the condensation of phenol and formaldehyde can result in three different forms designated as *para-para'* (I), *ortho-para'* (II), *ortho-ortho'* (III) depending upon the positions of the

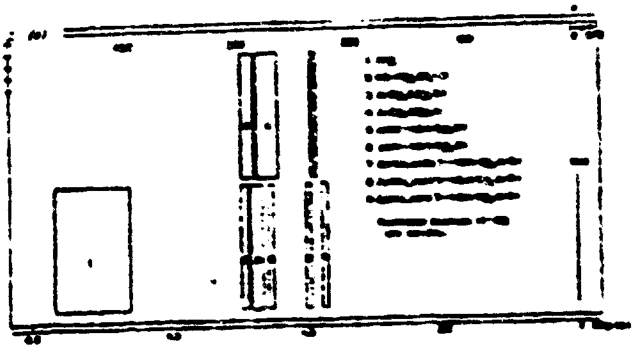

Figure 26: NMR Chemical Shift Region for Different Functional Groups of Phenol-Formaldehyde Resins in Dilute Solutions in Acetone.

J. C. Woodbrey, H. P. Higginbottom and H. M. Culbertson, J. Polymer Sci. Part A, 3, 1079(1965).

hydroxyl groups on the adjacent aromatic rings relative to the methylene bridge.

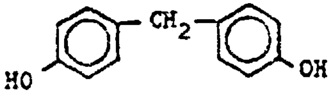

(I)

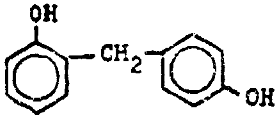

(II)

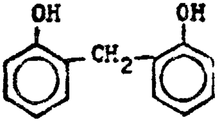

(III)

Hirst, *et al.*(69) has assigned the chemical shift for each of these three different configurations in dimers (Figure 27). The chemical shift of 3.75, 3.89, and 3.97 ppm observed for the methylene resonance in I, II, and III, respectively, are typical for larger moieties, and they form the basis for interpreting the data obtained in our studies.

Figures 28 to 32 contain the 220 MHz NMR spectra of the phenol-formaldehyde oligomers showing clearly hydroxyl, aromatic, and methylene resonance peaks. The spectra of cresol-formaldehyde oligomers (Figures 33 and 34) show the methyl resonance peaks. The splitting pattern of the absorption bands are not very well defined. This is in part a result of the large number of isomers even with relatively low molecular weight resins. For example, there are 13,203 linear isomeric structures for a polymer having only ten phenolic units tied together with methylene bridges through *ortho* or *para*-positions(70). As a result, there is a lack of complete equivalence of all the protons in a polymer chain.

The absorptions due to the phenolic hydroxyl protons are usually in the region from about 8.00 to 9.25 ppm. The

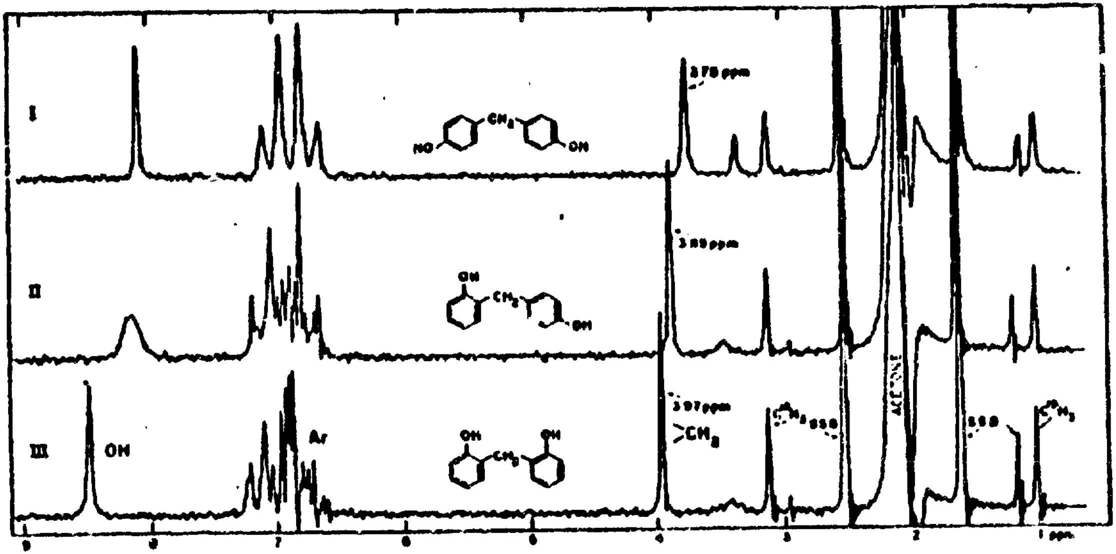

Figure 27: NMR Spectra of Phenol-Formaldehyde Dimers.

R. C. Hirst, D. M. Grant, R. E. Hoff and W. J. Burke, J. Polymer Sci., Part A, 3, 2091(1965).

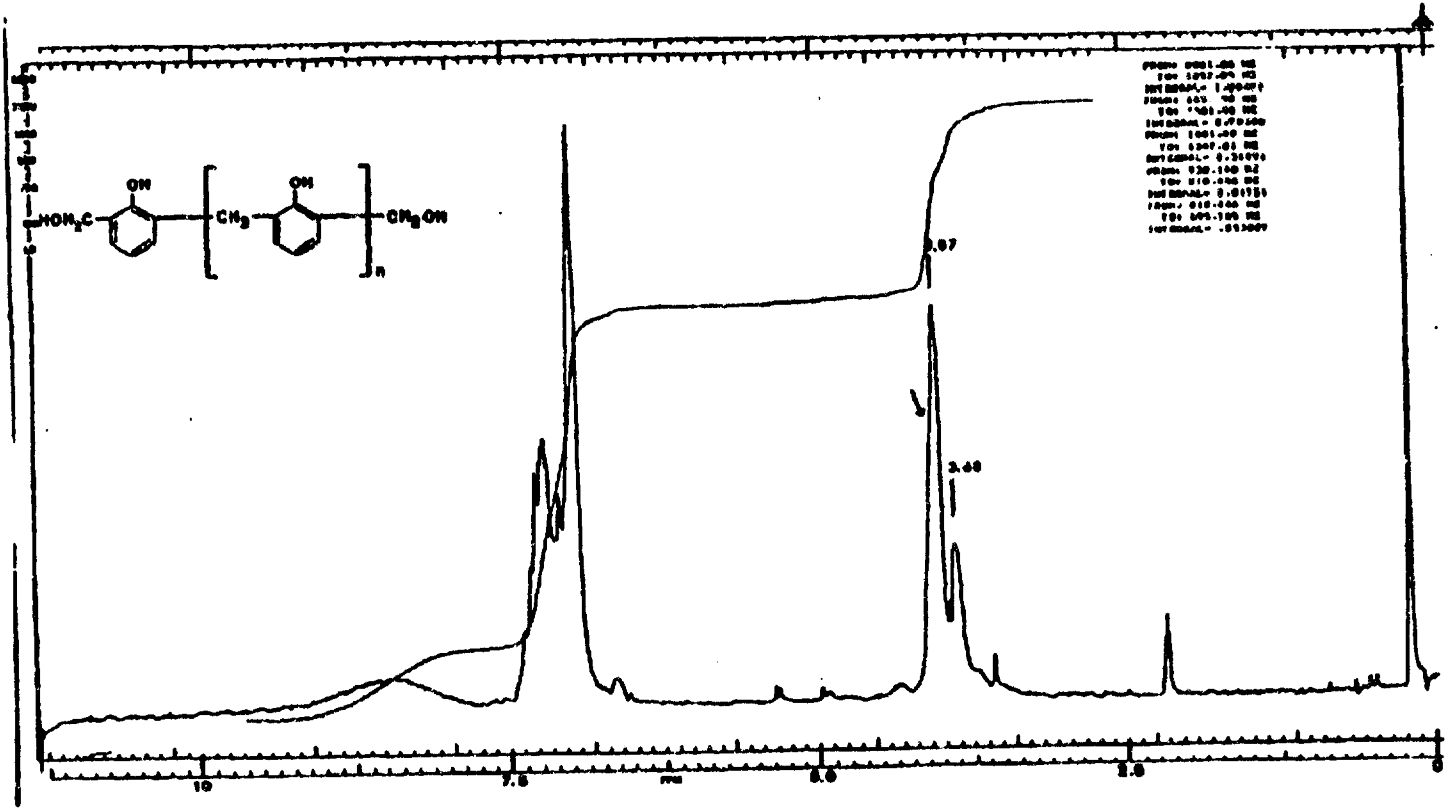

Figure 28: NMR Spectrum of Phenol-Formaldehyde Resin in d-Acetone.

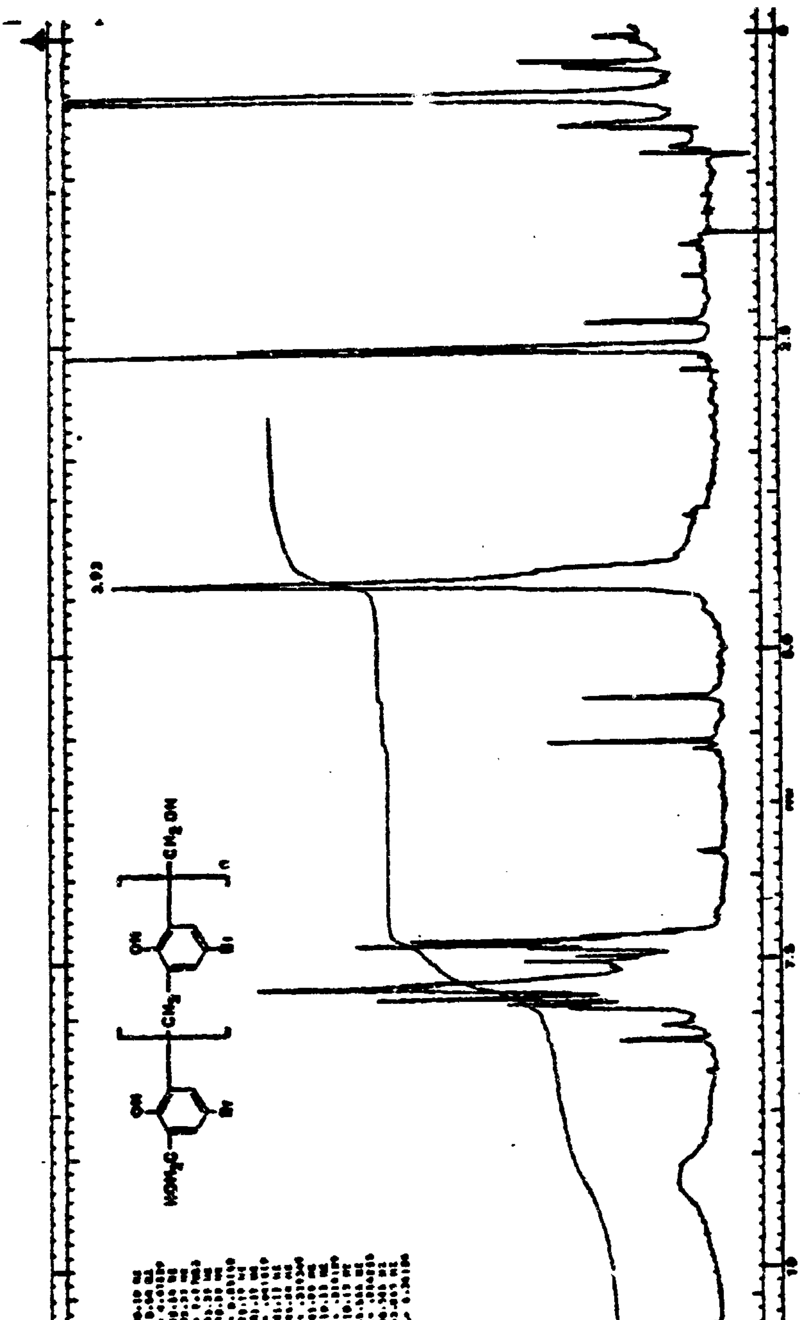

Figure 29: NMR Spectrum of p-Bromophenol-Formaldehyde Resin in d-Acetone.

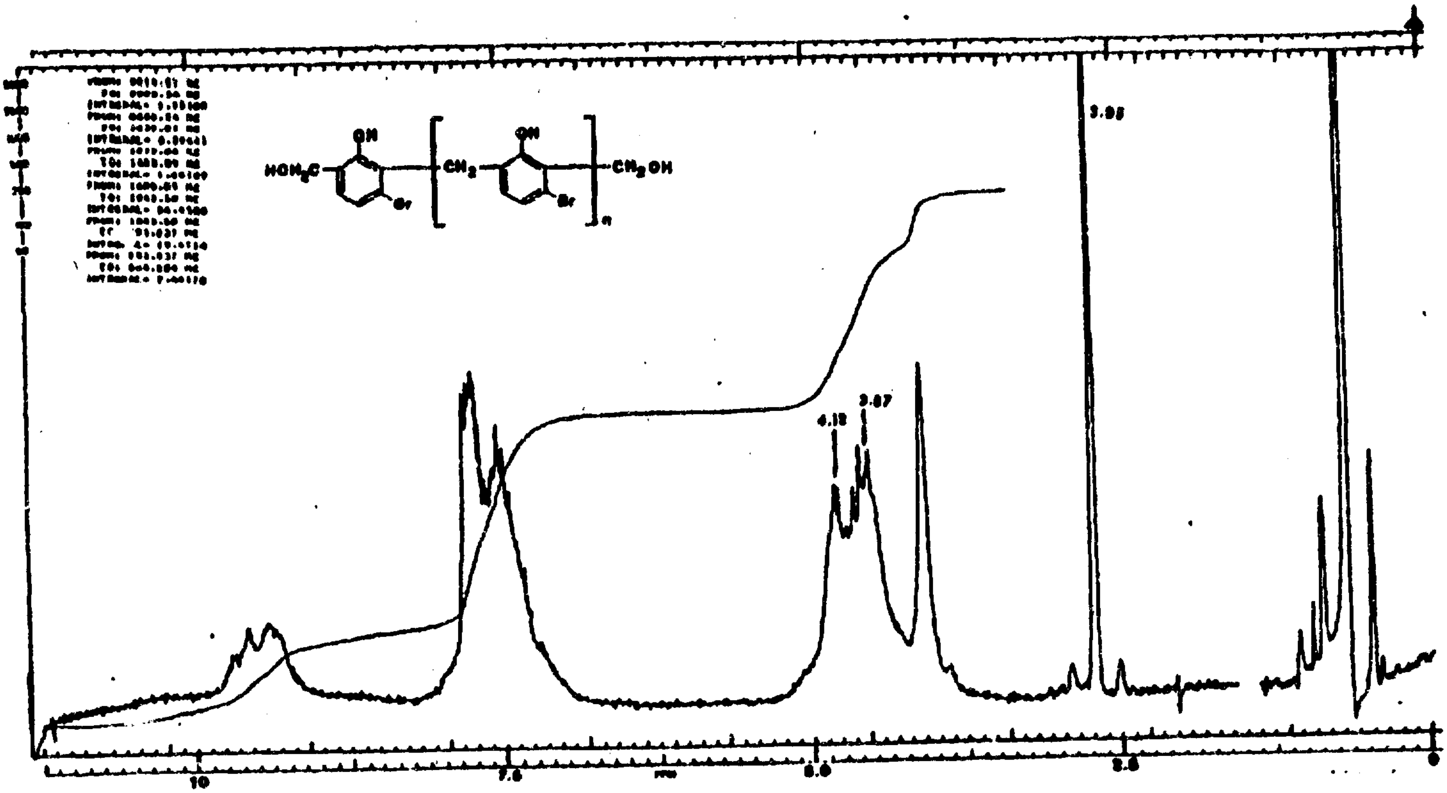

Figure 30: NMR Spectrum of m-Bromophenol-Formaldehyde Resin in d-Acetone.

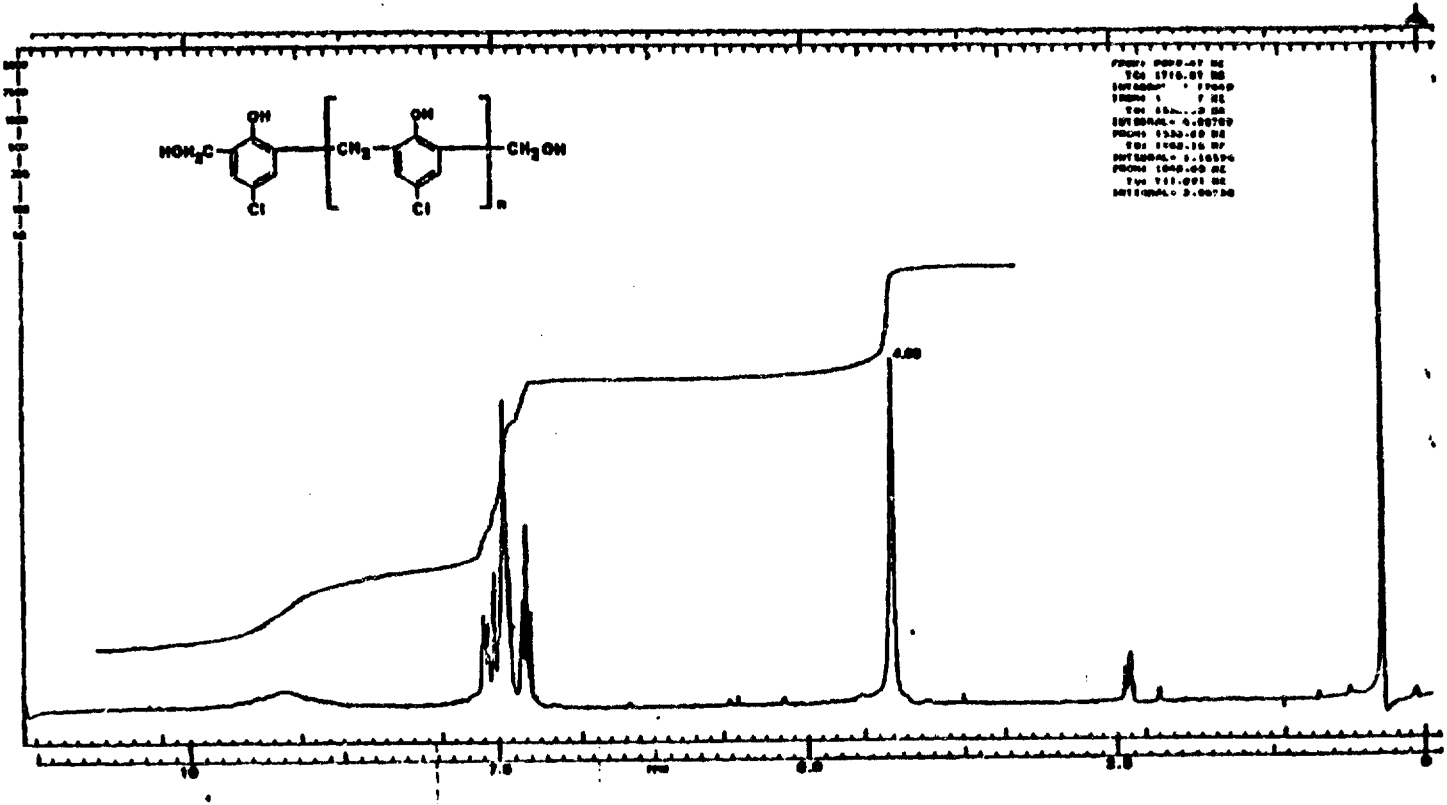

Figure 31: NMR Spectrum of p-Chlorophenol-Formaldehyde Resin in d-Acetone.

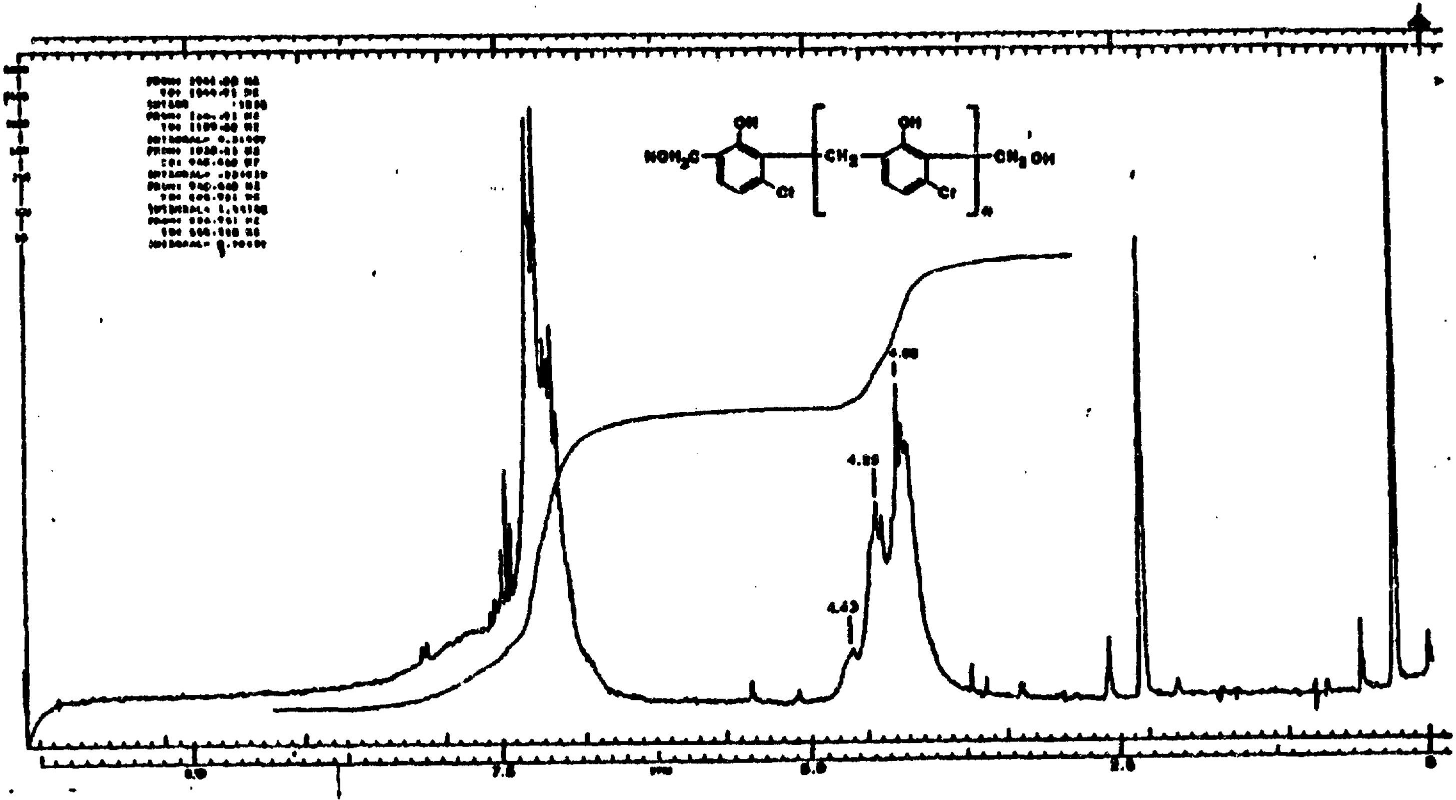

Figure 32: NMR Spectrum of m-Chlorophenol-Formaldehyde Resin in d-Acetone.

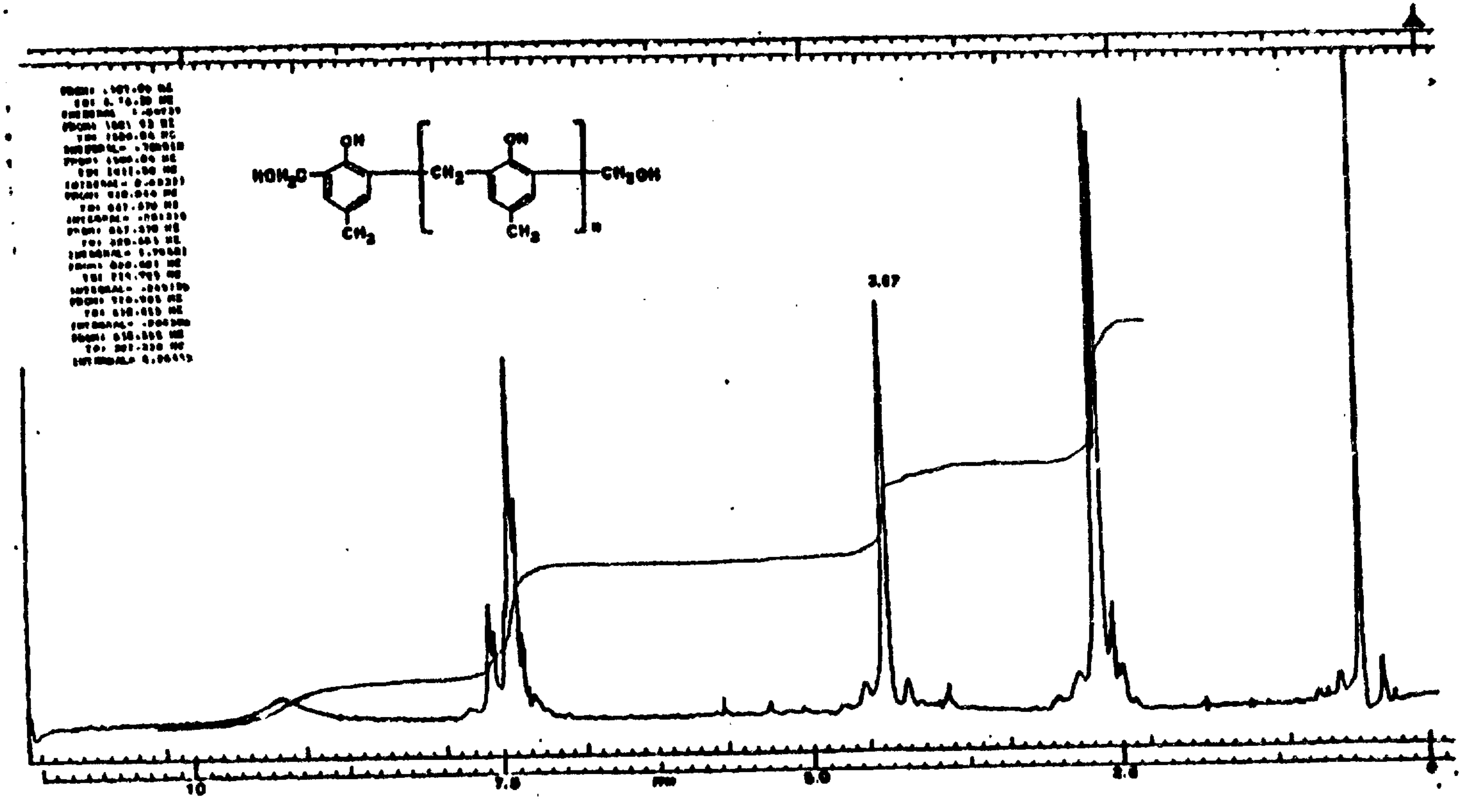

Figure 33: NMR Spectrum of p-Cresol-Formaldehyde Resin in d-Acetone.

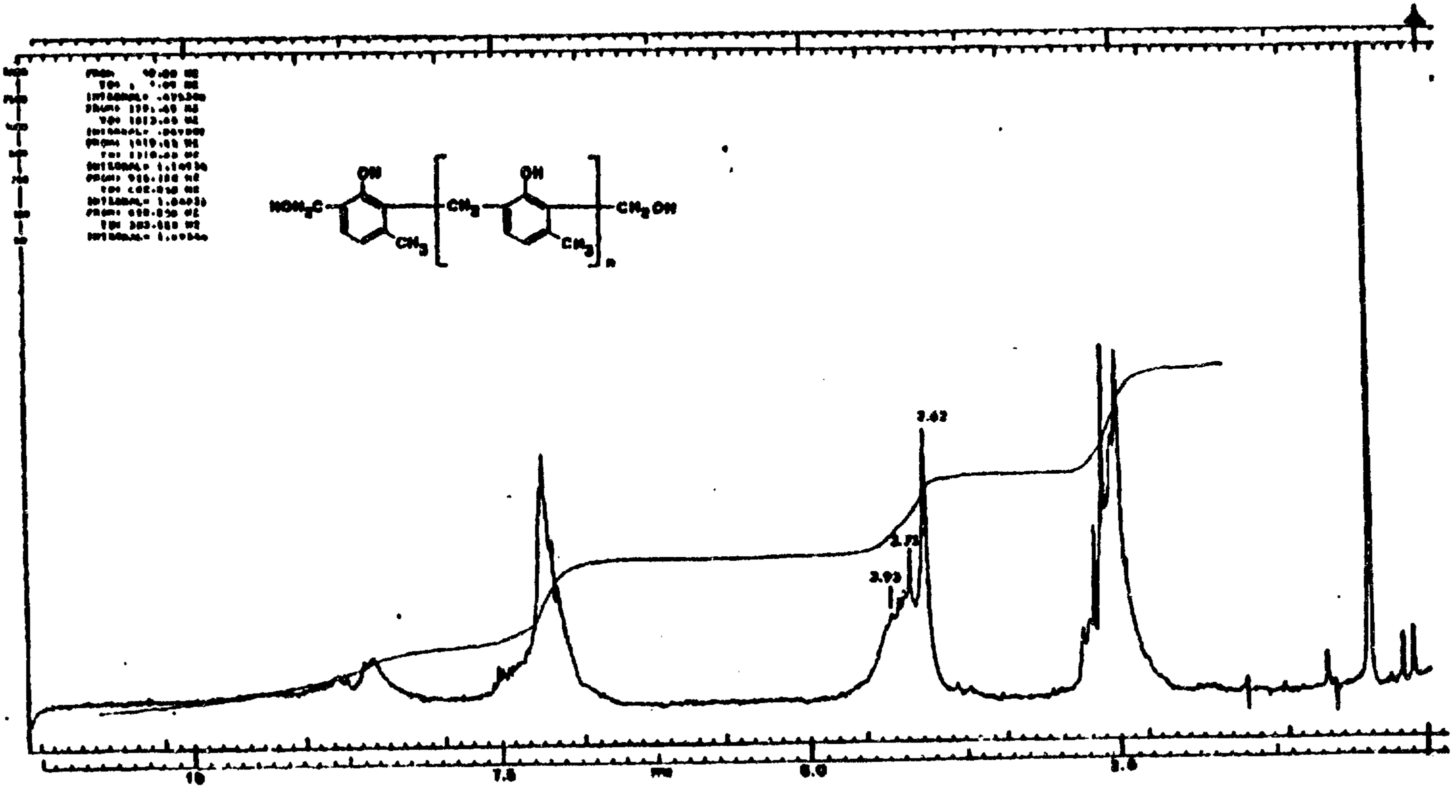

Figure 34: NMR Spectrum of m-Cresol-Formaldehyde Resin in d-Acetone.

aromatic protons observed in the region from 6.25 to 7.50 ppm. The methylene protons (except for those of *para*-substituted phenolic resins) can be resolved into peaks due to *p*,*p*'-, *o*,*p*'- and *o*,*o*'-methylene bridges (Figures 28, 30, 32, and 34). The *ortho*-*ortho*' resonance is observed as a shoulder on the *ortho*-*para* peak (Figure 28). In some of the *m*-substituted phenol formaldehyde oligomers these peaks are resolved (Figures 32 and 34). Similar observations have been found by Hirst(79) (Figure 35).

The substituent groups have altered the chemical shift of the methylene protons slightly. Differences in shift are related to the field effect arising from the substituents(71). The methyl groups (+I) move the chemical shift of methylene protons to higher field (3.87 ppm for PCP). On the other hand, halogens (-I) move the chemical shift to lower field (3.93 ppm for pBPF and 4.00 ppm for PCPF). The effects of halogens are in agreement with the order of electronegativity, that is, Cl > Br. For non-substituted and *meta*-substituted phenol-formaldehyde oligomers the chemical shift of methylene protons of a particular linkage, for example, *ortho*-*ortho*' methylene bridge, also increase in the order of electronegativity of the substituents: -Cl (4.25 ppm) > -Br (4.12 ppm) > -H (3.87 ppm) > $-CH_3$ (3.75 ppm).

The field effect arising from the electronic dipole moment of the substituents is dependent on the orientation of the dipoles and charges with respect to the C-H bond.

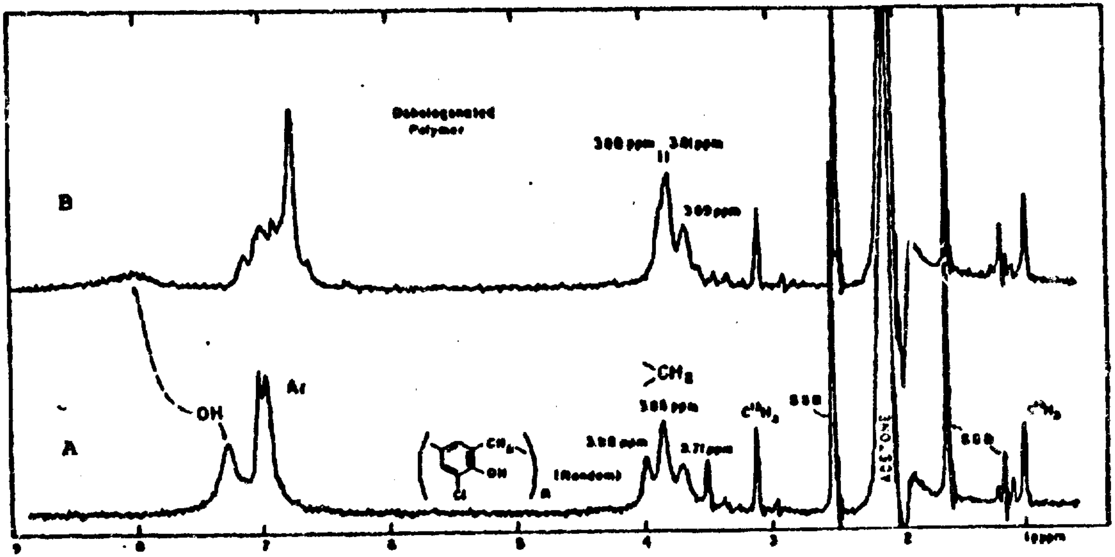

Figure 35: NMR Spectra of an o-Chlorophenol-Formaldehyde Polymer (A) and the Corresponding Dehalogenated Polymer (B).

R. C. Hirst, D. M. Grant, R. E. Hoff and W. J. Burke, J. Polymer Sci., Part A, 3, 2091(1965).

The *meta*-substituents are at the *para*-position with respect to the methylene protons, therefore, they have a greater influence on the chemical shift of the methylene protons than the *para*-substituents.

The possible side products such as, hemiformals, polyformals, and the dibenzyl ether type of bridges will give rise to absorptions in the 4.70-5.20 ppm region(68). These absorptions are not found in the NMR spectra of all the samples being studied.

Infrared spectra (Figures 36-39) reveal further details of the structure of phenol-formaldehyde resins. Many articles have appeared in the literature on the identification of phenolic resins by means of infrared spectroscopy(72-76). Secrest(67) has summed up the available results in the field and supplemented these with his own findings. Those results provide useful information on the assignments of absorption bands in this study.

Both the phenolic and aliphatic hydroxyl groups absorb strongly in the region of 3600-3100 cm^{-1}. The weak absorption due to the aromatic CH appears at 3010 cm^{-1} and may be masked by the hydroxyl absorption in the case of mCFP (Figure 39). The aliphatic hydrogens can be observed as a weak peak at 2900 cm^{-1}. The 1600 cm^{-1} band involves "quadrant stretching" of the benzene ring $C \overset{\cdots}{=} C$ bonds(77). The intensity of the absorption is dependent on the nature and position of the substituents. The absorption is stronger for *meta*-substituted phenols because of the dipole moment change provided by the

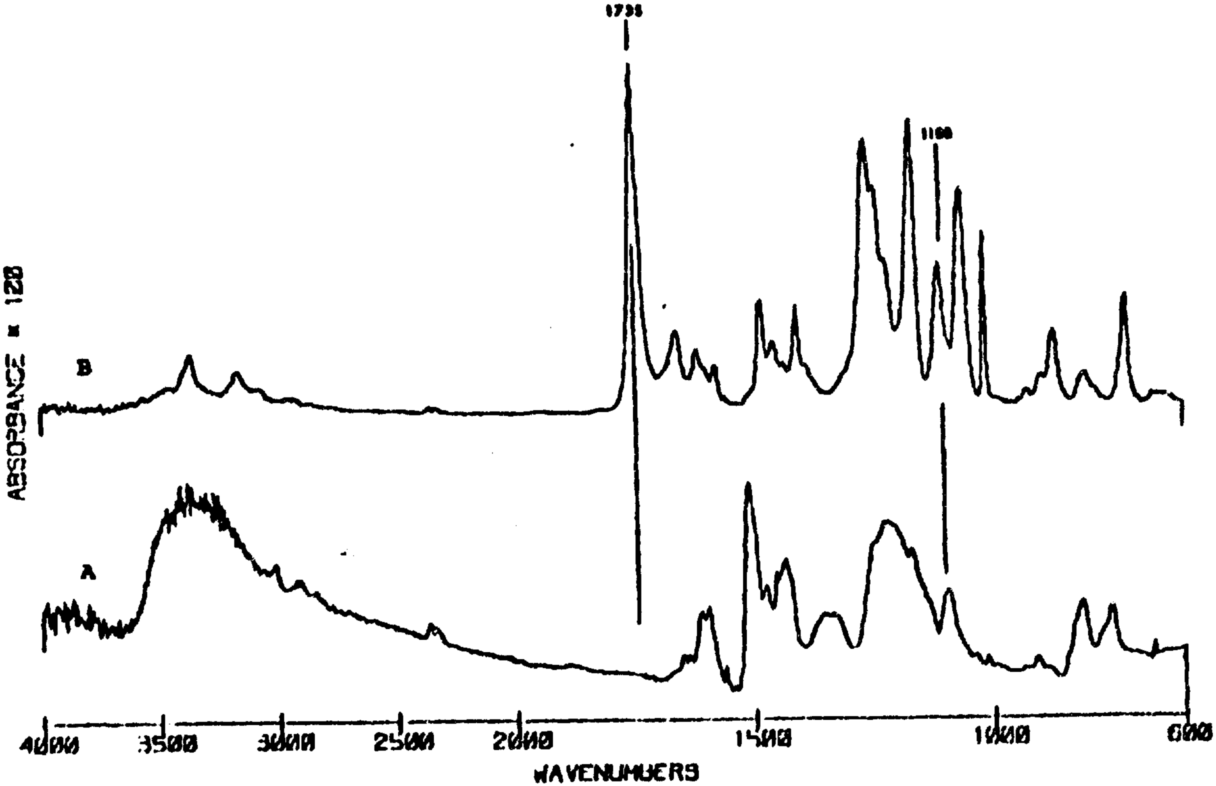

Figure 36: IR Spectra of (A) PF, and (B) X(C)pCPF. KBr Pellet.

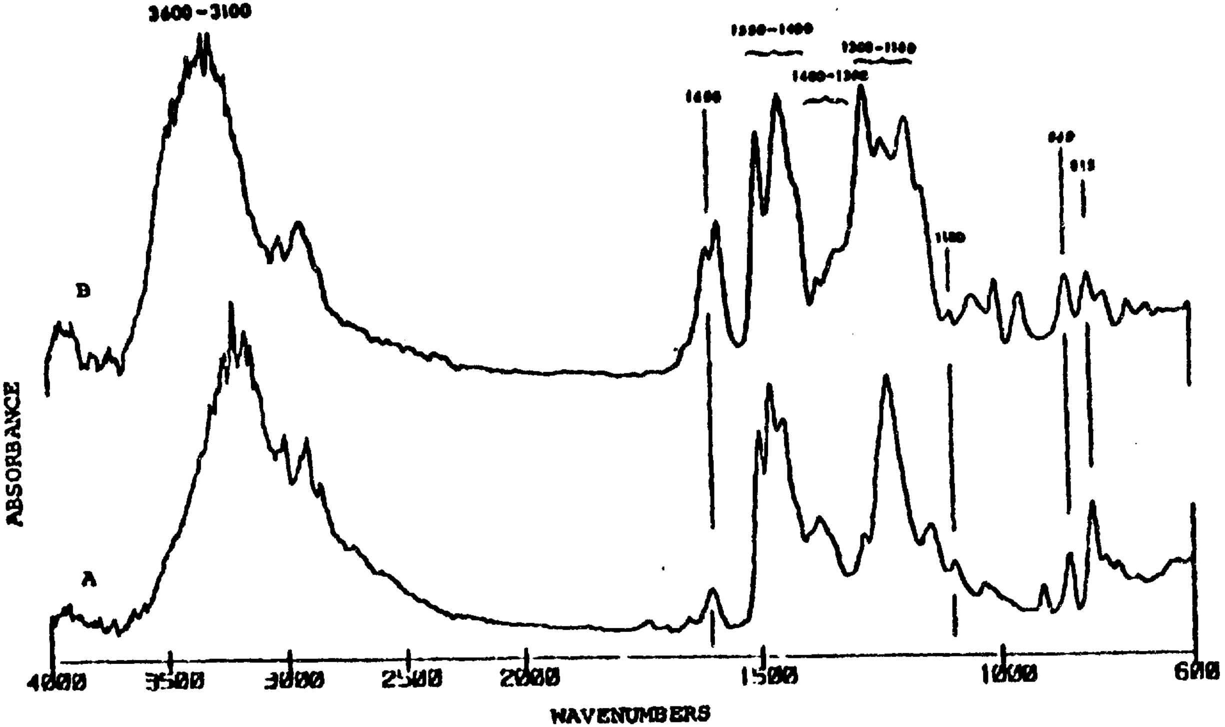

Figure 37: IR Spectra of (A) pCF, and (B) mCF. KBr Pellet.

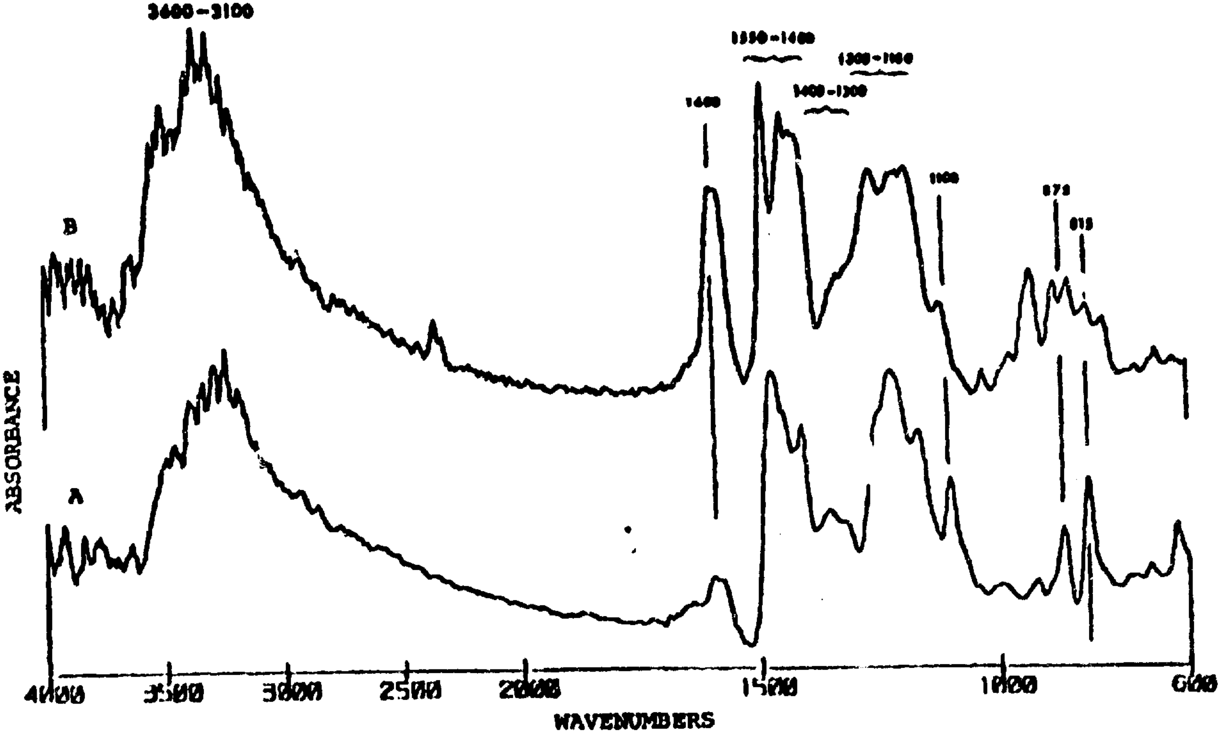

Figure 38: IR Spectra of (A) pBPF, and (B)mBPF. KBr Pellet.

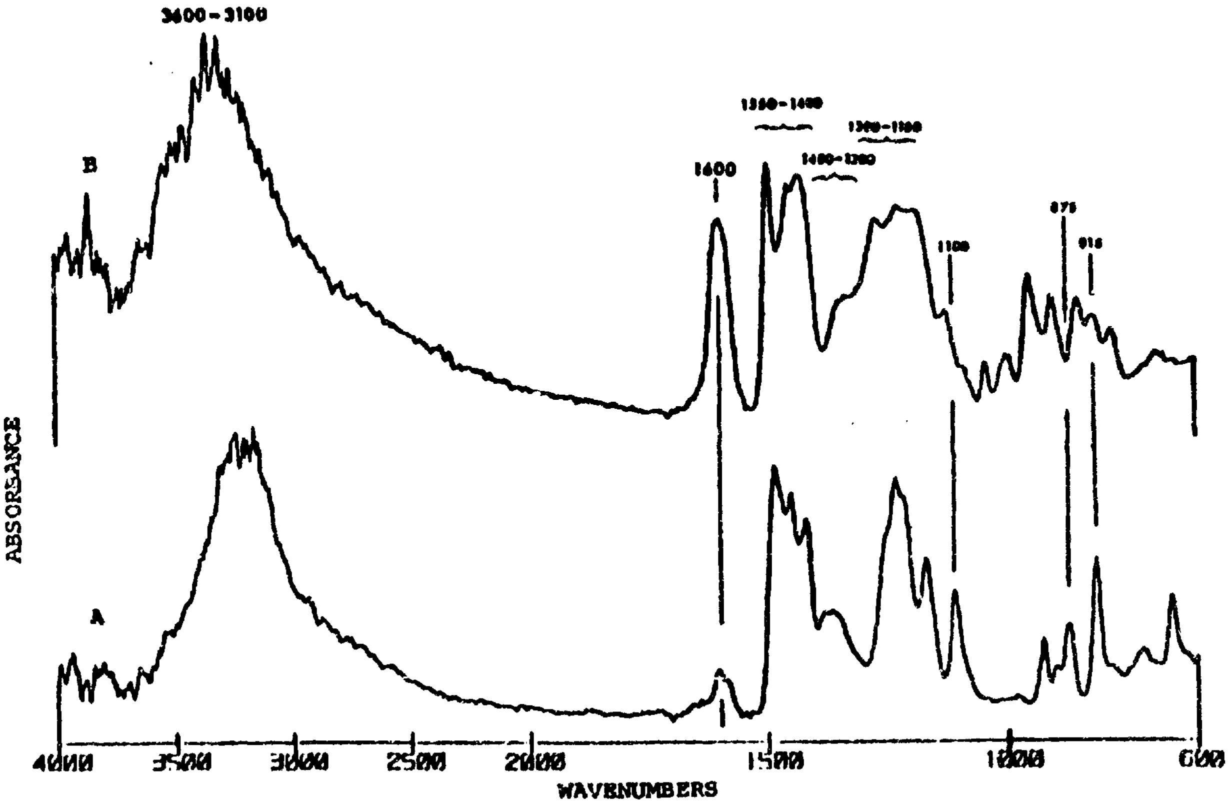

Figure 39: IR Spectra of (A) pCPF, and (B) mCPF. KBr Pellet.

unsymmetrical substituents. Two bands in the region of 1550-1400 cm^{-1} are due to semicircle stretching of the benzene ring(78). The band at 1450 cm^{-1} is stronger in the meta-substituted phenolic resins. The band between 1400-1300 cm^{-1} is assigned to the OH deformation of phenol(78). This band is absent in the spectrum of X(C)PP in which the hydroxyl groups are reacted with terephthaloyl chloride, while it remains in the spectrum of the resin cured through methylene linkages (Figure 40). Substituted phenols give rise to an absorption band in the region of 1300-1180 cm^{-1} due to C-O stretching vibration of phenol. Depending on the positions of the substituent the intensity and the position of the absorption of phenols vary. Detailed correlations are made for alkyl phenols in solution(80). The meta-substituted phenol absorbs strongly at 1300-1250 cm^{-1}. The band at 1100 cm^{-1} arises from the ether groups(67,81):

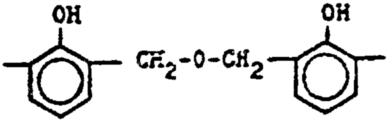

Aldehydes can develop by splitting of the dimethylene linkages(82):

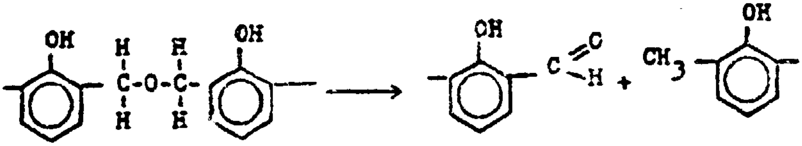

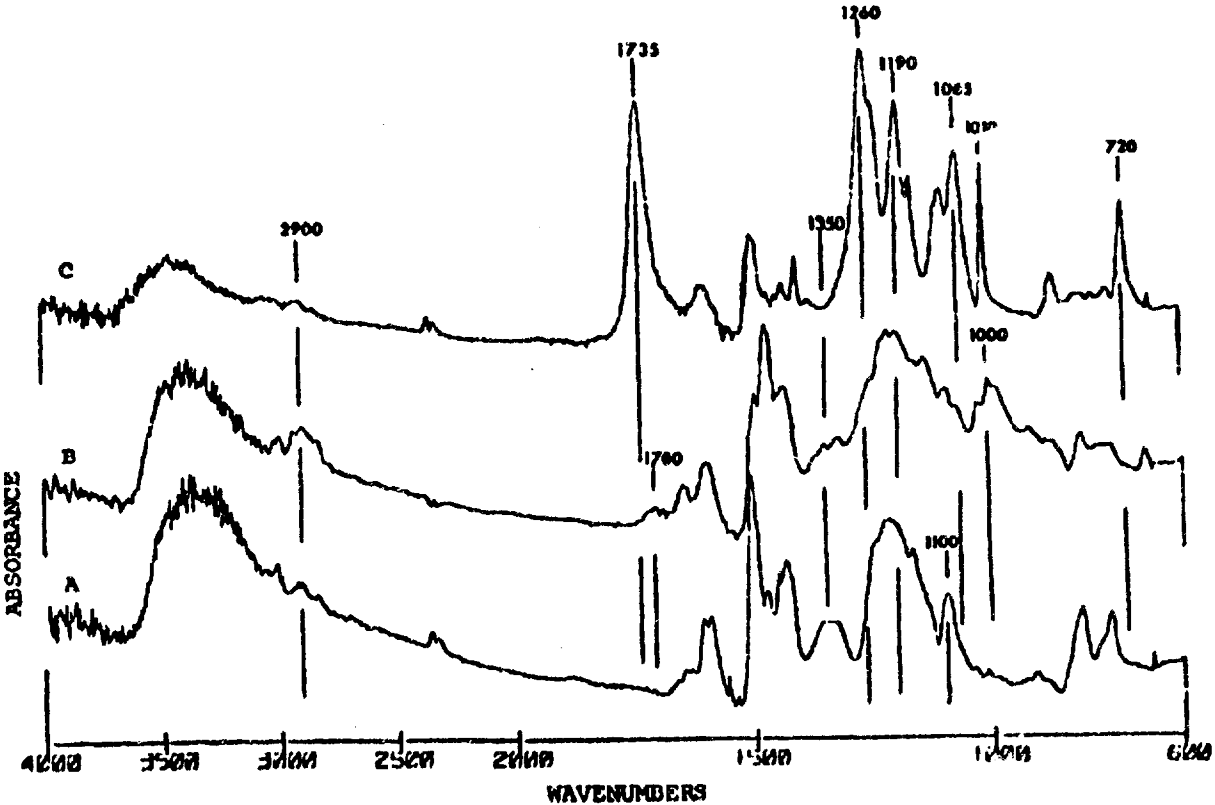

Figure 40: IR Spectra of (A) PF, (B) PF Cured with Formaldehyde, and (C) PF Cured with Terephthaloyl Chloride. KBr Pellet.

This mechanism offers the explanation for the existence of a weak band near 1710 cm^{-1} in the spectrum of the cured resin (Figure 40). One strong absorption band that is present in the spectra of all the phenolic resins of normal phenol and para-substituted phenols is at about 815 cm^{-1} due to the in-phase out-of-phase C-H bending vibrations of the substituted benzene ring(73,74,76,83). The para-substituted phenols (1:2:4:5 substituted benzene ring) also exhibit a strong absorption band at 860-875 cm^{-1}. This assignment is in agreement with that of Richards and Thompson(74), Bender(83), and Lucchesi(73).

The infrared spectra of phenolic resins cured with formaldehyde and terephthalcyl chloride are shown in Figure 40.

In the formaldehyde cured resin the changes are observed as an increased absorption at 2900 cm^{-1} from the methylene CH stretching, 1700 cm^{-1} from the aldehyde carbonyl groups, and 1000 cm^{-1} from the methylol groups(67).

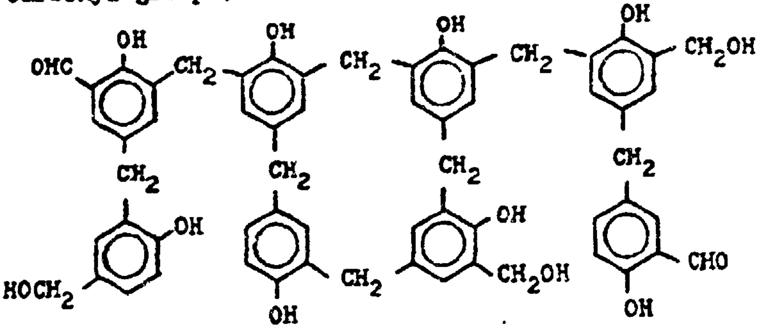

This result is in agreement with the crosslinked structure.

The curing of phenolic resins with terephthaloyl chloride may have occurred inter- and intra-molecularly with hydroxyls to form esters as suggested by Lei and Khamis(29):

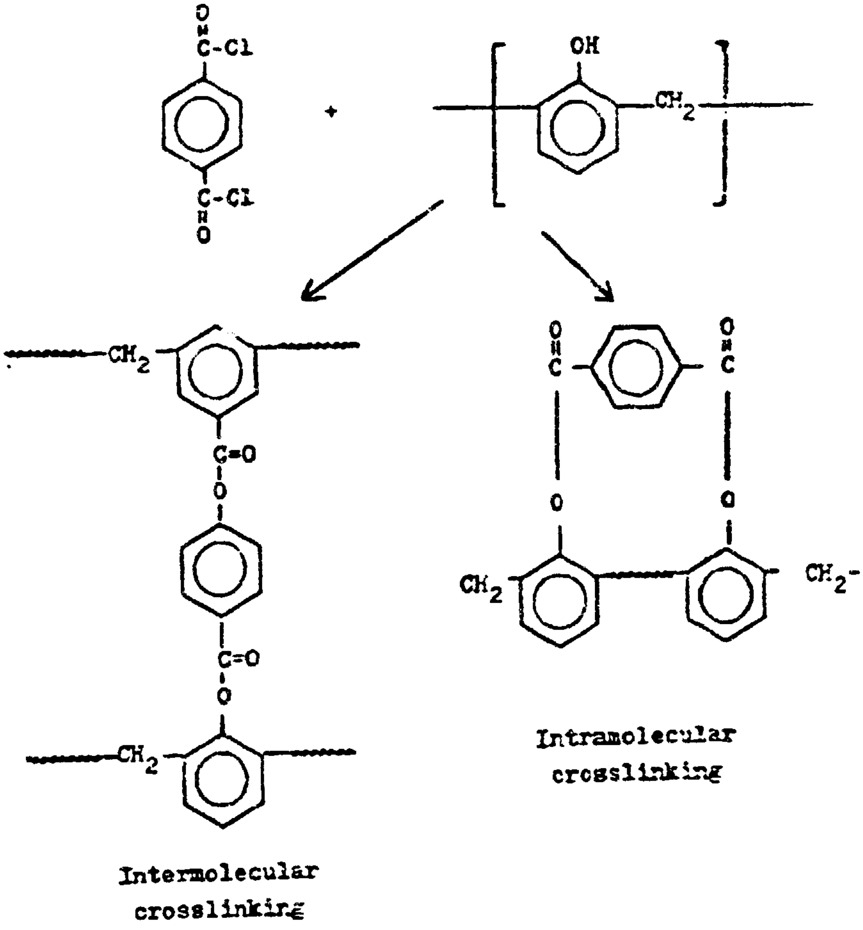

Intermolecular crosslinking

Intramolecular crosslinking

The resulting resin is expected to give absorptions at 1735, 1260, 1190, and 1065 cm^{-1} due to the carbonyl groups, the ester C-O groups, Ø-C-O, and C-O-C, respectively(84). The

C-H bending vibrations of para-substituted benzene ring of the curing agent give rise to a sharp band at 1010 cm^{-1}, where the 2 and 3 hydrogens move clockwise while the 5 and 6 hydrogens move counterclockwise(85). The sharp band at 720 cm^{-1} is assigned to the aromatic ring of the phthalate(87).

3.2.2 Number Average Molecular Weight Determination

For unsubstituted phenolic resin the structure is assumed to be the following simplified form:

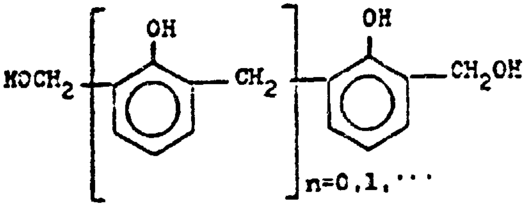

The various NMR integrals are defined as follows: A_1 = relative number of hydroxyl protons; A_2 = relative number of aromatic ring protons; A_3 = relative number of methylene protons; $m = (A_1 + A_2)/A_3$. The ratio, m, increases as the repeating unit, n, increases.

The value of $(A_1 + A_2)$ will increase from 6 (when n = 0) to 6 + 4n, and the value of A_3 will increase from 4 (when n = 0) to 4 + 2n. The value of m can be expressed in terms of n:

$$\frac{6 + 4n}{4 + 2n} = m$$

Therefore, the value of n can be calculated from:

$$m(n + 1)-2n-3 = 0 \; .$$

and the number-average molecular weight, $\overline{M}n$, is obtained:

$$\overline{M}n = 106n + 154.$$

For mono-substituted phenolic resins the value of n is given by:

$$m(2n + 4)-3n-5 = 0.$$

The number-average molecular weight for each different resin can be calculated from the following equations:

mBPF, pBPF: $\overline{M}n = 185n + 233$
mCPF, pCPF: $\overline{M}n = 140n + 188$
mCP, pCP: $\overline{M}n = 120n + 168.$

Table 4 shows the results obtained on the phenolic resins by using the above methods.

It should be noted that the calculations of m, n, and $\overline{M}n$, assume the absence of cyclic structures and branched isomers. The assumption may become invalid for some higher molecular weight resins. Also, the errors accompanying determinations of m and n increase greatly with increasing bridging contents and the molecular weight.

3.2.3 Thermal Properties of Cured Phenolic Resins

Summaries of the thermal analytical data of the phenolic resins crosslinked by formaldehyde and terephthaloyl chloride are shown in Tables 5 and 6, respectively. The oxygen index is plotted as a function of char yield as shown in Figure 41. An approximate correlation between oxygen index and char yield is found among samples containing no halogens according to the following relationship:

Table 4.

Number Average Molecular Weights, $\overline{Mn}$, of Oligomeric Phenolic Resins

	m	n	$\overline{Mn} \times 10^3$
PF	2.07	13.2	1.53
mBPF	1.44	6.33	1.40
pBPF	1.45	8.00	1.71
mCPF	1.48	23.0	3.42
pCPF	1.45	8.00	1.31
mCF	1.42	4.25	0.67
pCF	1.43	5.14	0.78

Table 5.

Thermal Analytical Data of Phenolic Resins Crosslinked via Methylene Linkages

Sample No.	Crosslinked Resins	Char Yield,% at 800°C, N_2	Oxygen Index,%
1	X(T)PF	57	35
2	X(F)PF	56	35
3	X(T)mCF	51	33
4	X(T)mCPF	32	26
5	X(F)mCPF	50	75
6	X(T)mBPF	38	50
7	X(F)mBPF	41	75

Table 6.

Thermal Analytical Data of Phenolic Resins Crosslinked via Ester Linkages

Sample No.	Crosslinked Resins	Char Yield,% at 800°C, N_2	Oxygen Index,%
8	X(C)PP	44	25
9	X(C)mCP	34	23
10	X(C)pCP	39	25
11	X(C)mCPP	39	39
12	X(C)mBPP	26	43
13	X(C)pCPP	46	42
14	X(C)pBPP	37	55

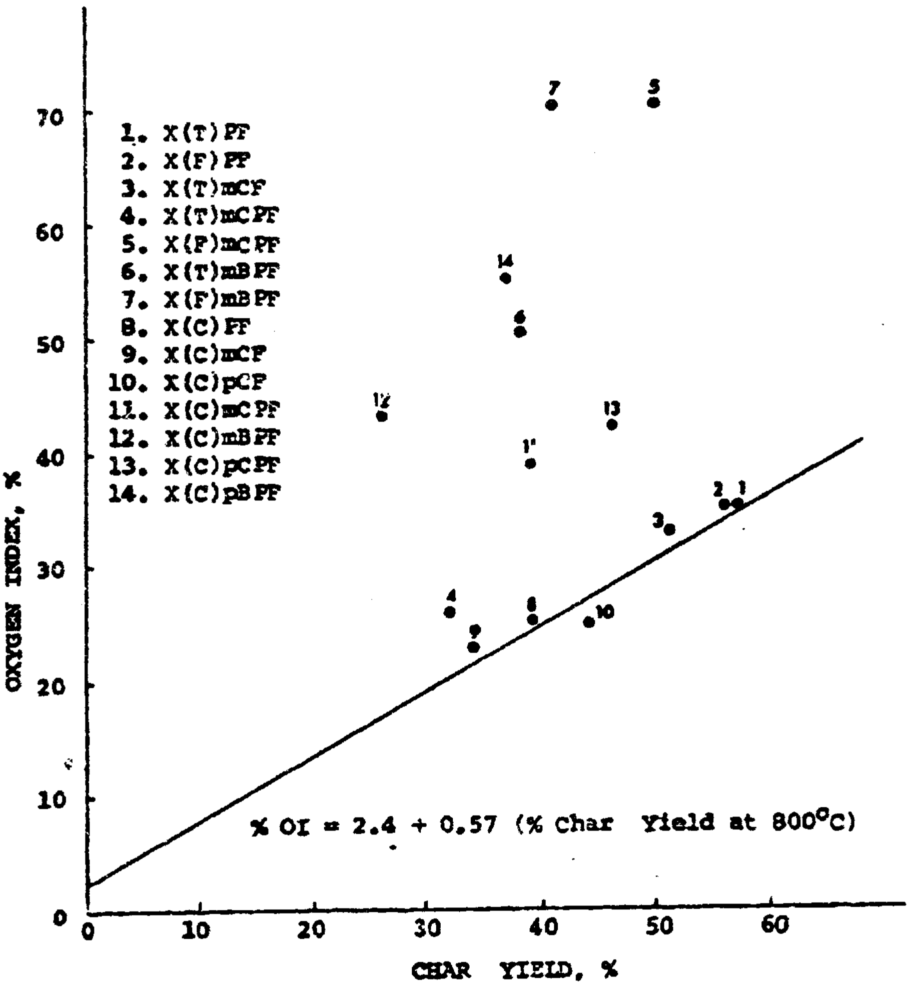

Figure 41: Correlation of Oxygen Index and Char Yield of Phenolic Resins.

$$\% \text{ OI} = 2.4 + 0.57 \, (\% \text{ char yield at } 800^{\circ}\text{C}).$$

Depending on the experimental conditions such as the sample forms and the criteria for the oxygen index measurements and the temperature defined for char yields, the intercept and the slope of the curve vary. Van Krevelan(5) obtains the following equation:

$$\% \text{ OI} = 17.5 + 0.4 \, (\% \text{ char yield at } 850^{\circ}\text{C}).$$

In general, brominated phenolic resins are found to have higher oxygen indices with lower char yields. The reason has been discussed earlier in terms of a gas-phase radical suppression mechanism and the loss of Br from the structure. The *para*-substituted phenolic resins cured *via* ester linkages give higher char yields and oxygen indices than the *meta*-substituted resins. The differences can be related to their reactivity towards crosslinking agents. In any one of the following proposed mechanisms(87) for the condensation of phenols and acid chlorides in the presence of tertiary amines, the acidity of phenols plays an important role:

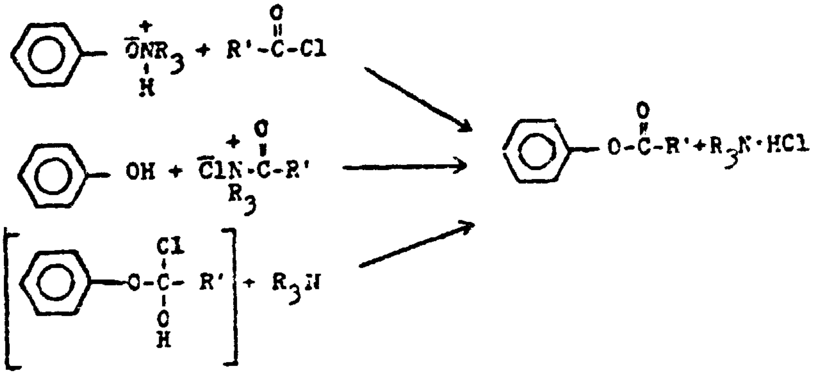

$\overset{+}{\bar{O}}NR_3$ + R'-C(=O)-Cl
OH + $\overset{+}{\bar{Cl}}N$-C(=O)-R'
R_3
O-C(Cl)(OH)-R'
+ R_3N
O-C(=O)-R'+$R_3N \cdot HCl$

Therefore, the para-substituted phenols which usually have smaller K_a values(88) than those of the meta-substituted phenols may result in a higher degree of crosslinking. The degree of crosslinking has been found to have a direct influence on char formation (Table 7)(89).

The results also show that s-trioxane-cured resins have lower char yields and oxygen indices than those of the corresponding formaldehyde cured resins. The infrared spectrum of X(T)mCPF (Figure 42) shows a strong ether absorption at 1100 cm^{-1} which is observed as a weak peak in the spectrum of X(F)mCPF. The methylol absorption at 1000 cm^{-1} is relatively stronger. The bands at 1250-1200 cm^{-1} and 940-900 cm^{-1} (strong) are the characteristics of aromatic ether such as methylene-1,2-dioxybenzenes ($\emptyset$-O-CH_2-O-$\emptyset$)(90). The relatively low intensity of the OH stretching absorption indicates that hydroxyl groups are involved in the s-trioxane crosslinking reactions. From the above observations the mechanisms for such reactions can be assumed to proceed the following way:

Table 7.

Char Yields as a Function of Degree of Crosslinking[*] of Phenol-formaldehyde Polymer

Polymer	Phenolic Hexa	Sol.Fraction	Char Yield, % at 800°C, N_2
1-a	-	1.00	43.2
1-b	8.3	0.76	50.2
1-c	6.9	0.51	51.2
1-d	4.2	0.41	58.9
1-e	2.8	0.21	62.9
1-f	1.9	0.09	64.7

[*] Curing by hexamethylenetetramine (hexa) at 157°C under Ar.

J.A. Parker and E.L. Winkler, NASA Tech. Rept.
TR R-276
Nov. 1967

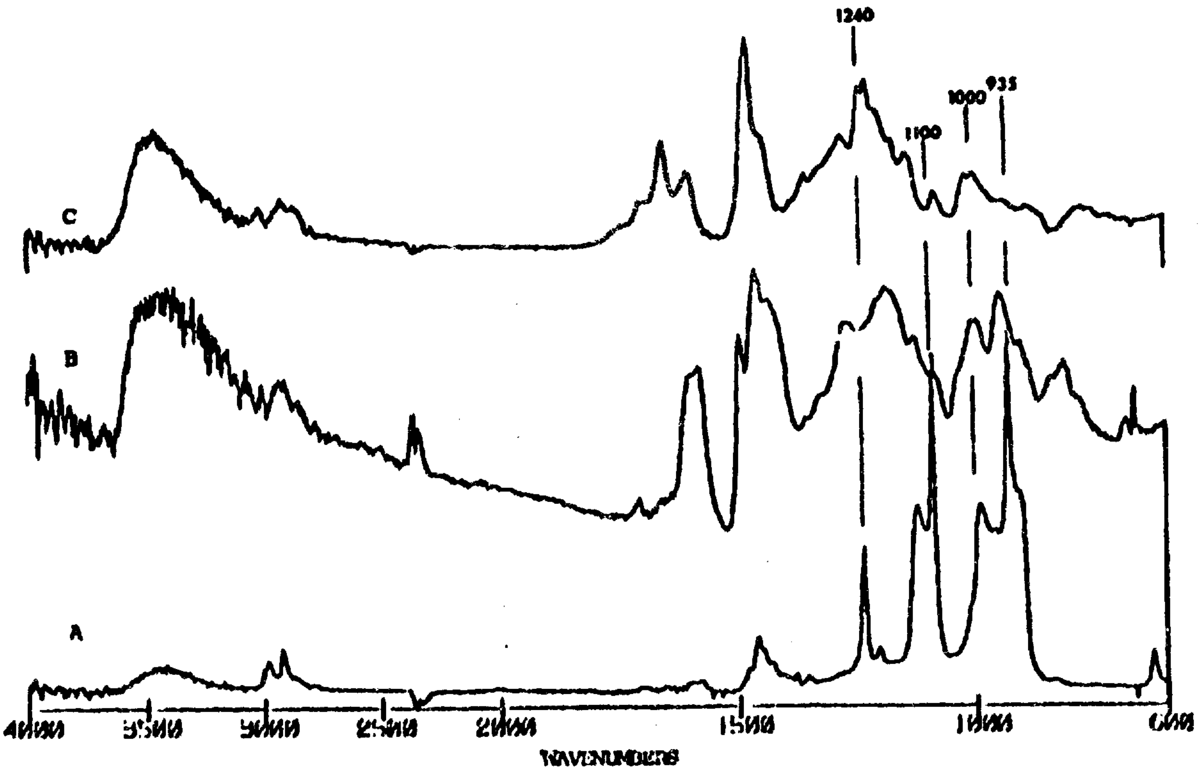

Figure 42: IR Spectra of (A) X(T)mCPF, (B) X(F)mCPF, and (C) X(F)PF. KBr Pellet.

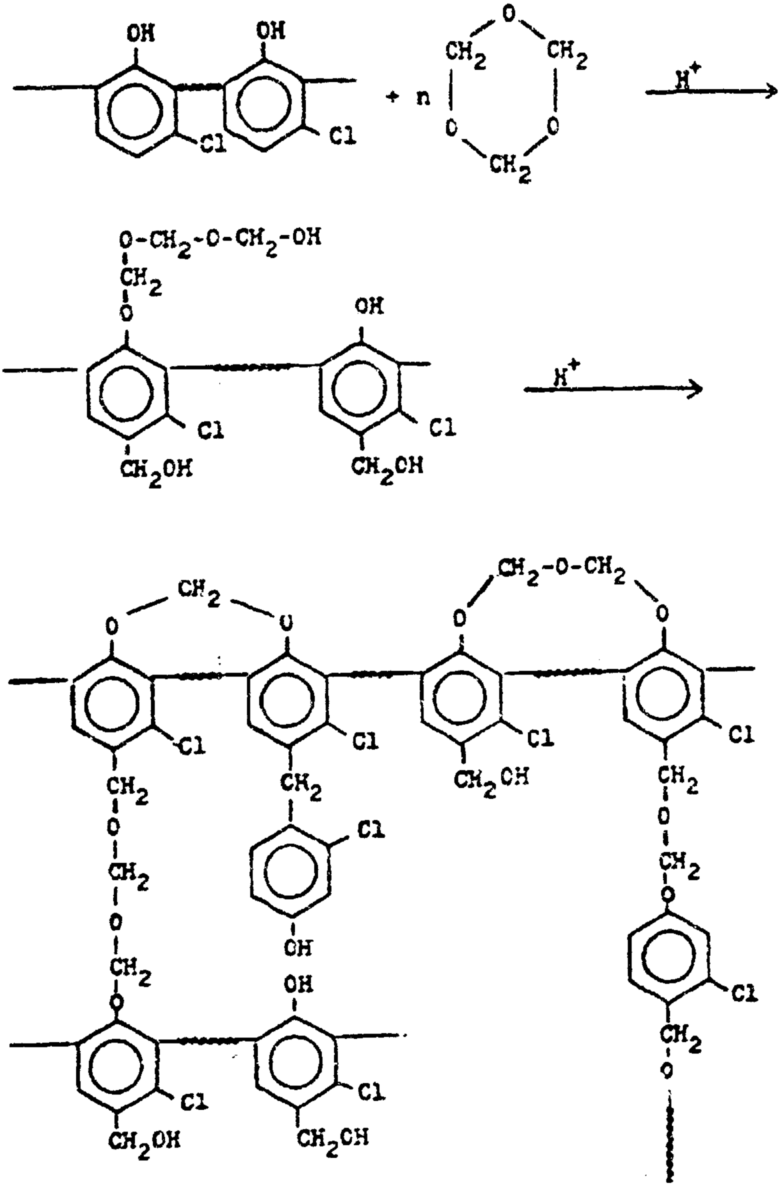
OH
OH
Cl
Cl
+ n
O
CH2
CH2
O
O
CH2
H+
O-CH2-O-CH2-OH
CH2
O
OH
Cl
Cl
CH2OH
CH2OH
H+
CH2
O
O
CH2-O-CH2
O
O
Cl
Cl
Cl
Cl
CH2
CH2
CH2OH
CH2
O
O
CH2
CH2
O
Cl
O
Cl
CH2
OH
CH2
OH
O
Cl
Cl
CH2OH
CH2OH

The final cured resins contains aliphatic ethers, methylols, methylene linkages and cyclic acetals.

3.2.4 Conclusion

The structures of the oligomeric phenolic resins have been studied by NMR and FT-IR spectroscopy. The oligomeric resins consist mainly of methylene linkages joining at the *ortho* and *para* positions of the phenolic nuclei. NMR spectra also provide an approximate estimation of the number-average molecular weight.

The crosslinked resins are made by using formaldehyde, s-trioxane and terephthaloyl chloride as the curing agents. The structures of the cured resins are studied by FT-IR spectroscopy. The formaldehyde cured resins contain a small amount of methylols and dibenzyl-type ethers. Based on the evidence from the infrared spectra the reactions between s-trioxane and the oligomeric resins are assumed to proceed *via*. cyclic acetal formation along with the conventional crosslinking through methylene bridges. Methylols and benzyl-type ethers are predominant in the structures.

Crosslinking of the oligomeric resins can also be achieved through the reaction of terephthaloyl chloride. The curing reactions may have occurred inter- and intramolecularly with the hydroxyls to form ester linkages.

The thermal analytical data demonstrate the improvement in oxygen index due to the presence of halogens in some of the resins.

3.3 Photo-Fries Rearrangement of Fluorene-Based Polyarylates

3.3.1 UV Spectroscopic Studies

The UV spectra of the polymers in methylene chloride are recorded periodically during the irradiation (Figures 43, 44, and 45). An increase in absorption in the region from 325 to 375 nm with a maximum at 355 nm for BPF-I and BCF-I are related to the hydroxybenzophenone structure if one takes into consideration the fact that low-molecular substituted benzophenone derivatives absorb in the region from 300 to 400 nm depending on the type and position of the substituent in the structure(91). The absorption maxima of polymeric benzophenone also differ markedly from one another(45,92). By comparing Figures 43 and 45, the increase is found to be less in the case of BCF-I. In the spectra of BDMPF-I (Figure 45) only slight changes in the region of 325-375 nm are observed. A more direct comparison of the changing rates is shown in Figure 46. The curves result from plotting the absorption at 350 nm for each sample as a function of irradiation time.

With the polyarylates examined in this work, the structural requirement to produce the photo-chemical-Fries rearrangement under UV irradiation is the presence of at least one unsubstituted position on the phenol rings *ortho* to the ester groups. Thus, BDMPF-I does not rearrange under the irradiation conditions. The substitution on one-half of the *ortho*-positions of the phenol rings with the methyl groups

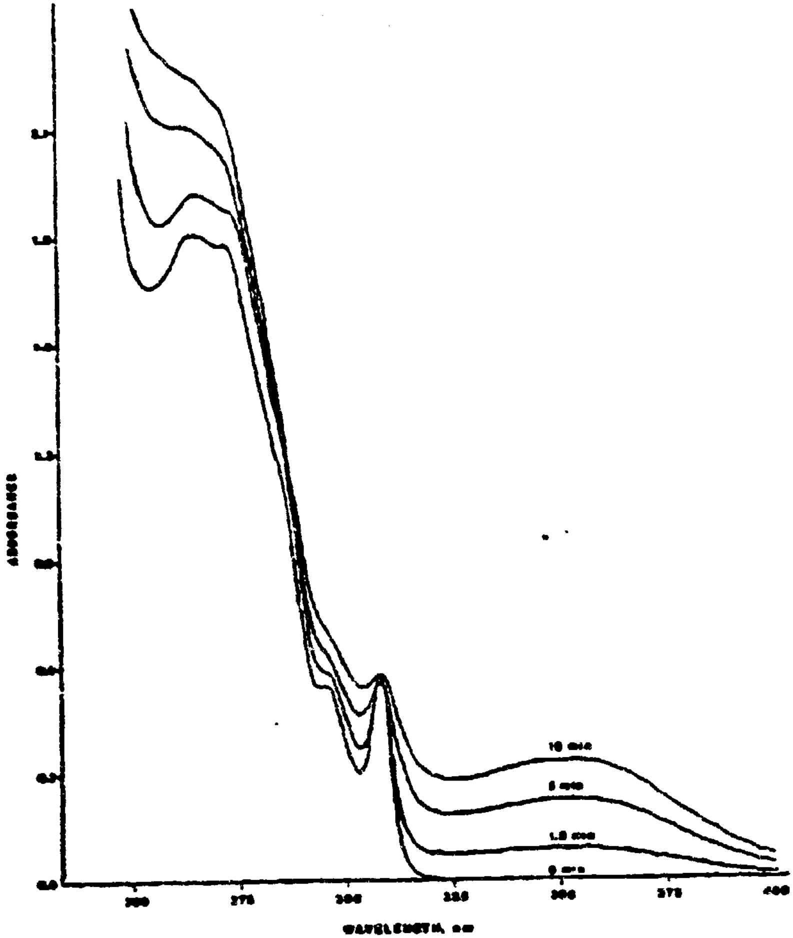

Figure 43: UV Spectra of BPP-I in Methylene Chloride Solution before and after Irradiation for Different Periods of Time.

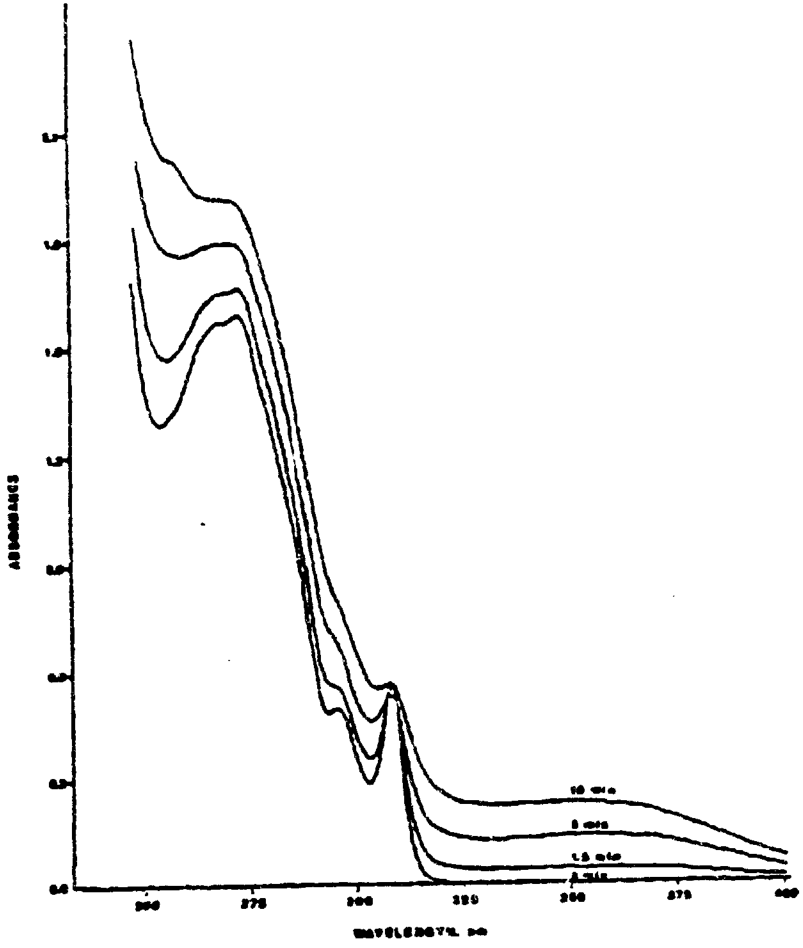

Figure 44: UV Spectra of BCF-I in Methylene Chloride Solution before and after Irradiation for Different Periods of Time.

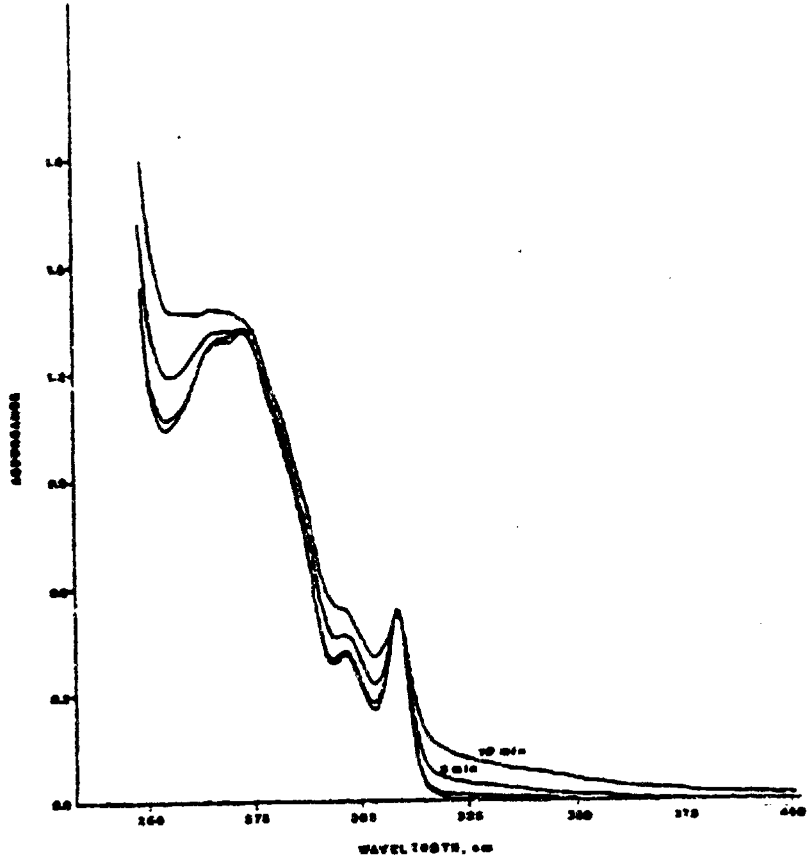

Figure 45: UV Spectra of BDMPF-I in Methylene Chloride Solution before and after Irradiation for Different Periods of Time.

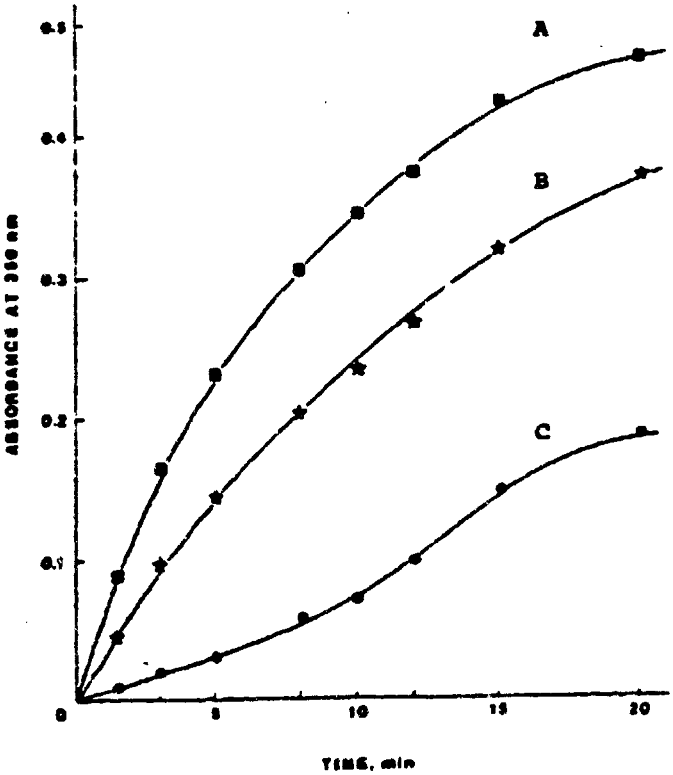

Figure 46: Changes in Absorbance at 350 nm with Irradiation time : (A) BPF-I, (B) BCF-I, and (C) BDMPF-I.

(*e*.g., BCF-I) apparently reduces the formation of *o*-hydroxybenzophenone.

3.3.2 FT-IR Spectroscopic Studies

Infrared spectra shown in Figures 47, 48 and 49 for the samples before and after 60 min. irradiation provide further information on the structural changes resulting from the rearrangement. The difference spectra are generated by digitally subtracting two spectra on a 1:1 basis assuming no change in thickness of the samples after irradiation. The absolute changes are obtained with the scale expanded 5 times.

In Figure 47 the OH stretching vibration is observed as a weak band in the region near 3300 cm^{-1}. Broadening and weakening of the band are due to the intramolecular hydrogen bonding between the hydroxyl group and the carbonyl group at the *ortho* position(93). The intermolecular hydrogen bonding causes a slight shift of the ester carbonyl absorption towards a lower frequency at 1745 cm^{-1}(47). The positive peak at 1630 cm^{-1} in the difference spectrum is attributed to the highly polarized hydroxybenzophenone carbonyl group(45,47). The ester C-O bond breaking involved in the photo-Pries rearrangement is observed as a decrease in intensity of a band at 1290 cm^{-1}. The most notable change in the difference spectrum is the increased absorption in the phenolic OH deformation and C-O stretching regions around 1220 cm^{-1} which also represents the Ø-C-O vibration(94).

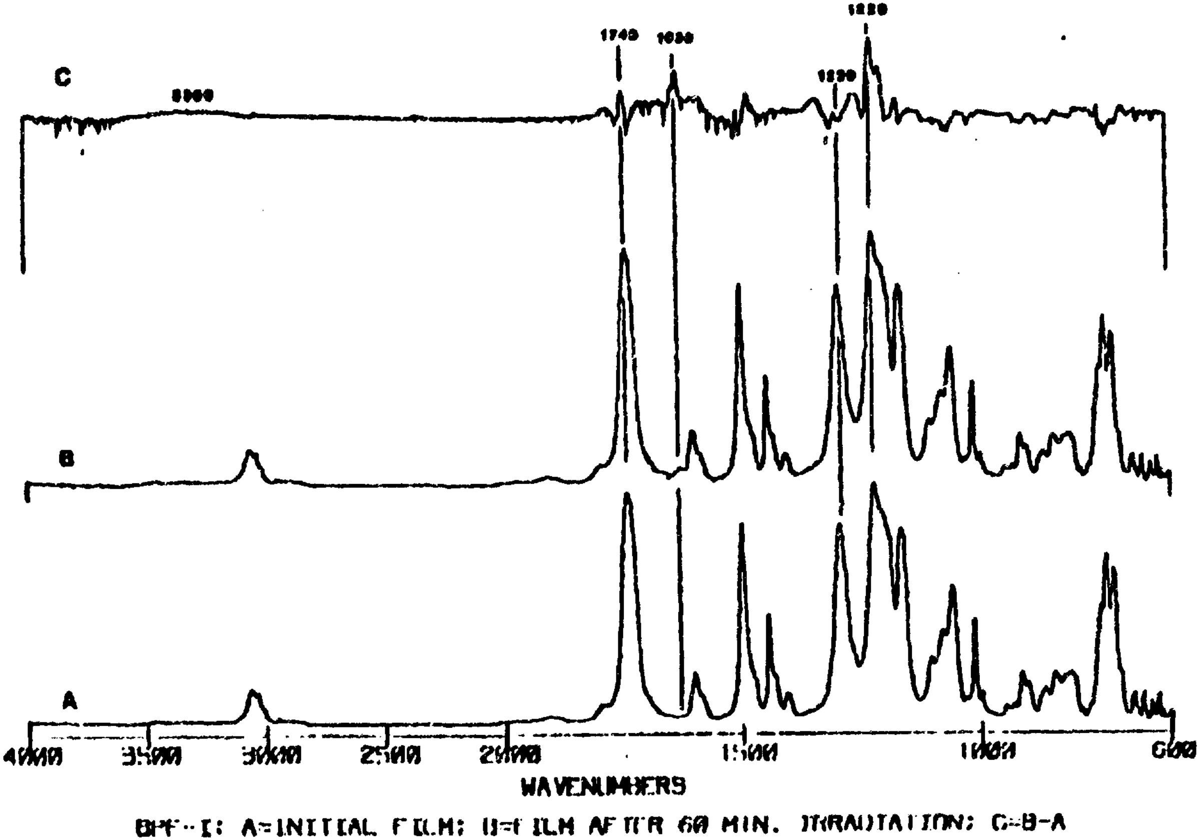

Figure 47: Infrared Spectra of (A) BPF-I, (B) BPF-I after 60 Min. Irradiation, and (C) Difference Spectrum B-A. Reflectance Attachment.

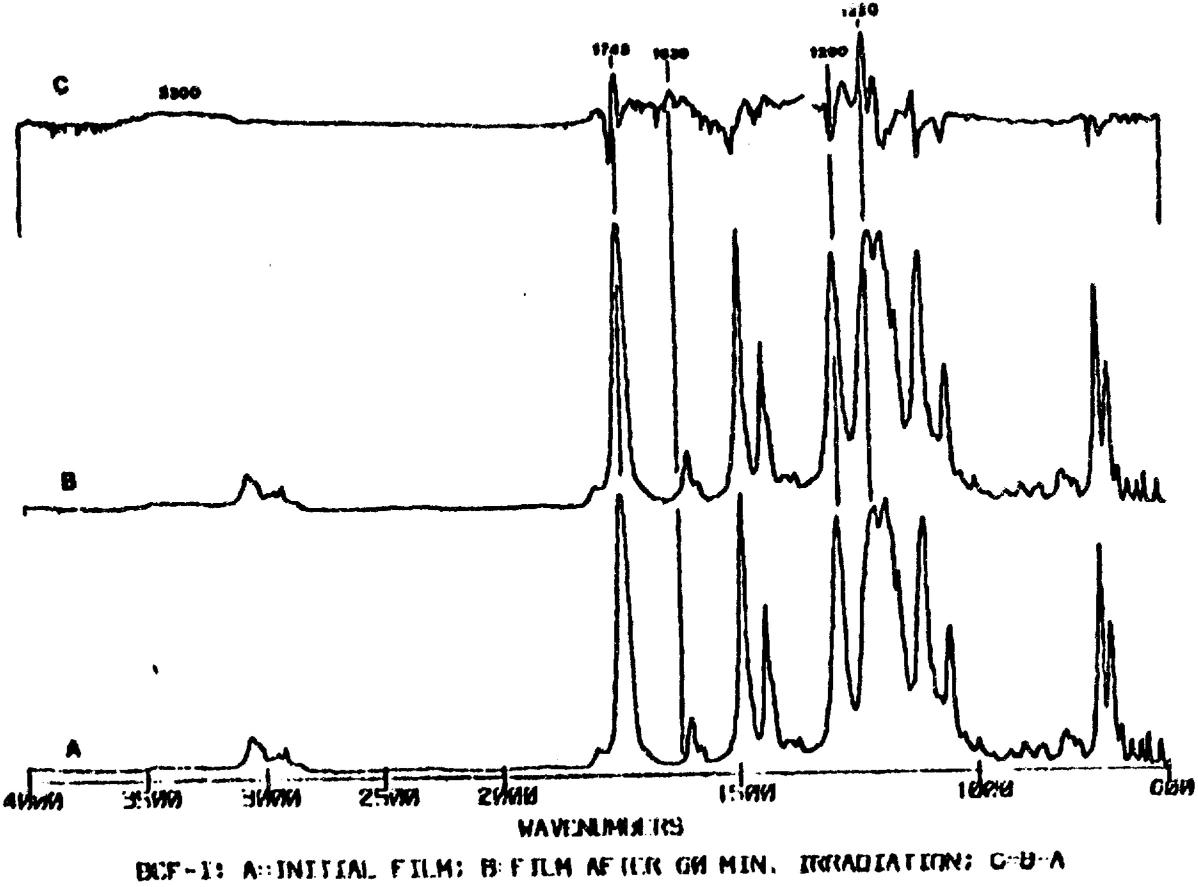

Figure 48: Infrared Spectra of (A) BCF-I, (B) BCF-I after 60 Min. Irradiation, and (C) Difference Spectrum B-A. Reflectance Attachment.

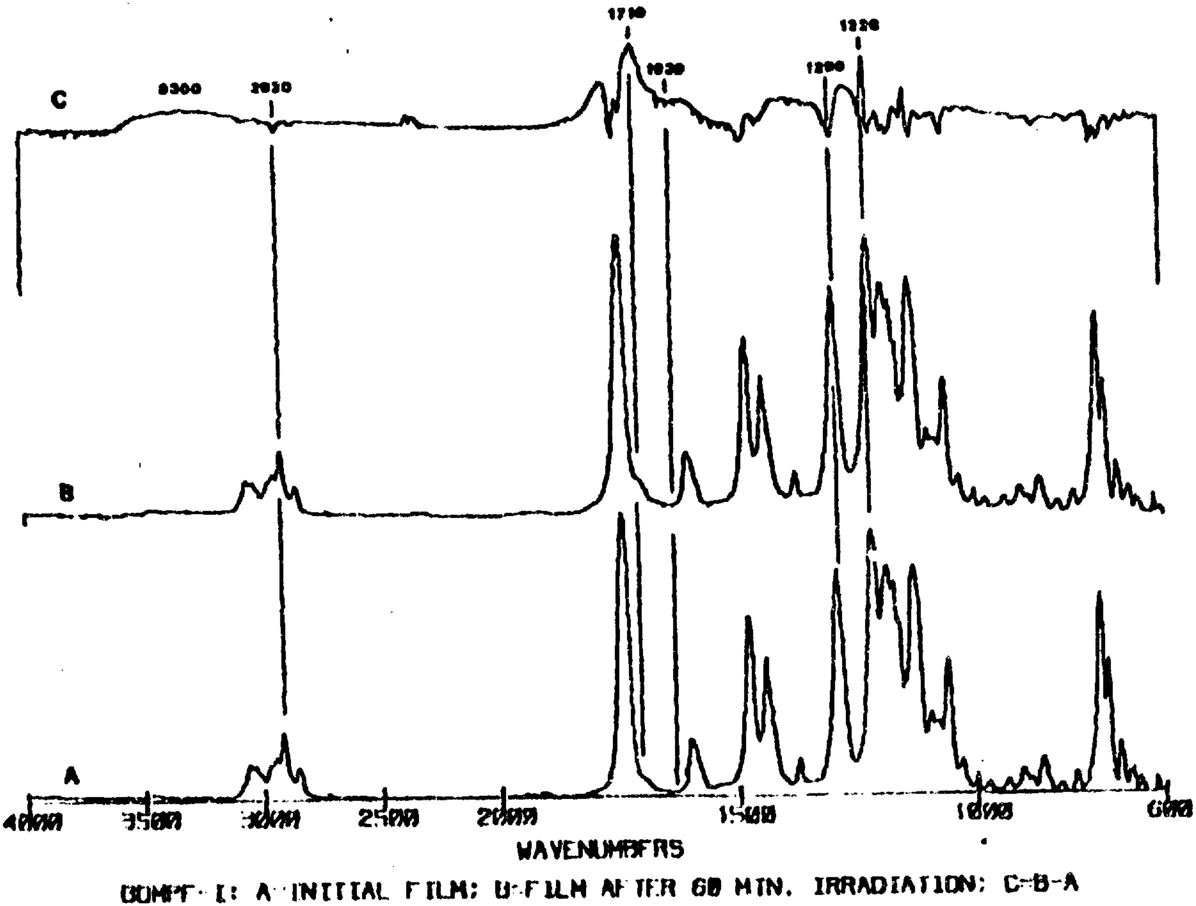

Figure 49: Infrared Spectra of (A) BDMPF-I, (B) BDMPF-I after 60 Min. Irradiation, and (C) Difference Spectrum B-A. Reflectance Attachment.

It is proposed that irradiation of BPF-I occurs with molecular rearrangement to form a new polymer compound, in part, of linear o-hydroxybenzophenone moieties as the product:

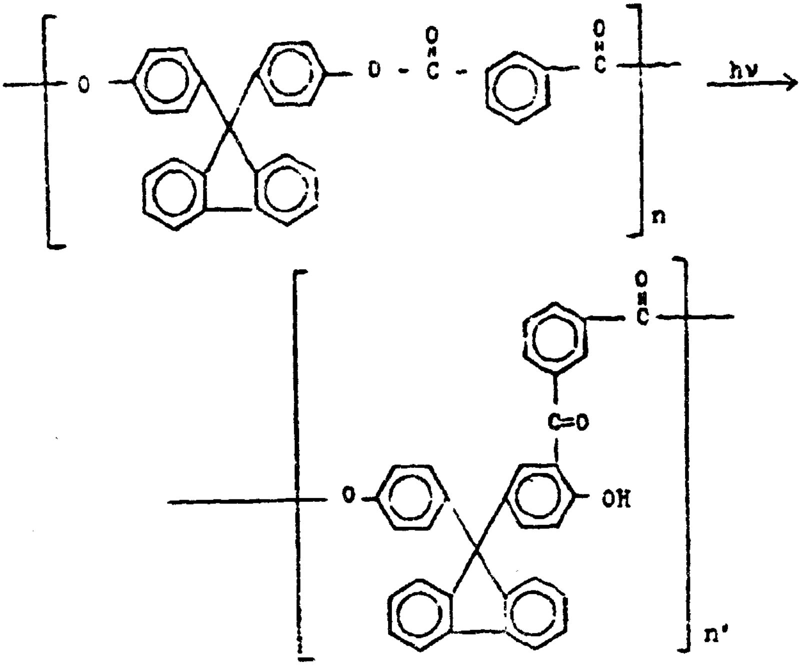

The spectral changes of BCF-I upon irradiation (Figure 48) are almost identical to that of BPF-I except for the less intense peak at 1630 cm^{-1} indicating the formation of o-hydroxybenzophenone is inhibited by the substitution of one of the *ortho*-positions in the phenol rings with the methyl groups. This is in agreement with the result from the UV spectroscopic observations.

A complete inhibition of the Fries rearrangement may occur in BCMPF-I. Figure 49 indicates no formation of hydroxybenzophenone (1630 cm^{-1}). Free hydroxyl groups are observed as a strong band at 3300 cm^{-1}. The hydroxyl groups are most likely to be the phenolic type which also gives rise to a sharp peak at 1220 cm^{-1} due to Ø-CH stretching vibration. The slightly decreased band at 2920 cm^{-1} indicates a loss of aliphatic hydrogens presumably from the methyl groups. A decreased absorption peak at 1745 cm^{-1} and an increased absorption peak at 1710 cm^{-1} are observed, suggesting the formation of an aromatic aldehyde at the expense of the ester group. The cleavage of the ester C-O bond is also evident, indicated by the negative difference band at 1290 cm^{-1}. Based on the above analysis the following reaction scheme is proposed for the UV degradation of BDMPF-I.

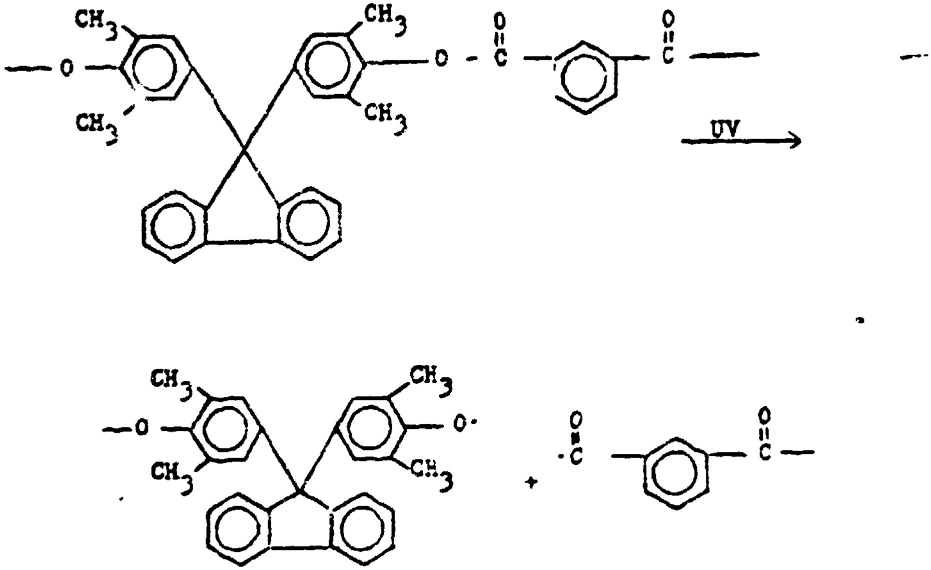

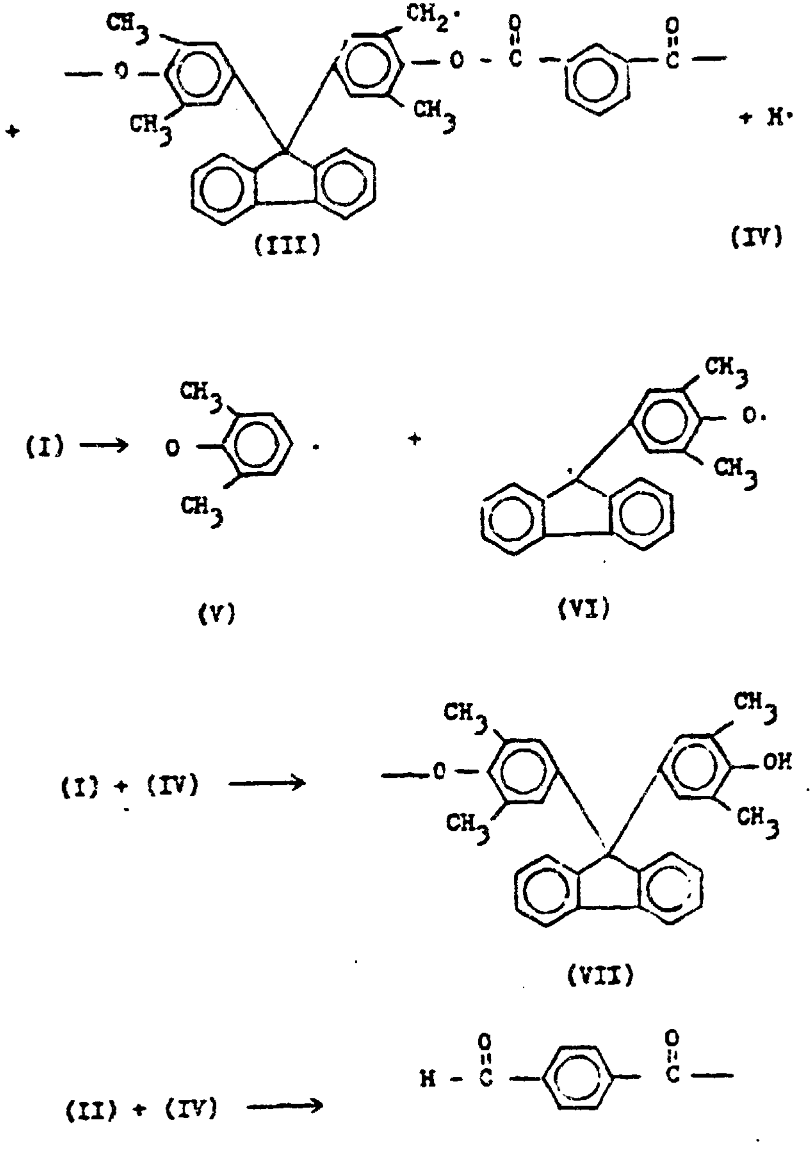
+
CH3
CH3
O
CH2·
CH3
O
C
O
C
+ H·
(III)
(IV)
(I) →
O
CH3
CH3
+
CH3
O·
CH3
(V)
(VI)
(I) + (IV) →
CH3
O
CH3
CH3
OH
CH3
(VII)
(II) + (IV) →
H
O
C
O
C
(VIII)

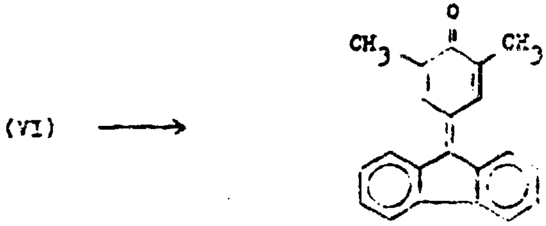

(IX)

The quinone structure (IX) may account for the yellow color of the irradiated sample. In the study of photo-degradation of a polycarbonate(95), a similar quinone structure (X) has been proposed as part of the degradation products.

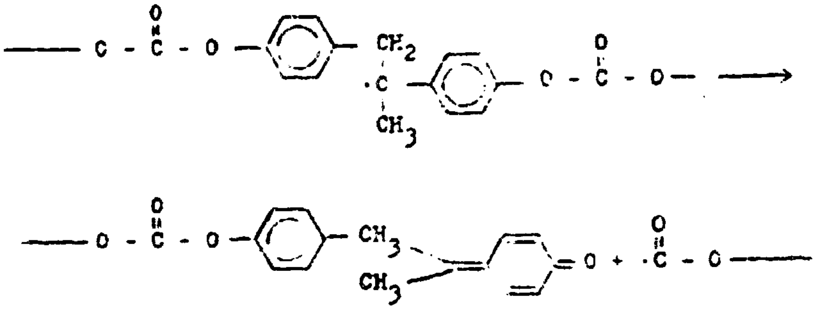

(X)

3.3.3 Conclusion

An investigation of the photo-Fries rearrangement in fluorene based polyarylates has been made. It is shown that the structural changes of the polymers having free ortho-positions on the phenol rings are connected with the formation of o-hydroxybenzophenone structures in the polymer as a result of the photo-Fries rearrangement. UV spectroscopy provides a direct detection of o-hydroxybenzophenone. Digital subtraction of infrared data obtained by Fourier Transform infrared spectroscopy has been applied in observing the chemical changes occurring in the photo-Fries rearrangement process. Substitution in the ortho-positions of the phenol rings results in a different route for degradation. The degradation products include the aldehyde moieties, phenols, and the possible quinone structures.

BIBLIOGRAPHY

1. H.F. Mark, S.M. Atlas, S.W. Shalaby, and E.M. Pearce, in "Flame-Retardant Polymeric Materials", M. Lewin, S.M. Atlas, and E.M. Pearce, Editors, Plenum Press, New York, 1975, p. 1.

2. ibid., p. 15.

3. C.P. Fennimore and F.J. Martin, Modern Plastics, 44, 141(1966).

4. J.A. Parker, G.M. Fohlen, and P.M. Sawko, paper presented at Conference on Transparent Aircraft Enclosures, Las Vegas, Nevada, Feb. 5-8, 1973.

5. D.W. Van Krevelen, Polymer, 16, 615(1975).

6. S.V. Vinogradova and Y.S. Vygodskii, Russian Chemical Reviews, 42(7), 551(1973).

7. V.V. Korshak, S.V. Vinogradova, and S.N. Salazkin, Vysokomolekul. Soedin., 4, 339(1962); Chem. Abs., 58, 3513c (1962).

8. B.V. Chandik, Modern Plastics, Oct., 72(1977).

9. H.G. Cooke, SPE Tech. Papers, 5, Paper No. 77, 1959; Chem. Abs., 53, 15628d (1959).

10. I. Wiesner, Czech., 107,058 (1963); Chem. Abs., 60, p. 9,433d (1964).

11. Y. Yamozaki, Japan Kokai, 75, 27,843(1975); Chem. Abs., 83, p. 98,517k (1975).

12. K. Kamada, Y. Kinoshita, and H. Nakanishi, Japan Kokai Tokkyo Koho, 79, 15,954(1979); Chem. Abs., 90, 205247r (1979).

13. C.V. Wittenwyler, Modern Plastics, Dec., 62(1978).

14. M.S. Lin and E.M. Pearce, Unpublished work.

15. L.I. Komarova, S.N. Salazkin, I.A. Bulgakova, M.I. Kalaniya, S.V. Vinogradova, and V.V. Korshak, J. Polymer Sci.; (Polymer Chemistry), 16, 1643(1978).

16. A. Bayer, Ber. dtsch. Chem. Ges., 5, 25(1872); A. Knop and W. Scheib, "Chemistry and Application of Phenolic Resins", Springer-Verlag, New York, 1979, Chapter 1, Ref. 4.

BIBLIOGRAPHY (Continued)

17. G. Kleeberg, *Liebigs Ann. Chem.*, *263*, 283(1891).

18. A. Luft, *U.S.*, 735,278 (1902).

19. L.H. Baekeland, *U.S.*, 942,699 (1907).

20. K.J. Saunders, "Organic Polymer Chemistry", Chapman and Hall, London, 1973, p. 282.

21. A. Knop and W. Scheib, "Chemistry and Application of Phenolic Resins", Springer-Verlag, New York, 1979, p. 35.

22. S.R. Sandler and W. Karo, "Polymer Syntheses", Academic Press, New York, 1977, Vol. 2, p. 46.

23. K.J. Saunders, "Organic Polymer Chemistry", Chapman and Hall, London, 1973, p. 287.

24. N.J.L. Megson, "Phenolic Resin Chemistry", Butterworth, London, 1958, p. 15.

25. R.W. Martin, "The Chemistry of Phenolic Resins", Wiley, New York, 1956, p. 7.

26. N. Kornblum, R.A. Smiley, R.K. Blackwood, and P.C. Iffland, *J. Amer. Chem. Soc.*, *77*, 7269(1955).

27. J. Economy, L. Wohrer, and F. Frechette, *J. Fire Flammability*, *3*, 412(1972).

28. A. Knop and W. Scheib, "Chemistry and Application of Phenolic Resins", Springer-Verlag, New York, 1979, p. 93.

29. G. Lei and A. Khamis, *Polymer Preprints*, *19*, No. 2, 713(1978).

30. W.L. Hawkins, "Polymer Stabilization", Wiley-Interscience, New York, 1972, p. 192.

31. *ibid.*, p. 197.

32. E.J. O'Connell, *J. Amer. Chem. Soc.*, *90*, 6550(1968).

33. A. Heller, *Mol. Photochem.*, *1*, 2571(1969).

34. V.I. Stenberg, "Photo-Fries Reaction and Related Rearrangements", in O.L. Chapman, Ed., "Organic Chemistry", Vol. 1, Dekker, New York, 1967, p. 127.

BIBLIOGRAPHY (Continued)

35. J.D. Anderson and C.R. Reese, *Proc. Chem. Soc.*, 217(1960).

36. H. Kobsa, *J. Org. Chem.*, **27**, 2293(1962).

37. R.A. Finnegan and J.J. Mattice, *Tetrahedron* **21**, 1015(1965).

38. C. Pac and S. Tsutsomi, *Bull. Chem. Soc. Jap.*, **37**, 1392(1964).

39. E.A. Caress and I.E. Rosenberg, *J. Org. Chem.*, **36**, 769(1971).

40. D.P. Kelley and J.T. Pinhey, *Tetrahedron Lett.*, No. 46, 3427(1964).

41. H. Obara, H. Takahashi, and H. Hirano, *Bull. Chem. Soc. Jap.*, **42**, 560(1969).

42. D. Bellus, *Advan. Photochem.*, **8**, 109(1971).

43. J.D. Anderson and C.R. Reese, *J. Chem. Soc.*, 1781 (1963).

44. J.E. Guillet, *Naturwissenschaften*, **59**, 503(1972).

45. S.B. Maerov, *J. Polymer Sci.*, **A3**, 487(1965).

46. S.M. Cohen, R.H. Young, and K.H. Markhart, *J. Polymer Sci.*, Part A-1, **9**, 3263(1971).

47. V.V. Korshak, S.V. Vinogradova, S.A. Siling, S.R. Rafikov, Z.TA. Fomina, and V.V. Rode, *J. Polymer Sci.*, Part A-1, **1**, 157(1969).

48. ASTM D1652-73, Standard Method of Test for Epoxy Content of Epoxy Resins, *ASTM*, **28**, 341(1975).

49. H. Lee and K. Neville, "Handbook of Epoxy Resins", McGraw-Hill, New York, 1967, pp. 4-17.

50. P.W. Morgan, *Macromolecules*, **3**, 536(1970).

51. G. Lask and H.G. Wagner, "Eighth Symposium on Combustion", Williams and Wilkins, Baltimore, 1962, p. 432.

52. H.B. Palver and D.J. Seery, *Combustion and Flame*, **4**, 213(1960).

BIBLIOGRAPHY (Continued)

53. C.P. Fenimore and F.J. Martin, Combustion and Flame, 10, 135(1966).

54. G. Fryburg, National Advisory Committee for Aeronautics - Technical Notes, 2102, 1950.

55. P.C. Warren, SPE Journal 27, 17(1971).

56. W.A. Rosser, H. Wise, and J. Miller, "Seventh International Symposium on Combustion", Butterworth, London, 1959, p. 175.

57. H. Wise and W.A. Rosser, "Ninth International Symposium on Combustion", Butterworth, London, 1963, p. 733.

58. E.C. Creitz, J. Res. National Bureau of Standards, 74A(4), 521(1970).

59. E.C. Creitz, J. Res. National Bureau of Standards, 65A(4), 389(1961).

60. E.R. Larsen, J. Fire and Flammability/Fire Retardant Chemistry, 1, 4(1974).

61. L. Pauling, "The Nature of the Chemical Bond", Cornell University Press, Ithaca, New York, 1948, p. 53.

62. Y.P. Khanna and E.M. Pearce, Unpublished results (1975).

63. Y.P. Khanna, Ph.D. Thesis, Polytechnic Institute of New York, Brooklyn, N.Y., (1980).

64. H. Lee and K. Neville, "Handbook of Epoxy Resins", McGraw-Hill, New York, 1966, pp. 5-18.

65. P.C. Painter, J. Havens, W.W. Hart, and J.L. Koenig, J. Polymer Sci., Polymer Physics Ed., 15, 1237(1977).

66. N.J.L. Megson, "Phenolic Resin Chemistry", Academic Press, New York, 1958, p. 107.

67. P.J. Secrest, Official Digest, 37, 187(1965).

68. J.C. Woodbrey, H.P. Higginbottom and H.M. Culbertson, J. Polymer Sci., Part A, 3, 1079(1965).

69. R.C. Hirst, D.M. Grant, R.E. Hoff, and W.J. Burke, J. Polymer Sci., Part A, 3, 2091(1965).

BIBLIOGRAPHY (Continued)

70. K.L. Williamson, N.C. Jacobus, and K.T. Soucy, J. Amer. Chem. Soc., 86, 4021(1964).

71. L.M. Jackman and S. Sternhall, "International Series of Monographs in Organic Chemistry", Vol. 5, Applications of Nuclear Magnetic Resonance Spectroscopy in Organic Cyemistry, 2nd Ed., Pergamon Press, New York, 1969, p. 67.

72. R.J. Grisenthwaite and R.F. Hunter, J. Appl. Chem., 6, 324(1966).

73. C.A. Lucchesi, Official Digest 30, No. 397, 212(1958).

74. R.E. Richards and H.W. Thompson, J. Chem. Soc., 1220 (1968).

75. D.D. Shrene, Anal. Chem., 84, 1692(1952).

76. D.D. Shrene, "Synthetic Organic Coating Resins", Organic Analysis, Vol. 3, Interscience, New York, 1956, p. 132.

77. N.B. Colthup, L.H. Daly, and S.E. Wikerley, "Introduction to Infrared and Raman Spectroscopy", 2nd Ed., Academic Press, New York, 1975, p. 260.

78. ibid., p. 261.

79. R.E. Richards and H.W. Thompson, J. Chem. Soc., 1260 (1947).

80. D.D. Shrewsbury, Spectrochim. Acta, 16, 1294(1960).

81. A. Knop and W. Scheib, "Chemistry and Application of Phenolic Resins", Springer-Verlag, New York, 1979, p. 44.

82. ibid., p. 48.

83. H.L. Bender, Modern Plastics, 30, 136(1953).

84. N.B. Colthup, L.H. Daly and S.E. Wikerley, "Introduction to Infrared and Raman Spectroscopy", 2nd Ed., Academic Press, New York, 1976, Chapt. 9.

85. ibid., p. 268.

86. ibid., p. 292.

BIBLIOGRAPHY (Concluded)

87. P.W. Morgan, "Condensation Polymers", Interscience New York, 1965, p. 153.

88. R.T. Morrison and R.N. Boyd, "Organic Chemistry", 3rd Ed., Allyn and Bacon, Boston, 1973, p. 788.

89. J.A. Parker and E.L. Winkler, NASA Technical Report, TR R-276, Nov. 1967.

90. N.B. Colthup, L.H. Daly and S.E. Wikerley, "Introduction to Infrared and Raman Spectroscopy", 2nd Ed., Academic Press, New York, 1976, p. 312.

91. V.V. Rode, E.YE. Said-Galiyer, Bull. Acad. Sci., USSR, 2149(1969).

92. J.S. Humphrey, Polymer Preprints, 8, 453(1968).

93. A.V. Stuart and G.B.B.M. Sutherland, J. Chem. Phys., 24, 559(1956).

94. N.B. Colthup, L.H. Daly, and S.E. Wikerley, "Introduction to Infrared and Raman Spectroscopy", 2nd Ed., Academic Press, New York, 1975, p. 318.

95. J.S. Humphrey, A.R. Shultz, and D.B.G. Jaquise, Macromolecules, 6, No. 3, 305(1973).

96. A. Baeyer, Ann., 202, 76(1980).

97. F.F. Blicke and R.A. Patelski, J. Amer. Chem. Soc., 58, 273(1936).

98. H.L. Bradlow and C.A. VanderWerf, J. Amer. Chem. Soc., 70, 654(1948).

99. G.A. Olah, "Friedel-Crafts and Related Reactions", Vol. 3, Wiley, New York, 1963, p. 560.

100. R.M. Silverstein, G.C. Bassler, and T.C. Morrill, "Spectrometric Identification of Organic Compounds", 3rd Ed., Wiley, New York, 1974, p. 185.

101. U. Gaur and B. Wunderlich, Macromolecules, 13, No. 6, 1618(1980).

END
FILMED
DTIC